



UNIVERSITY OF
KWAZULU-NATAL

INYUVESI
YAKWAZULU-NATALI

**HISTO-PHYTOCHEMICAL EVALUATION AND
CHARACTERISATION OF THE FOLIAR STRUCTURES
OF *TAGETES MINUTA* L. (ASTERACEAE)**

JESAMINE J. RIKISAHEDEW

A research dissertation submitted in fulfilment of the academic requirements for
the degree of Master of Science in
Biological Sciences

School of Life Sciences

College of Agriculture, Engineering and Science University of KwaZulu-Natal
Westville South Africa

December 2018

Supervisor

Prof Y. Naidoo

Co-supervisor

Prof Y. H. Dewir

PREFACE

The research contained in this dissertation was completed by the candidate while based in the Discipline of Biological Sciences, School of Life Sciences of the College of Agriculture, Engineering and Science, University of KwaZulu-Natal, Westville, South Africa. The financial assistance of the National Research Foundation (NRF) towards this research is hereby acknowledged. Opinions expressed, and conclusions arrived at, are those of the author and are not necessarily to be attributed to the NRF.

The contents of this work have not been submitted in any form to another university and, except where the work of others is acknowledged in the text, the results reported are due to investigations by the candidate.

As the candidate's supervisor(s) I have approved this dissertation for submission.

Signed: Prof Y. Naidoo (Supervisor)

Email: naidooy1@ukzn.ac.za

Date: 5 December 2018



Signed: Dr Y.H. Dewir (Co-supervisor)

Email: ydewir@hotmail.com

Date: 5 December 2018

DECLARATION: PLAGIARISM

I, Jesamine Jöneva Rikisahedew, declare that:

(i) the research reported in this dissertation, except where otherwise indicated or acknowledged, is my original work;

(ii) this dissertation has not been submitted in full or in part for any degree or examination to any other university;

(iii) this dissertation does not contain other persons' data, pictures, graphs or other information, unless specifically acknowledged as being sourced from other persons;

(iv) this dissertation does not contain other persons' writing, unless specifically acknowledged as being sourced from other researchers. Where other written sources have been quoted, then:

a) their words have been re-written but the general information attributed to them has been referenced;

b) where their exact words have been used, their writing has been placed inside quotation marks, and referenced;

(v) where I have used material for which publications followed, I have indicated in detail my role in the work;

(vi) this dissertation is primarily a collection of material, prepared by myself, published as journal articles or presented as a poster and oral presentations at conferences. In some cases, additional material has been included;

(vii) this dissertation does not contain text, graphics or tables copied and pasted from the Internet, unless specifically acknowledged, and the source being detailed in the dissertation and in the References sections.

Signed: Jesamine J. Rikisahedew

Email: 211508867@stu.ukzn.ac.za

Date: 5 December 2018

ABSTRACT

Plants have been used as ethnomedicine for millennia. In recent years, there has been an upward surge of interest in the use of plants as medicine due to the interest in drugs with fewer side effects as well as the fight against antibiotic resistance. This study is based on *Tagetes minuta*, an aromatic essential herb that is cultivated for its high percentage essential oils which have been used in the treatment of various ailments. In addition, *T. minuta* contains a myriad of secondary metabolites that serve in numerous industrial and clinical applications. The aim of this study was to characterise the foliar structures responsible for the production, storage, and exudation of these useful compounds, as well as to examine the chemical constituents of the crude organic solvents derived from the leaves of *T. minuta*. The potential for green synthesis of silver nanoparticles from the crude methanolic extract and its potential as an antibacterial was also determined. Stereomicroscopy and scanning electron microscopy revealed the presence of uniseriate non-glandular trichomes on the foliar surfaces, as well as large pellucid secretory cavities. Histochemical analyses on the non-glandular trichomes showed that they are capable of storing various bioactive compounds, which is a novel discovery for this species. The development of the subdermal secretory cavities show that the cells undergo autolysis in order to form a schizolysigenous cavity in mature leaves, which was revealed using light microscopy. The ultrastructure of the secretory epithelium within the secretory cavity was analysed using transmission electron microscopy, which displayed the changes of the plastids to contain lipid molecules as well as an increase in vesicles indicating the presence of essential oils. Phytochemical analysis on the crude organic solvents derived from the leaves of *T. minuta* revealed the presence of alkaloids, sterols, saponins, terpenoids, phenols, and lipids. Gas-chromatography mass-spectrometry was carried out to reveal that the constituents with the highest percentage were 9-octadecen-1-ol (4.51 %), β -sitosterol (6.07 %), olean-12-en-3-one (7.47 %), and 3-methyl-1-butanol (14.77 %), all of which cause bacterial growth inhibition, as well as showing acaricidal activity, and anticancer properties in studies focussed on clinical applications. Silver nanoparticles were successfully synthesised from the methanolic leaf extract, which was confirmed using UV-visible spectroscopy and energy dispersive x-ray analysis. UV-visible spectrum of synthesised silver nanoparticles showed maximum peak at 442 nm, and

transmission electron microscopy revealed the silver nanoparticles to be spherical in shape, ranging from 10 to 50 nm in diameter. Preliminary antimicrobial activity was determined using the agar well diffusion method, which showed growth inhibition against *E. coli*, *S. aureus*, methicillin-resistant *S. aureus*, *B. subtilis* and *P. aeruginosa*. This study has shown that *T. minuta* contains numerous bioactive compounds that have pharmacological and medicinal uses, as well as characterising the non-glandular trichomes present on the adaxial and abaxial leaves for the first time. The synthesis of silver nanoparticles from the methanolic extract of *T. minuta* in this study is novel, and shows promise for cheaper, more effective, and less risky nanotechnological applications.

PUBLICATIONS AND CONFERENCE CONTRIBUTIONS FROM THIS THESIS

Details of contribution to publications that form part and/or include research presented in this dissertation:

Publication 1: Rikisahedew, J.J. and Naidoo, Y., 2018. Phyto-histochemical evaluation and characterisation of the foliar structures of *Tagetes minuta* L. (Asteraceae). South African Journal of Botany 115, 328–329.

Author contributions: The candidate carried out experimental research, captured all research data, interpreted results and formulated the discussion, completed the abstract, and presented research outcomes during an oral and poster presentation.

Presentation 1: Rikisahedew, J.J. and Naidoo, Y., 2018. Phyto-histochemical evaluation and characterisation of the foliar structures of *Tagetes minuta* L. (Asteraceae). South African Journal of Botany 115, 328–329. 44th Annual Conference of the South African Association of Botanists, Pretoria, South Africa. Oral and poster presentation.

ACKNOWLEDGEMENTS

This work would not have been possible without the National Research Foundation (NRF), who supported this dissertation financially. I also acknowledge the University of KwaZulu-Natal (UKZN) Westville campus, for allowing the use of facilities and resources needed for this project.

I am indebted to my supervisors, Prof Yougasphree Naidoo and Prof Yasser H. Dewir, for their useful comments, remarks and engagement through the learning process of this Master's dissertation. Thank you for maintaining an open-door policy that always made me feel welcome.

To the colleagues and friends that I have made in my years spent in office 05-074, thank you for offering assistance without hesitation, hours of enlightening discourse, and many weekends of fun. You have become my work family.

Thank you to the staff at the Microscopy and Microanalysis Unit (MMU) at the UKZN Westville campus, particularly Mr Vishal Bharuth and Mr Subashen Naidu, for always being willing to assist with my research and providing the support and necessary facilities. In addition, thank you to Prof Lin for allowing me the use of his microbiology lab, without which this project would remain incomplete.

To my younger siblings, thank you for giving me the motivation and drive to aim higher.

I owe the greatest thanks to my partner, Caveshen Rajman, for his never-faltering support through this difficult but rewarding journey. I don't often get to express my gratitude to you. You have always been my primary motivator.

I wish to dedicate this dissertation to my late mother, Gonasagree Pillay, whose memory has inspired every achievement I have ever made.

TABLE OF CONTENTS

PREFACE.....	i
DECLARATION: PLAGIARISM	ii
ABSTRACT	iii
PUBLICATIONS AND CONFERENCE CONTRIBUTIONS FROM THIS THESIS ..	v
ACKNOWLEDGEMENTS	vi
TABLE OF CONTENTS	vii
LIST OF TABLES	ix
LIST OF FIGURES	x
LIST OF ABBREVIATIONS	xii
CHAPTER 1: INTRODUCTION.....	1
1.1 Traditional medicine	1
1.2 Botanical description of <i>Tagetes minuta</i> L.	2
1.3 Rationale of the study	5
1.4 Aims and Objectives:.....	5
CHAPTER 2: LITERATURE REVIEW.....	7
2.1 Introduction.....	7
2.2 Asteraceae family and the <i>Tagetes</i> genus	8
2.3 The genus <i>Tagetes</i>	9
2.4 Phytochemical studies on <i>Tagetes minuta</i>	11
2.5 Trichome types and functions.....	15
2.6 Secretory cavities	21
CHAPTER 3: FOLIAR STRUCTURES AND HISTOCHEMICAL ANALYSES OF <i>TAGETES MINUTA</i> L. LEAVES	23
3.1 Abstract.....	23

3.2 Introduction.....	24
3.2 Methods and Materials.....	26
3.3 Results and Discussion	30
3.8 Conclusion	49
CHAPTER 4: PHYTOCHEMICAL ANALYSES AND ANTIBACTERIAL POTENTIAL OF <i>TAGETES MINUTA</i> L.	50
4.1 Abstract.....	50
4.2 Introduction.....	51
4.3 Methods and Materials.....	53
4.4 Results and Discussion	57
4.5 Conclusion	62
CHAPTER 5: GREEN SYNTHESIS OF SILVER NANOPARTICLES FROM <i>TAGETES MINUTA</i> L. AND ITS ANTIBACTERIAL POTENTIAL.....	64
5.1 Abstract.....	64
5.2 Introduction.....	65
5.3 Methods and Materials.....	67
5.4 Results and Discussion	70
5.5 Conclusion	77
CHAPTER 6: GENERAL CONCLUSIONS AND RECOMMENDATIONS FOR FURTHER RESEARCH	78
6.1 Main findings	78
6.2 Future recommendations.....	79
CHAPTER 7: REFERENCES.....	80
APPENDIX A - Table A 1:	99
APPENDIX A - Table A 2:	100
APPENDIX B – Antibacterial activity	101

LIST OF TABLES

CHAPTER 4

Table 4. 1 : Preliminary phytochemical analysis of the crude leaf extracts of <i>Tagetes minuta</i>	59
Table 4. 2 : Phytochemical compounds with % peak area >1 in the methanolic extract of <i>T. minuta</i> by GC-MS.	61
Table 4. 3: Preliminary screening of antibacterial activity of silver nanoparticles derived from leaves of <i>T. minuta</i>	62

CHAPTER 5

Table 5. 1 : Preliminary screening of antibacterial activity of silver nanoparticles derived from leaves of <i>T. minuta</i>	76
---	----

LIST OF FIGURES

CHAPTER 1

- Figure 1. 1** Vegetative growth and flowers of *Tagetes minuta*..... 4
- Figure 1. 2** Worldwide distribution of *Tagetes minuta*. 4

CHAPTER 2

- Figure 2. 1** Chemical structures of constituents most abundant in the essential oil of *Tagetes minuta*..... 14
- Figure 2. 2** Non-glandular trichomes types of Asteraceae. 18
- Figure 2. 3** Multicellular non-glandular trichomes types of Asteraceae. 20
- Figure 2. 4** Secretory cavity types: intercellular spaces. 22

CHAPTER 3

- Figure 3. 1** Vegetative growth and flowers of *Tagetes minuta* at the University of Kwazulu-Natal Westville campus. 30
- Figure 3. 2** Stereomicrographs of the leaves of *Tagetes minuta*..... 32
- Figure 3. 3** Secretory cavities of *Tagetes minuta*. 35
- Figure 3. 4** Scanning electron micrographs of the non-glandular trichomes on the adaxial surface of young leaves of *Tagetes minuta*. 36
- Figure 3. 5** Single non-glandular trichomes of *Tagetes minuta*..... 38
- Figure 3. 6** Mites on the surface of *Tagetes minuta* (*Tyedeidae*). 40
- Figure 3. 7** Development of the secretory cavity in *Tagetes minuta*. 43
- Figure 3. 8** Development of non-glandular trichome. 44

Figure 3. 9 Histochemical observations on the non-glandular trichomes of <i>Tagetes minuta</i> : a) Coomassie Blue. b) Wagner’s reagent. c) Ruthenium red. d) Nile Blue. e) Sudan III and IV. f) Acridine orange. g) Phloroglucinol. h) Ferric chloride. i) Autofluorescence.....	45
Figure 3. 10 Electron micrographs of plastids in leaves of <i>Tagetes minuta</i>	47
Figure 3. 11 Electron micrograph of cells within the oil complex	48

CHAPTER 4

Figure 4. 1 GC-MS chromatogram of crude methanolic extract of <i>T. minuta</i> leaves ..	60
---	----

CHAPTER 5

Figure 5. 1 Photographs of silver nanoparticle synthesis using <i>T.minuta</i> extract from leaves.....	71
Figure 5. 2 UV-Vis absorption spectra of reduction of silver ions to silver nanoparticles after 30 min reaction.....	71
Figure 5. 3 HR-TEM images of silver nanoparticles in low and high magnification. ..	72
Figure 5. 4 Frequency histogram for silver nanoparticle size range.....	73
Figure 5. 5 EDX spectrum of synthesised silver nanoparticles using leaf extract of <i>T. minuta</i>	74
Figure 5. 6 FTIR spectrum of the synthesised silver nanoparticles.....	75

LIST OF ABBREVIATIONS

AgNP	Silver nanoparticles
Chl	Chloroplast
EDX	Energy dispersive X-ray
EL	Epidermal layer
EO	Essential oil
FEGSEM	Field emission scanning electron microscopy
FTIR	Fourier transform infrared spectroscopy
GC-MS	Gas-chromatography mass-spectrometry
Li	Lipid
M	Mitochondria
NGT	Non-glandular trichomes
Pg	Plastoglobuli
PS	Parenchymal sheath
S	Starch granules
SC	Secretory cavity
SE	Secretory epithelium
SEM	Scanning electron microscopy
SP	Secretory product
SPR	Surface plasmon resonance
TEM	Transmission electron microscopy
UV-Vis	UV-visible spectrometry
Ve	Vesicle

CHAPTER 1: INTRODUCTION

1.1 Traditional medicine

South Africa is recognised as being one of the most ecologically biodiverse countries in the world. It is home to approximately twenty-four thousand plant species, of which ten thousand are endemic (Algotsson, 2009). The economic growth of South Africa's population is heavily reliant on the biodiversity of the country in the form of local agriculture, recreational wellbeing and entrepreneurship (Street and Prinsloo, 2013).

Traditional medicine is firmly rooted in the culture and history of many communities around the world. Many of these practices have gained popularity as sources of alternative and complementary medicines such as Ayurveda, Chinese herbal medicines, and traditional African medicines (Fabricant and Farnsworth, 2001). Since the early 2000s, traditional medicine has been a fast-flourishing market due to the growing emphasis on healthy living and concerns over the side effects of mainstream drugs. Contemporary medicine is constantly searching for new treatments as several antibiotics and other life-saving drugs have been rendered ineffective due to the rise in drug resistance (Zuber and Takala-Harrison, 2018). New drugs can take years in research and development before being released to the public for use. This has contributed to the upward rise in the use of traditional medicines worldwide. Recent examples of this are the uses of various plants in the treatment of malaria and tuberculosis (Ngarivhume et al., 2015; Madikizela et al., 2017).

In many developing countries, traditional healthcare plays a vital role in meeting the primary healthcare needs of their populations. Through centuries of refinement, herbal remedies are prepared based on the plant being utilised and what condition is being treated. These methods include infusions, macerations, tinctures, and inhalation of powdered plant material (Nafiu et al., 2017).

Traditional medicine in South Africa is referred to as '*Umuthi*' and has become an increasingly popular industry. Rural poverty and weak healthcare systems are the driving forces for approximately 60-80% of South Africans who rely on traditional medicine for

an array of ailments (Mander et al., 2007). This industry continues to flourish due to the country's rich plant biodiversity which boasts at least four thousand indigenous ethnobotanically-significant species (Van Wyk et al., 2009). Researchers are actively exploring the 'Umuthi' markets for botanical resources that yield bioactive compounds which could be medicinally beneficial.

1.2 Botanical description of *Tagetes minuta* L.

Tagetes minuta is an aromatic essential plant with a broad spectrum of biological activities among which are medicinal, antioxidant and antibacterial properties (Shirazi et al., 2014). It has been reported in literature that *T. minuta* produces highly volatile essential oils that are widely used in the cosmetic and perfumery industries, as flavouring agents in food and beverages, as well as a natural herbal medicine (Vasudevan et al., 1997).

The genus *Tagetes* belongs to the Asteraceae family, of which *T. minuta* is an herbaceous plant that produces composite flowers in the rainy season. A synonym of *T. minuta* is *T. glandulifera* Schrank. The species' name of *T. minuta* is derived from the Latin word 'minute' meaning small in reference to the size of the capitula. It is a weed of late summer that disappears at the beginning of the colder seasons after the completion of its life cycle (Chamorro et al., 2008). This species is indigenous to South America and Mexico (common name: Mexican marigold) but has become naturalised in South Africa (common names: Khakibos, Unukani, Mbanje) since the Spanish colonisation. This plant grows best on soil with good drainage and grows up to 1.5 metres high. It is commonly used in the agricultural industry as the roots secretions are known to deter weeds from growing in its nearby vicinity.

Tagetes minuta is a widely distributed plant in South Africa and is used for different purposes in different regions of the country. It has been used for the treatment of headaches, body pain and epilepsy by either smelling the strong scent, chewing the leaves or rubbing a paste made of the herb on the affected part, e.g. head, joints (Igwaran et al., 2017; Karimian et al., 2014; Kyarimpa et al., 2014; Vasudevan et al., 1997). The plant's essential oil has also been used in the control of *Rhipicephalus microplus* (common tick)

in cattle by reducing the spread via the halt in the tick reproduction cycle (Andreotti et al., 2013). This indicates that the plant has a strong acaricidal activity and thus has promise as an insecticide as well. Solvent extractions from other species in this genus have also been shown to have promising anticancer properties (Gakuubi et al., 2016; Kashif et al., 2015).



Figure 1. 1 Vegetative growth and flowers of *Tagetes minuta*. **a)** Mature plant growing alongside a verge at the University of KwaZulu-Natal (Westville campus), **b)** Fully expanded mature pinnatisect leaves **c)** Tubular flowers of *T. minuta*.

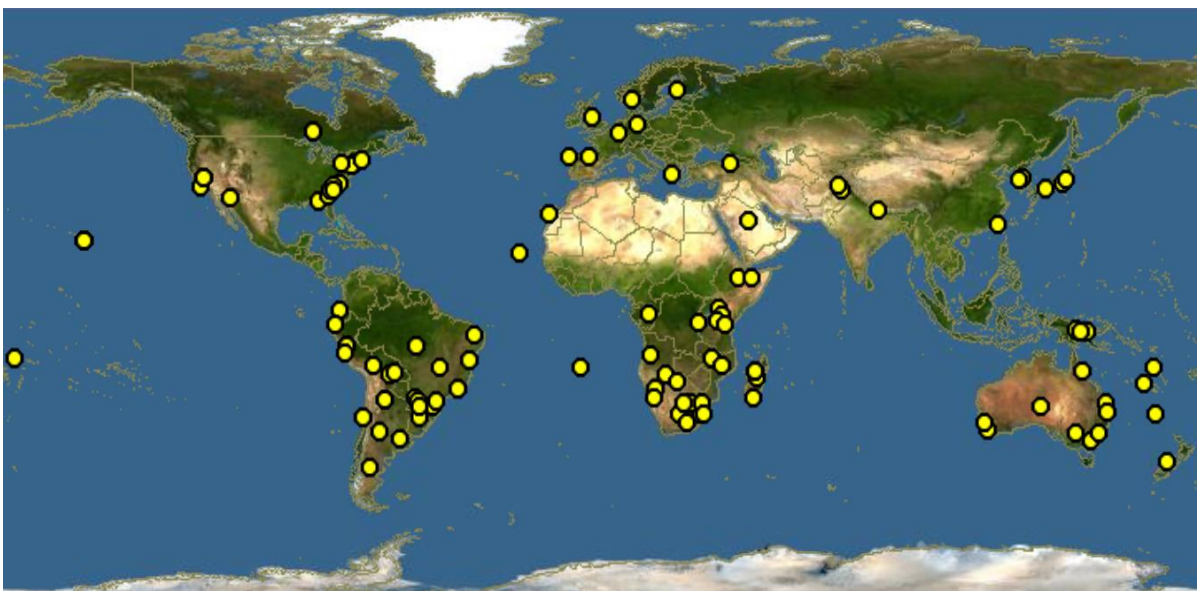


Figure 1. 2 Worldwide distribution of *Tagetes minuta*, image adapted from Global Biodiversity Information Facility webpage. (Source: <http://www.discoverlife.org> accessed on 23/08/18)

1.3 Rationale of the study

The active constituents of medicinal plant extracts have been shown to treat various ailments and diseases that can lead to the development of novel and more cost-effective treatments. *Tagetes minuta* has been examined for its phytochemical properties (Arora et al., 2015; Shahzadi and Shah, 2015; Gakuubi et al., 2016) and its essential oils have been used to treat malaria vectors and some types of cancer (Ibrahim and Mohamed, 2017; Kimutai et al., 2017; Kyarimpa et al., 2014).

In South Africa, *T. minuta* is listed as an invasive species (SANBI, 2015). However, there are beneficial uses for its phytochemicals, indicating the potential use of *T. minuta* as an underutilised minor crop. Scarce research was conducted on the foliar micromorphology and ultrastructure of this species as well as no description of the mode by which the various phytochemicals are secreted. This project describes and reviews the micromorphology of the adaxial and abaxial surfaces of emergent, young, and mature leaves to identify and determine trichome density, subdermal secretory structures, as well as to analyse the histo-phytochemical properties of phytochemicals in *T. minuta*.

Trichome morphological attributes have additionally been key qualities in plant taxonomic investigations. The morphology of trichomes, chemical nature of the secretory products, and how the secretory products are exuded are vital aspects that need to be addressed. In addition, the methanolic extract from the leaves of *T. minuta* was used in the screening of preliminary antibacterial activity as well as determining the potential for green synthesis of silver nanoparticles.

1.4 Aims and Objectives:

The aims and objectives of this study as per chapter are outlined below:

Chapter 3:

Aim: Examine and describe the foliar structures and secretory cavities of *T. minuta* using various microscopy techniques.

Objective 3.1: Employ the use of stereomicroscopy and scanning electron microscopy to image and describe the foliar surface structures such as trichomes, secretory cavities and stomata of the leaves.

Objective 3.2: Describe the internal cellular organelles and components of the cells within the secretory cavities of the leaves.

Objective 3.3: Reveal the internal structures of trichomes with regard to phytochemical classes using histochemical staining techniques.

Chapter 4:

Aim: Elucidate the location and composition of the phytochemicals of the leaves of *T. minuta* using a variety of histochemical and phytochemical analyses.

Objective 4.1: Investigate the various compound classes present in the crude organic solvent extracts of the leaves using phytochemical tests.

Objective 4.2: Elucidate the chemical constituents of the crude methanolic extract using GC-MS.

Objective 4.3: Determine the antibacterial potential of the methanolic extract against gram positive and gram negative bacteria.

Chapter 5:

Aim: Determine the potential for green synthesis of silver nanoparticles using the methanolic extract of *T. minuta* as well as screen for antibacterial activity.

Objective 5.1: To produce silver nanoparticles derived from the crude methanolic extract using green synthesis techniques.

Objective 5.2: To screen for antibacterial activity of the synthesised silver nanoparticles against selected gram positive and gram negative bacteria.

CHAPTER 2: LITERATURE REVIEW

2.1 Introduction

Traditional medicines refer to plant materials that are used for curative, preventative, or rehabilitative treatment in accordance with traditional or cultural principles (Cunningham, 1990). In many developing countries, where traditional medicine is the only form of therapy, it fulfils the function of primary healthcare (Dauskardt, 1990; Bisi-Johnson et al., 2017). Due to its potential in treating various ailments and diseases naturally and effectively, this sector continues to grow worldwide (Nair and Chanda, 2007). The biological screening and isolation of bioactive compounds from medicinal plants is the most common source of drug discovery and have resulted in the production of many clinically used medicines (Balunas and Kinghorn, 2005). Pharmacognosy is the chemical study of the natural products from herbal sources (Cardellina, 2002).

The high quantities of extractable organic substances plants produce such as essential oils, tannins, saponins, rubber, and dyes are economically viable as raw materials for various scientific and commercial applications (Balandrin et al., 1985). The secondary metabolites have little bearing in the primary metabolism of the plant, but serve ecological roles as pollinator attractants, chemical defences against insects and other predators, and as chemical adaptors to environmental stresses (War et al., 2012). These metabolites tend to be synthesised at specific developmental stages of the plant's growth, and are produced, stored, and liberated from specialised cell types on and within the plant's organs (Werker, 2000).

Secretory structures in plants include trichomes, mucilage ducts, hydathodes, nectaries, and laticifers (Fahn, 2000). These structures are specialised cell formations that are responsible for the production of secondary metabolites that protect the plant from numerous biotic and abiotic stressors (Werker, 2000). The morphoanatomical and phytochemical analyses of these structures enable the understanding of how useful bioactive compounds are produced, and how they can be utilised efficiently for medicinal and pharmacological applications.

2.2 Asteraceae family and the *Tagetes* genus

The Asteraceae family (syn. Compositae) is named for the Greek word ἀστήρ which means ‘star’, in reference to composite star-like form of inflorescence. With approximately 20000 species and 1300 genera, it is the largest family of flowering plants (Bremer, 1987; Adedeji and Jewoola, 2008). Three subfamilies are recognized in Asteraceae, namely the Asteroideae, the Cichorioideae (syn. Lactucoideae), and the Barnadesioideae (Bremer et al. 1992). The family has a worldwide distribution, colonising a wide variety of habitats, but are most common in semi-arid and arid regions of the subtropics (Achika et al., 2014). Many species of Asteraceae have been deliberately introduced to countries worldwide for medicinal use, food, and horticulture – making it an economically vital family (Barkley et al., 2006).

Most Asteraceae species are known to have foliar structures known as trichomes and/or secretory cavities that enable the production of chemical compounds, often in the form of essential oils (Venkatachalam et al., 1984). Trichomes are appendages that resemble small hairs and are found on the surface of leaves, stems, and sepals (Werker, 2000). They vary in structure, size and function. Non-glandular trichomes serve to protect the plant against herbivores and pathogens, whilst decreasing damage caused by UV-B rays and can act as an insecticide (Adebooye et al., 2012) whereas glandular trichomes accumulate and secrete essential oils that characterise the plant as aromatic and can also be used therapeutically (Wagner, 1991). Secretory structures manifest a high degree of morphological diversity and are fairly common in Asteraceae species. The secretory cavities of species found in the Asteraceae family is well-documented in those plants that are cultivated and harvested for their essential oils and similar bioproducts (Werker et al., 1994; Monteiro et al., 1999; Milan et al., 2006; Lizarraga et al., 2017; Filartiga et al., 2017; Bezerra et al., 2018).

2.3 The genus *Tagetes*

Tagetes minuta L. is an annual aromatic herb from the Asteraceae family. The taxonomical grouping for this plant is among the largest, with approximately 1000 genera and more than 23000 species (Sadia et al., 2013). The genus *Tagetes* comprises 56 species (Bandana et al., 2018). The most common *Tagetes* species include *T. minuta*, *T. erecta*, *T. patula*, and *T. tenuifolia*. *Tagetes minuta* is the most widely studied plant from this genus due to its high-grade percentage of essential oil that has versatile uses in the perfume, food, and ethnomedicinal industries (Singh et al., 2003).

Taxonomic classification of *Tagetes minuta* L. (Bandana et al., 2018):

Kingdom	:	Plantae
Subkingdom	:	Viridiplantae
Infrakingdom	:	Streptophyta
Superdivision	:	Embryophyta
Division	:	Tracheophyta
Class	:	Magnoliopsida
Superorder	:	Asteranae
Order	:	Asterales
Family	:	Asteraceae
Genus	:	<i>Tagetes</i>
Species	:	<i>Tagetes minuta</i> L.

Common and local names of *Tagetes minuta* L. (Qureshi et al., 2007; SANBI, 2015)

English	:	wild marigold, stinking Roger, Mexican marigold, Muster John Henry
India	:	Jungli gainda
Spain	:	huacatay, enana
Angola	:	ekaibulo

Brazil	:	chinchilla, coora, cravo de mato, rabo de rajao, suique
Chile	:	quinchihue
Germany	:	wild sammetblume
Kenya	:	ang'we, mubangi, nyanjaga, omotioku
Madagascar	:	mavoadala
Portugal	:	cravo de defuncto
Paraguay	:	agosto, suico
South Africa	:	khakibos, kleinafrikander, mbanje, insangwana, unukani

Synonyms of *Tagetes minuta* include *T. bonariensis* Pers., *T. glandulifera* Schrank, *T. glandulosa* Link, *T. montana* (Hort) DC., and *T. porphyllum* Vell (Maheshwari, 1972; Bandana, 2018). The species name of *T. minuta* is derived from the Latin word 'minutes' meaning small, in reference to the size of the capitula. It is a weed of spring and it disappears at the start of winter after completion of its life cycle (Chamorro et al., 2008). This species is indigenous to South America and Mexico (common name: Mexican marigold) but has become naturalised in South Africa since the Spanish colonisation. *Tagetes minuta* grows best on soil with good drainage and grows up to two metres high. This plant is commonly used in the agricultural industry, as the root secretions are known to deter weeds from growing in its nearby vicinity.

Tagetes minuta is known as an aromatic essential plant that exhibits rich natural product chemistry. It produces highly volatile essential oils that are widely used in the cosmetic, perfumery and food industries, as well as being used as ethnomedicine (Vasudevan et al., 1997). This plant is widely distributed in South Africa and is used for different purposes in different regions of the country. It has been documented in literature that it is used for treatment of headaches, body pain, and epilepsy by either smelling the strong scent or chewing the leaves or rubbing a paste made of the herb on the affected part, e.g. head, joints. Several papers have documented the medicinal use of extracts of *T. minuta* (Vasudevan et al., 1997; Kyarimpa et al., 2014), which report high levels of effectiveness.

2.4 Phytochemical studies on *Tagetes minuta*

Phytochemical screening of medicinal plants enables the development of novel therapeutic compounds with an improved efficacy to address variable health-related issues.

Tagetes minuta is cultivated primarily due to its richness in essential oil, which is present in all organs except the stem (Singh et al., 2003). In addition to the essential oil, *T. minuta* also produces various secondary metabolite compounds including monoterpenes, sesquiterpenes, flavonoids, aromatics, and thiophenes (Singh et al., 1995; Lawrence, 1996; Bansal et al., 1999; Brene et al., 2009; Sadia et al., 2013).

The major components of *T. minuta* oil are (*Z*)- β -ocimene, hydrocarbons (limonene), acyclic unsaturated monoterpenoids, ketones, dihydrotagetone, tagetones (*E*, *Z*), and ocimenones (*E*, *Z*) (Kyarimpa et al., 2014; Tiwari et al., 2016; Igwaran et al., 2017).

Meshkalasadat et al. (2010) characterised the volatile components of *T. minuta* cultivated in Iran using nano-scale injection. Their study indicated that the essential oil is rich in monoterpene hydrocarbons (28.3%), oxygenated monoterpenes (45.2%), sesquiterpene hydrocarbons (2.5%), oxygenated sesquiterpenes (3.7%), diterpenes (0.6%), and other compounds (17.2%).

The variation in essential oil content and composition of *T. minuta* in North India was studied by Tiwari et al. (2016) using gas chromatography-mass spectrometry (GC-MS) and gas chromatography with flame-ionization detector (GC-FID) for analysis. The essential oil content varied from 0.52 to 0.78% in the different growth stages of the crop (flower initiation, full flowering, late flowering, and seed setting stages). The main constituent of the essential oil was found to be monoterpenoids (80.5-92.9%).

In Argentina, Gil et al. (2002) studied three wild accessions of *T. minuta* for the composition of thiophenes and concluded that there were only quantitative differences. The major constituents of the essential oil were dihydrotagetone, α -phellandrene, limonene, *o*-cymene, β -ocimene, and tagetenone.

In South Africa, Mohammad et al. (2010) showed that the main components of the essential oil were β -ocimene (32.0%), and dihydrotagetone (16.4%); while Igwaran et al.

(2017) used GC-MS analyses to determine the main compounds to be β -ocimene (14.4%), m-tert-butyl-phenol (9.41%), 2,6-dimethyl-, (E)-5,7-octadien-4-one (7.14%), hydro-methyl-naphthalene (5.58%) and spathulenol (4.56%).

Tankeu et al. (2013) reported chemotypic variation of the *T. minuta* essential oil extracted from South African plants, revealing two major chemotypes – (E)-tagetone, dihydrotagetone, and (Z)-tagetone as the characteristic marker constituents for Chemotype 1; while (Z)- β -ocimene, (E)-ocimenone, and (Z)-ocimenone characterised Chemotype 2. This supplements the findings of Senatore et al. (2004), which also identified two chemotypes for this species. One chemotype is characterised by a higher content of tagetones in samples from the United Kingdom, and higher content of ocimenes and ocimenones in samples taken from South Africa and Egypt.

In 2014, Al-Musayeib et al. isolated nine compounds and identified two of them to be novel compounds (5-methyl-2,2',5',2'',5'',2''',5''',2''''-quinquethiophene and quercetagetin-6-O-(6-O-caffeoyl- β -d-glucopyranoside) from the methanolic extract of *Tagetes minuta*, which shows significant antioxidant activity.

Lizarraga et al. (2017) analysed the chemical composition of the essential oils of *T. minuta* and *T. terniflora*. They deduced that the oil of *T. minuta* was characterised mainly by high percentages of tagetone (56.2%) and cis- β -ocimene (19.9%), with lower amounts of dihydrotagetone (10.4%) and limonene (2.4%); whereas *T. terniflora* showed high percentages of tagetones (60.6%) and ocimenones (10.3%).

Ibrahim et al. (2018b) isolated a new compound called 'tagetnoic acid' from the hexane fraction of the leaves of *T. minuta*. This compound has been described as a strong lipoxygenase inhibitor with IC_{50} of 1.17 μ M as compared to the synthetic inhibitor indomethacin (IC_{50} 0.89 μ M). This suggests that the consumption of *T. minuta* leaves may alleviate inflammatory disorders.

Tagetes minuta is both a cultivated crop and an invasive weed, based on the country. This means that the differences in the chemical profile of essential oil can be attributed to both anthropogenic and environmental factors, not limited to:

- (i) method of harvesting
- (ii) geographic location of the plant
- (iii) growth stage of the harvested plants
- (iv) the plant organs used
- (v) climatic conditions of growth

Chemotypes are a result of genotypic \times environmental interactions (Tankeu et al., 2013), which leads to variations in the chemical composition of essential oil from *Tagetes minuta*.

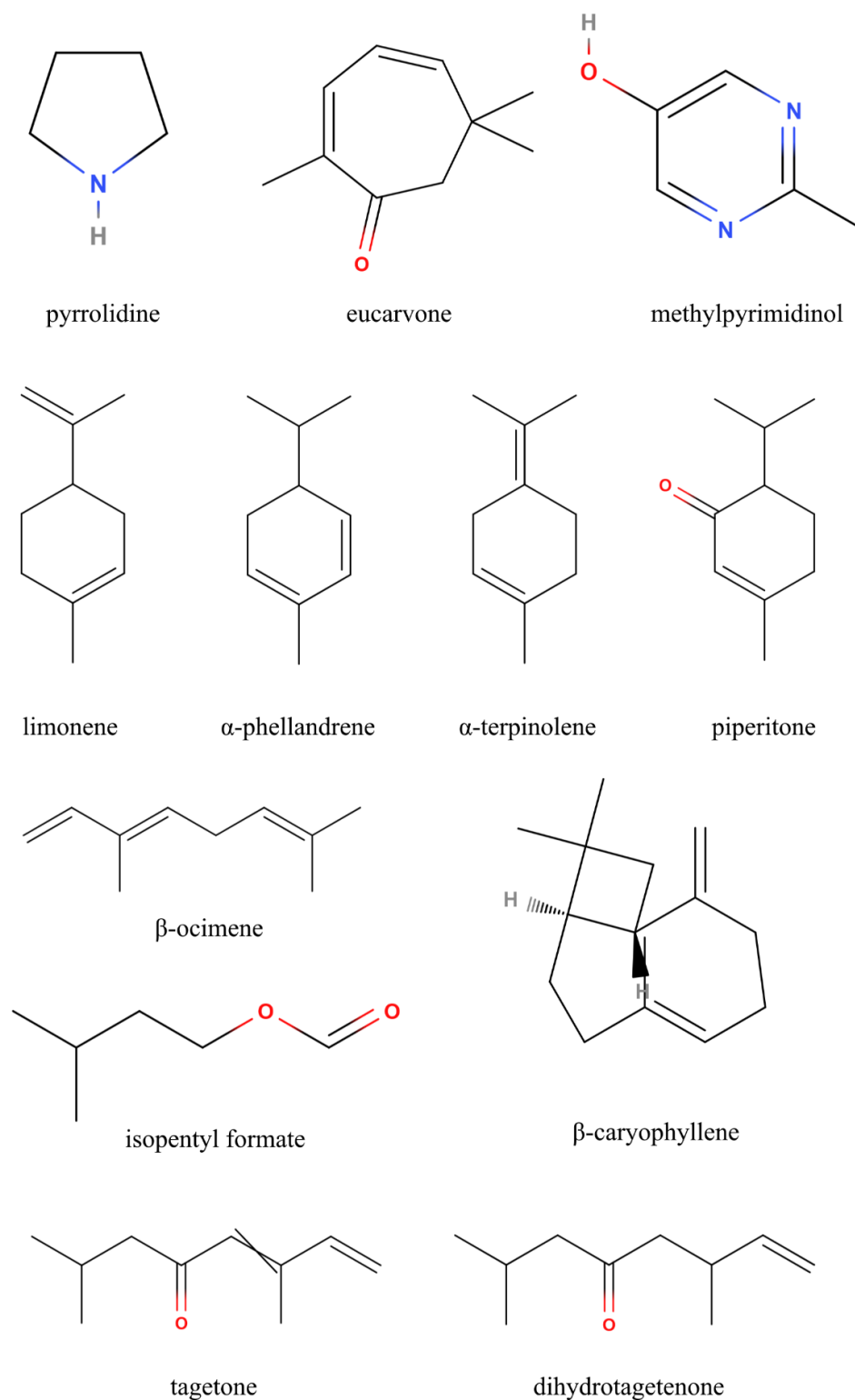


Figure 2. 1 Chemical structures of constituents most abundant in the essential oil of *Tagetes minuta* (Adapted from Sadia et al., 2013; Igwaran et al., Lizarraga et al., 2017).

2.5 Trichome types and functions

Trichomes are epidermal appendages that resemble small hairs on the surfaces of leaves, stems, roots, and flowers of almost all angiosperms (Wagner et al., 2004). They have served roles in the mechanisms of plants to adapt to a range of biotic and abiotic stressors (Levin, 1973; Fahn, 2000; Wagner et al., 2004). Trichomes vary in shape, size, location, and the ability to store and secrete bioactive compounds (Levin, 1973; Wagner, 1991). More than 300 types of plant trichomes have been described (Aschenbrenner et al., 2013). Conventionally, research on trichomes has focused primarily on the metabolic pathways in some types of trichomes (Schilmiller et al., 2008; Spyropoulou et al., 2014); however, studies show that trichomes can act as a defence syndrome against insects that feed on the plant, both mechanically and chemically (Levin, 1973; Wagner et al., 2004). Plants induce the growth of a denser cover of foliar trichomes in response to insect damage, as well as stimulating an increase in secondary metabolites (such as tannins, terpenoids, and alkaloids) that deter predators (Agrawal, 2006; War et al., 2012).

The classification of trichome types has been subjective; however, there are two major categories, glandular (secretory) and non-glandular. As trichomes can be used for taxonomic purposes, these can be subdivided further according to their relative morphological characteristics (Kim et al., 2011). Glandular trichomes are named for their terminal secretory head and ability to produce, sequester, accumulate, and exude specialised secondary metabolites that deter predators by causing the plant to become unpalatable, or secreting substances that attract pollinators (Levin, 1973; Wagner, 1991). Non-glandular trichomes are often called 'simple' trichomes as their functions are mostly aligned with their mechanical properties such as size, shape, and density (Matsuki et al., 2004; Wagner et al., 2004). They may be unicellular, multicellular, or branched and are associated with the texture of the epidermal surface of plants (Adedeji and Jewoola, 2008; Gairola et al., 2008).

Non-glandular trichomes (NGT) form early in the development of plant organs and often senesce shortly before the plant reaches maturity (Wagner et al., 2004). Werker (2000) suggests that dead trichomes on mature plant organs may still serve mechanical functions such as water absorption and abrasion protection. Non-glandular trichomes are most commonly associated with plant defence. Agrawal and Fishbein (2006) demonstrated the

ability of a plant to increase (non-glandular) trichome density as a result of herbivory from caterpillars; however, Wagner et al. (2004) suggest that the increase in NGT density is a precursor to the production of defence phytochemicals. The shape of non-glandular trichomes can give an indication of its mechanical function on the plant – ‘hooked’ trichomes often serve to increase the chances of seed dispersal (given the NGT can be found on the seed coating), and ‘spiked’ trichomes immobilise and impale insects (Levin, 1973).

Brewer et al. (1991) examined the effect of foliar trichomes in 38 plant species on water repellence with the conclusion that plants with leaf trichomes are more water repellent. Sletvold and Agren (2012) identified an increase in trichome production on *Arabidopsis lyrata* to be responsible for an improvement of the plant under drought conditions. In 2016, Mo et al. demonstrated a similar increase of trichome formation for drought-tolerant genotypes of *Citrullus lanatus* as compared to the domesticated, drought-sensitive variants of the watermelon. Gonzales et al. (2008) determined that mechanical damage induced density of glandular trichomes, while non-glandular trichome density increased in experimental drought conditions in *Madia sativa*. These studies exhibit the ability of trichome density to affect and limit water loss by transpiration by increasing the resistance of the leaf-air boundary (Galdon-Armero et al., 2018).

By employing the use of histochemical techniques and electron microscopy, Tozin et al. (2016) demonstrated the ability of non-glandular trichomes from three Lamiaceae and four Verbenaceae species to store bioactive compounds. Based on the understanding that the cells of non-glandular trichomes are metabolically active in the early stages of development (Mayekiso et al., 2008), they were able to exhibit the presence of lipids, terpenes, alkaloids, and phenolic compounds within the cells of non-glandular trichomes from these plants. It is not clear as to whether non-glandular trichomes are capable of the production and liberation of the bioactive compounds they store, but this has been evidenced in plants from the Cistaceae and Apiaceae family (Tattini et al., 2006; Weryszko-Chmielewska and Chwil, 2014, respectively).

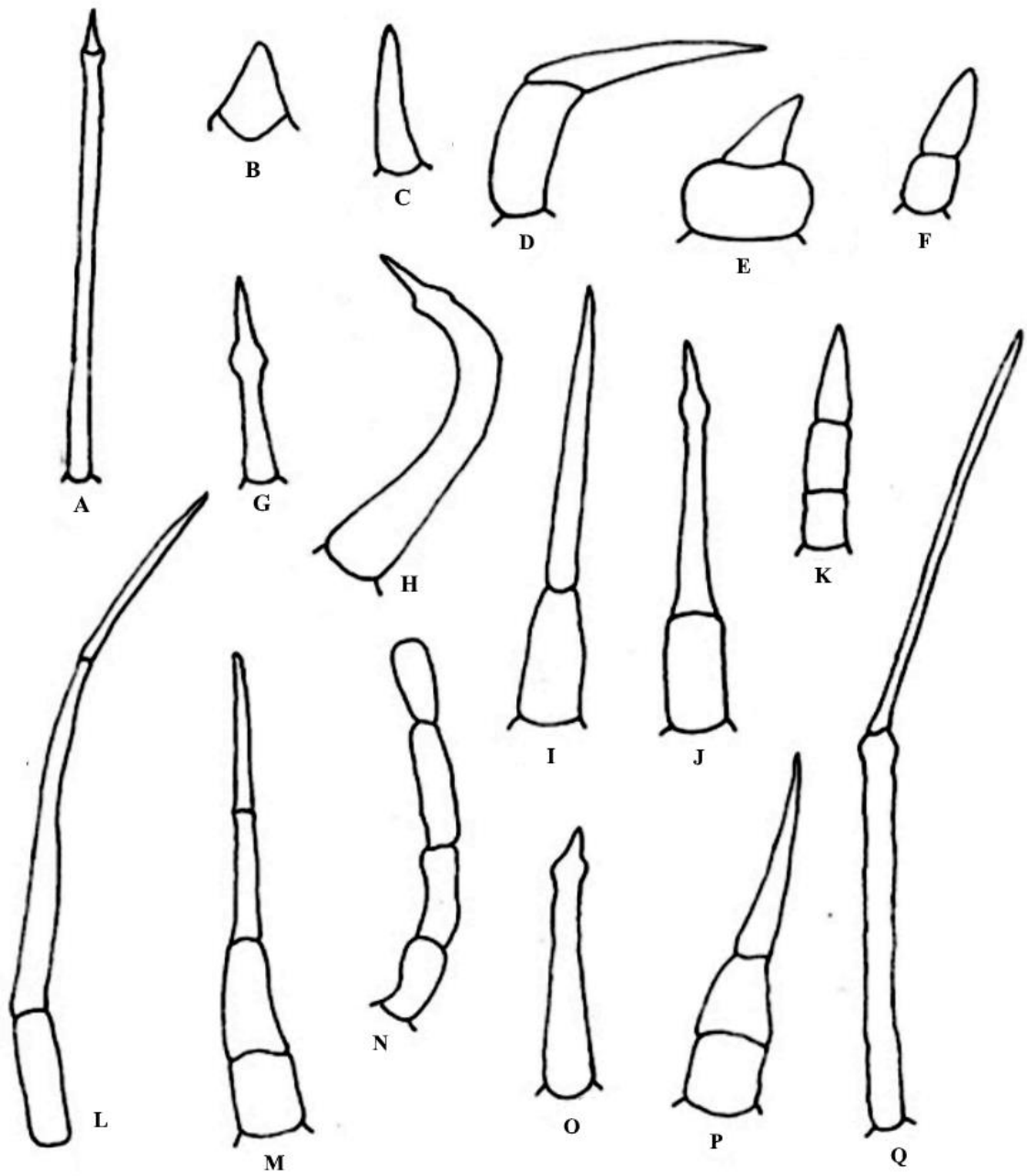


Figure 2. 2 Non-glandular trichomes types of Asteraceae (adapted from Adedeji and Ajewoola, 2008):

- (A) unicellular trichome (narrow)
- (B) unicellular trichome (spine-like)
- (C) unicellular trichome (spike-like)
- (D) bicellular hooked trichome
- (E) bicellular trichome (large basal cell)
- (F) bicellular trichome (normal basal cell)
- (G) unicellular spiked trichome
- (H) unicellular hooked trichome
- (I) bicellular trichome (normal basal cell)
- (J) bicellular trichome (spiked apical cell)
- (K) multicellular trichome (pointed apical cell)
- (L) multicellular trichome (acicular apical cells)
- (M) multicellular trichome (tapered apical cell)
- (N) multicellular trichome (rounded apical cell)
- (O) unicellular trichome (pointed apical cell)
- (P) multicellular trichome (tapered apical cell, normal basal cells)
- (Q) bicellular long trichome (acicular cells)

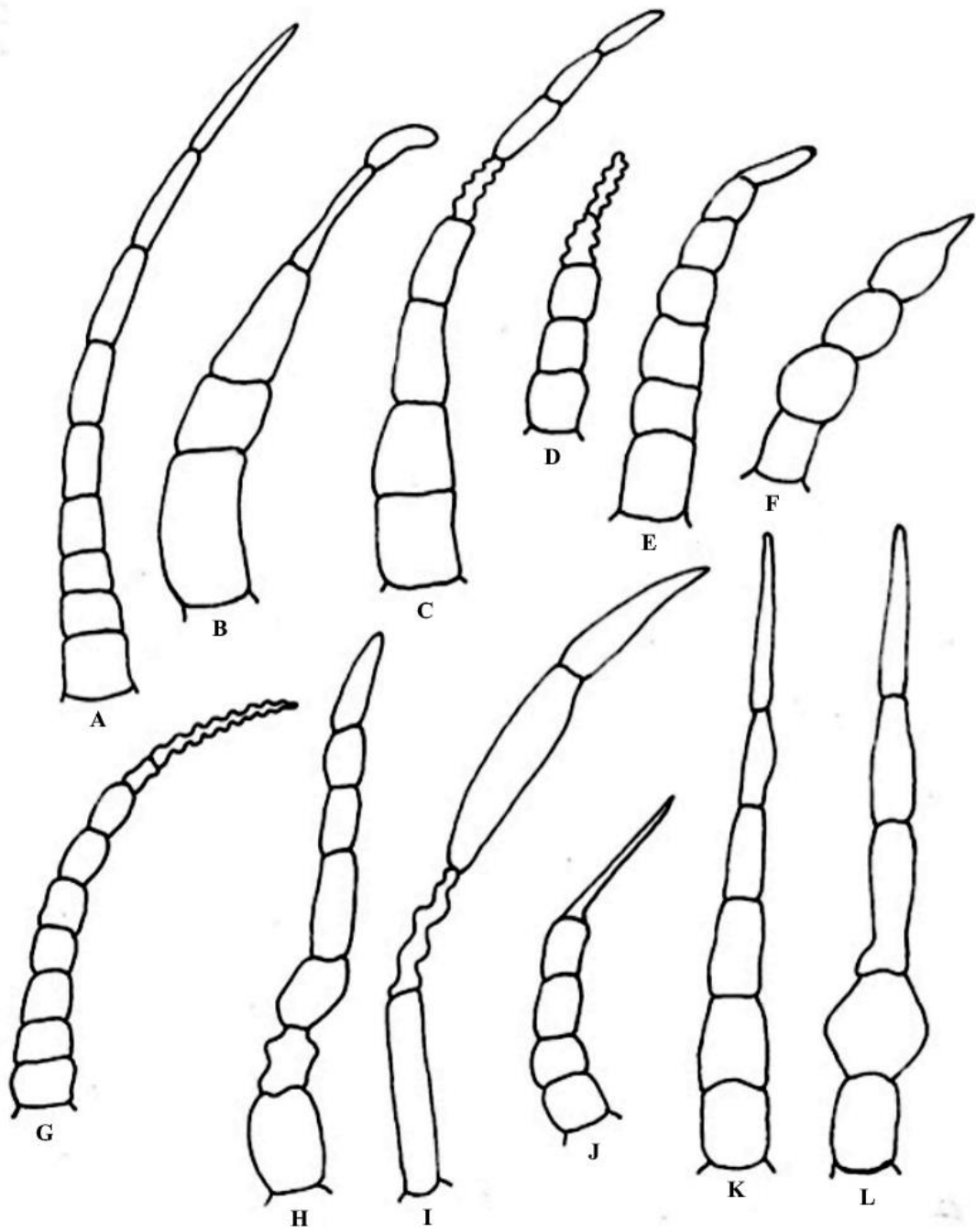


Figure 2. 3 Multicellular non-glandular trichomes types of Asteraceae (adapted from Adedeji and Ajewoola, 2008):

- (A) apex pointed
- (B) apex sickle-shaped
- (C) with one shrivelled cell
- (D) two shrivelled apical cells
- (E) apical cell globular
- (F) apical cell acicular at the end, bulbous cells
- (G) apical cell shrivelled
- (H) one cell slightly shrivelled
- (I) one cell shrivelled
- (J) apical cell acicular
- (K) pointed apical cell
- (L) pointed apical cell (bulbous basal cells)

2.6 Secretory cavities

Plant secretory cavities are glands in plant organs that are made up of specialised glandular cells surrounding a secretion-filled space (Turner et al., 1998). They often contain essential oils, lipids, resins, alkaloids, flavonoids, tannins, or mucilage (Fahn, 1979, Bartoli et al., 2011). There are three primary types of developmental secretory cavities: schizogenous, lysigenous, and schizolysigenous (Turner et al., 1998).

Schizogenous cavities are formed by the separation of a single glandular cell that appears as a distinct intercellular space (lumina) lined by secretory epithelial cells (Tolke et al., 2017). Lysigenous cavities are formed by the disintegration of several cells, whereby the secretory cells degenerate as they release their secretory product into the developing space by a process known as holocrine secretion (Arora and Kumar, 2108). Schizolysigenous cavities form as an amalgamation of the previous two processes: the cavity develops from a single cell, but the epithelial cells on the periphery of the forming gland undergo autolysis in order to enlarge the storage cavity (Turner et al., 1998; Machado et al., 2017).

In the genus *Tagetes*, Sacchetti et al. (2001) showed that the secretory cavities of *T. patula* seedlings were schizogenous as it formed a distinct intercellular canal bordered by endodermal epithelial cells. Using transmission electron microscopy, they were able to demonstrate that the cells on the periphery of the secretory cavity were more electron dense and contained many more osmiophilic vesicles and plastids than its neighbouring parenchymatic cells.

Russin et al. (1992) studied the changes in the chemical composition of the secretory products of *T. erecta* during the development phase until late flowering of the plant. Their results showed that indole comprised almost 99% of the secretory product, which is a metabolite not commonly stored in its free state in vegetative plant organs. More interestingly, the ratio of indole to piperitone varied with plant development and aging. This also served as the first report in *Tagetes* of secretory products existing separately from the lamina tissues, implying that secretory cavities produce as well as store metabolic end products that change in concentrations based on the needs and developmental growth of the plant.

Lopez et al. (2009) and Lizarraga et al. (2017) described the secretory cavities of *T. minuta* as pellucid, elliptic glands (70 – 200 μ m) that are covered by a parenchymal sheath made up of cutinised epithelial cells. Both studies described the secretory cavities as being found along the entire phyllaries. In senescent leaves, the secretory cavity collapses inward due to the fragility of the epithelial cells along its periphery.

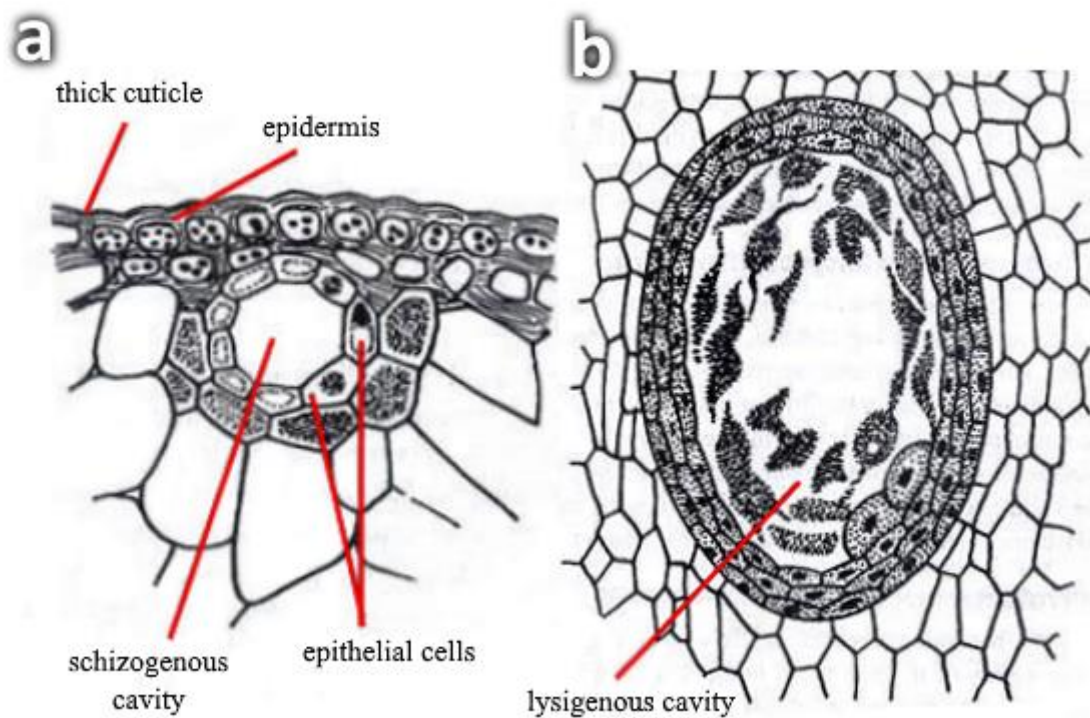


Figure 2. 4 Secretory cavity types: intercellular spaces: a) schizogenous intercellular space in *Bryophyllum* stem. b) lysigenous intercellular space in leaf of *Sequoia sempervirens* (Adapted from Fahn, 2000; Bartoli et al., 2011; Bombo et al., 2017).

CHAPTER 3: FOLIAR STRUCTURES AND HISTOCHEMICAL ANALYSES OF *TAGETES MINUTA* L. LEAVES

3.1 Abstract

Many species in *Tagetes* are known for producing essential oils and commercially useful bioactive compounds. The objective of this study was to investigate the micromorphological features of the internal and external foliar structures of *Tagetes minuta* that produce and store these compounds. This was accomplished using stereomicroscopy, light microscopy, scanning electron microscopy, transmission electron microscopy, and histochemical analyses. The findings show that the trichomes on the surface of *T. minuta* leaves appear to be linear and non-glandular, but still maintains the ability to store various bioactive compounds within as shown by histochemical analyses. The development of the subdermal secretory cavities show that the cells undergo autolysis in order to form a schizolysigenous cavity in mature leaves. Ultrastructure of the parenchymal sheath and secretory epithelium within the secretory cavity show the changes of the plastids to contain lipid and osmiophilic molecules. These findings are novel for *T. minuta* and enable a better understanding of the exudation process in order to optimise essential oil production for industrial applications.

Keywords: histochemistry; non-glandular trichomes; micromorphology; microcopy; secretory cavity

3.2 Introduction

Tagetes minuta is a member of the Asteraceae family, which comprises 1535 genera and approximately 23 000 species and is the largest family of angiosperms (Shen et al., 2018a). Many of these species have substantial medicinal, ornamental, and economic values due to their chemical composition and biological activities (Vidic et al., 2016). *Tagetes minuta* is commonly known as Mexican marigold, and is native to South America. It has since been naturalised in Europe, Asia, North America and Africa since the Spanish colonisation (Meshkatalasadat et al., 2010). This plant has a long history of human use as both food and allopathic medicine (Tereschuk et al., 1997; Scrivanti et al., 2003; Senatore et al., 2004). Infusions and extracts prepared from the leaves of *T. minuta* have been used to treat intestinal diseases, alleviate headaches and symptoms of epilepsy (Igwaran et al., 2017; Vasudevan et al., 1997).

Species belonging to *Tagetes* are characterised by the macroscopic punctate oil glands that are found on the abaxial leaf surfaces, which produce and store '*Tagetes oil*'. This essential oil is marketed due to its medicinal properties and various health benefits (Lopez et al., 2009; Sadia et al., 2013). The secretory cavity, the primary focus of the oil complex in *Tagetes* is relatively well-documented in literature, however, the subject of the foliar trichomes on *T. minuta* is a contentious topic (Lopez et al., 2009; Lizarraga et al., 2017). Trichomes are specialised hair-like epidermal appendages that have been shown to play a role in the plant defence system against biotic threats such as predators as both a physical barrier and by the mediation of chemical defences, as well and abiotic factors such as sunlight in the way of reflecting excess radiation (Valverde et al., 2001; Kariyat et al., 2018). Depending on the plant species, these structures can be found on the leaves, stems, roots, and even seed coats (Levin, 1973). Trichomes can be classified as either glandular or non-glandular based on their shape and function, with the most distinct morphological difference being the absence of a glandular head in the non-glandular trichomes (Werker, 2000). Due to the lack of a glandular head, non-glandular trichomes are considered to act exclusively as mechanical barriers; whereas glandular trichomes are responsible for the storage and/or exudation of biologically active phytochemicals (Levin, 1973; Werker, 2000).

The trichomes of *T. minuta* have been described as both glandular (Cappellari et al., 2013) and non-glandular (Lizarraga et al., 2017) with seemingly no consensus. The purpose of this study was to determine the trichome type and further investigate the secretory cavities of *T. minuta* using stereo- and electron microscopy, as well as elucidate the chemical classes of the phytochemicals stored in its trichomes using histochemical analyses.

3.2 Methods and Materials

3.2.1 Plant collection

Fresh (emergent, young, and mature) leaves of *T. minuta* were collected from a population at the University of KwaZulu-Natal Westville campus located at 29.817°S 30.940°E in Durban, South Africa. A voucher specimen was confirmed and deposited at the UKZN Westville Herbarium (accession number 18216, voucher number 01).

3.2.2 Stereomicroscopy

Both the adaxial and abaxial leaf surfaces at three developmental stages (emergent, young, and mature) were examined using the Nikon AZ100 Stereomicroscope, and images captured with the Nikon DXM 1200C camera using NIS-Elements Software with an emphasis on the foliar structures.

3.2.3 Scanning Electron Microscopy (SEM)

3.2.3.1 Chemical fixation

Fresh leaf material was cut into 3 mm² sections and were fixed in 2.5 % glutaraldehyde for 24 hrs. The sections were subsequently subjected to three washes (5 min each) with 0.1 M sodium phosphate buffer (pH 7.0), followed by post-fixation in 0.5 % osmium tetroxide for 2 hrs. Thereafter, the sections were washed three times for 5 min each with sodium phosphate buffer. The samples were then subjected to graded dehydration series in ethanol (25 %, 50 %, 75 %, and 100 %) for two sessions (5 min each) and two sessions (10 min each) in the 100 % ethanol, and were then critically-point dried using a Quorum K850 Critical Point Dryer. The sections were fixed using carbon conductive tape onto aluminium stubs and sputter-coated with gold using the Polaron SC 500 Sputter Coater. The viewing and imaging were performed using a LEO 1450 SEM at 5 kV and a working distance of 7 – 10 mm.

3.2.3.2 Freeze fracture

Fresh leaves were fractured along the midrib for analysis. The samples were cut into 2 cm² sections for freeze fracture. They were prepared by quenching rapidly in subcooled liquid nitrogen and fractured using forceps. Thereafter the fractured segments were dried using the Edwards-Modulyo freeze dryer at -60°C for 48 hrs in a vacuum of 10⁻² Torr. The fractured segments were mounted onto brass stubs and secured with carbon conductive cement. The samples were sputter-coated with gold using a Polaron SC 500 sputter coater and imaged on a LEO 1450 SEM with a working distance of 12 mm.

3.2.3.3 Cryo-scanning electron microscopy (Cryo-SEM)

Cryo-SEM was performed using a Quorum PP3000T coupled to a Zeiss UltraPlus FEGSEM. Fresh leaf material was cryo-fixed in a liquid nitrogen slush before being transferred to a vacuum chamber held at -135°C. The samples were then fractured, etched, and coated in platinum. The sections were viewed at 2 kV.

3.2.4 Light Microscopy and transmission electron microscopy (TEM)

Leaves from three developmental stages were trimmed to 2 mm² and fixed in 2.5 % glutaraldehyde for 24 hrs. Samples were rinsed three times in 0.1 M sodium phosphate buffer (pH 7.0) and post-fixed in 0.5 % osmium tetroxide for 2 hours. Samples were rinsed thrice in sodium phosphate buffer before undergoing dehydration using a graded series of acetone (25 %, 50 %, 75 %, for two 5-minute sessions, and 100 % for two 10-minute sessions). Propylene was used as a clearing agent, which was used in conjunction with a graded series of Spurr's resin (Spurr, 1969) for infiltration of the leaf tissues at 25 %, 50 %, 75 %, and 100 %, of resin in the propylene solution. Samples were then placed in silicone moulds in whole resin and polymerised at 70°C for 8 hrs.

The sections were cut using a Reichert Jung Ultracut-E ultramicrotome. Semi thin sections (0.5 µm) were used to determine the regions of interest. The survey sections were stained with 1 % toluidine blue and imaged using the Nikon Eclipse 80i light microscope

equipped with a Nikon DS-Fi1 camera and NIS-Elements D imaging software. Ultrathin sections (90 – 120 nm) were collected on copper grids and stained with 2.5 % uranyl acetate and lead citrate. The ultrathin sections were viewed using the JEOL 1010 TEM equipped with an Olympus MegaView III CCD camera and iTEM software.

3.2.5 Histochemical tests

Fresh leaf sections (100 - 120µm) were obtained using an Oxford ® Vibratome Sectioning System, and were stained with the reagents listed below. The purpose of this was to detect and analyse the localisation of specific cellular phytochemicals in the leaf structure. The images were captured on a Nikon Eclipse 80i compound light microscope.

a. Lipids

Nile Blue – The fresh sections were stained with 2 % Nile Blue for 1 minute at 37°C and then transferred to 1 % acetic acid for 1 min. Sections were rinsed with distilled water, mounted, and viewed. Pink staining indicates the presence of neutral lipids such as fats and oils, whereas blue staining indicates the presence of acidic lipids such as phospholipids (Demarco, 2017).

Sudan III/IV – Sections were stained for 10 min before being rinsed in 70 % ethanol and viewed. Tissues that stained red/orange indicates the presence of lipids or cutin (Buda et al., 2009).

b. Lignins

Phloroglucinol – The fresh sections were immersed in phloroglucinol stain for 5 min and rinsed with distilled water. A pink/red colouration indicates the presence of lignins (Jensen, 1962).

Acridine orange – The fresh sections were immersed for 10 min in the fluorescent dye and rinsed with distilled water. They were viewed under blue light, where a yellow/green fluorescence distinguishes the lignified cell walls, and red

colouration indicates non-lignified tissues. The red/orange colour indicates cells undergoing apoptosis which indicates cell viability (Gupta and De, 1983).

c. Phenolic compounds

Ferric Chloride – The fresh sections were immersed for 20 min in the stain before being thoroughly washed with distilled water. Sections were mounted in glycerine. Brown/black deposits indicate the presence of phenolic compounds (Zarate and Yeoman, 1994).

Autofluorescence – No stains were used, but fresh sections were viewed under UV light. Phenolic compounds emit a blue/green fluorescence, as well as some terpenoids (Demarco, 2017).

d. Proteins

Coomassie Blue – The fresh sections were immersed in 0.25 % Coomassie blue for 10 min and then transferred to 7 % acetic acid. After washing in distilled water, sections were mounted in glycerine. Proteins stain blue (Demarco, 2017).

e. Alkaloids

Wagner's Reagent – The fresh sections were stained for 20 min before being washed with distilled water. Alkaloids stain with red/brown colouration (Demarco, 2017).

f. Mucilage and pectins

Ruthenium Red – The fresh sections were stained for 2 min before being rinsed with distilled water. The pink/red colouration indicates the presence of acidic mucilages and pectins (Colombo and Rascio, 1977).

3.3 Results and Discussion

3.3.1 Vegetative growth and flowering

Tagetes minuta is an erect annual herb that is capable of reaching 2 m tall (Fig 3.1 a). It matures in summer, when the stem turns a distinct red-brown colour. The glossy, green leaves are arranged alternately on the stem and are pinnately dissected. The small white-yellow florets (10 – 15mm) are supported by fused involucre bracts. Each capitula is formed from 5 – 10 florets, which groups together to form a clustered panicle on flowering plants (Fig 3.1 b).

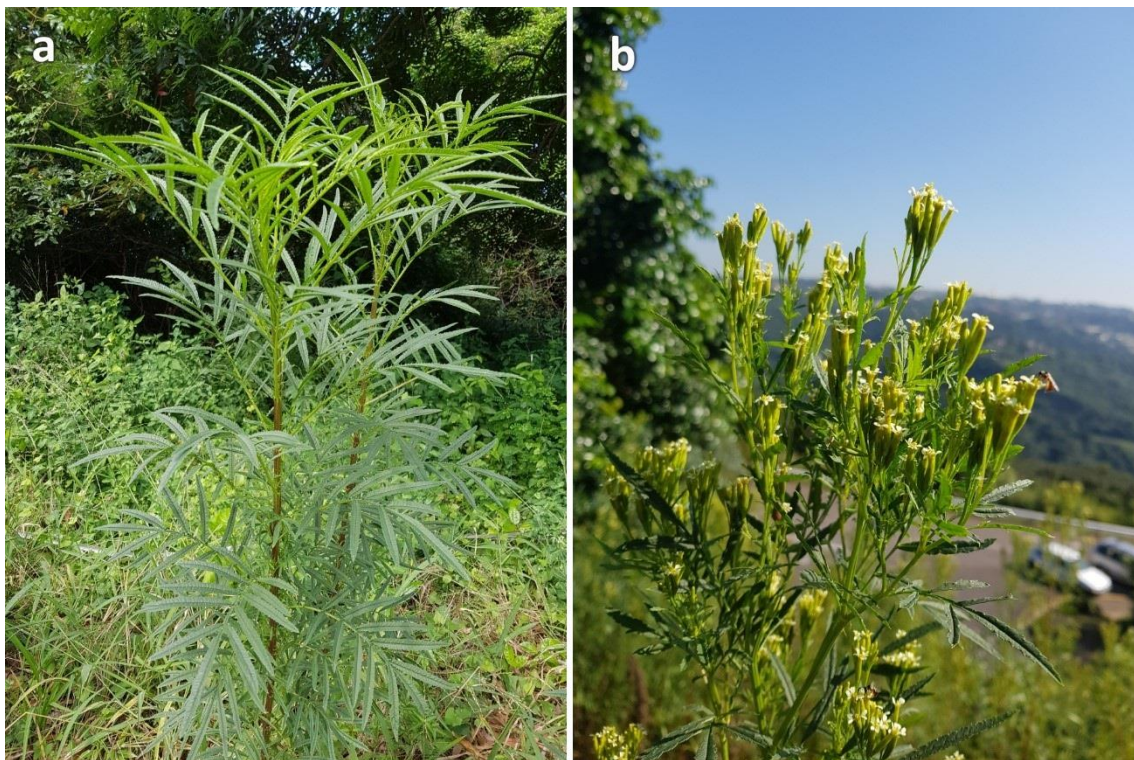


Figure 3. 1 Vegetative growth and flowers of *Tagetes minuta* at the University of Kwazulu-Natal Westville campus: a) Young plant at the vegetative stage. b) Mature plant at the flowering stage.

3.2 Stereomicroscopy

The pinnatisect leaves of *T. minuta* are long and narrow (3 – 15 cm in length and 2 – 8.5 cm in width), elliptic-lanceolate, and have an acute apex with serrated margins (Fig 3.2). Stereomicroscopy images shows that the adaxial surfaces are a darker green in the mature leaves, with a light green-yellow colour on the emergent and young leaves. They reveal the presence of non-glandular trichomes which appear translucent on both the adaxial and abaxial surfaces, with a denser cover on the abaxial leaf surface (Fig 3.2a inset). Between the developmental stages, it appears that there are considerably fewer trichomes on the mature leaves as compared to the emergent and young leaves.

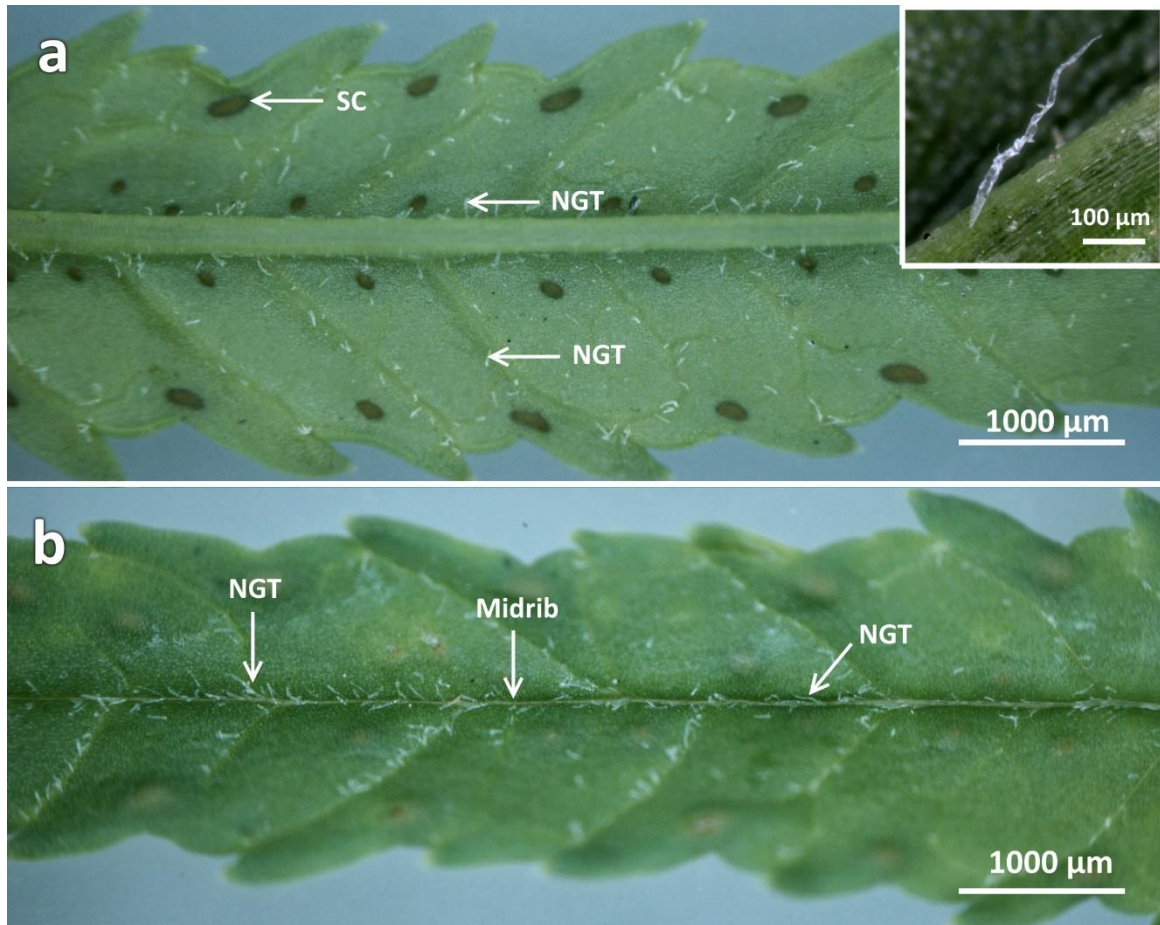


Figure 3. 2 Stereomicrographs of the leaves of *Tagetes minuta*: a) Abaxial surface of a young leaf showing non-glandular trichomes. Inset: isolated trichome on venation. b) Adaxial leaf surface of a young leaf showing trichomes growing along the midrib and major venation. SC: secretory cavity; NGT: non-glandular trichome.

There are macroscopic oil ‘glands’ on the under-surface of the leaves which appear as dark-yellow translucent spots. It is apparent that these oil glands are complex and multicellular (Fig 3.2 a). The dots are noticeably larger and more ellipsoid the closer they are to the margin of the leaves, while the pellucid glands found along the midvein are considerably smaller and rounder. The oil glands, while still visible on the adaxial surface of the mature leaves, are less pronounced than on the young leaves (Fig 3.2 b).

3.3 Secretory cavities

The stoma are anomocytic, with a limited number of subsidiary cells. They are in close proximity to the oil glands, hereafter referred to as secretory cavities. The secretory cavities range from 75 to 200 μm in diameter. The secretory cavity (Fig 3.3 a) is round and is noticeably present closer to the midvein while the more ellipsoid-shaped cavity (Fig 3.3 b) is distributed along the leaf margins and phyllaries. The secretory cavities are not immediately obvious from electron micrographs as they are covered by epidermal cells on the abaxial and adaxial leaf surfaces, except at the sites of exudation. These appear as slight depressions on the surface (Fig 3.3 c). The secretion of oils on the abaxial leaf surface in a young leaf can be seen under SEM (Fig 3.3 d). Likewise, under cryo-SEM, the oils from the secretory cavity appear on the leaf surface as globules (Fig 3.3 e) that were released under pressure from the vacuum. An image of the cross-section through an oil globule frozen in subcooled liquid nitrogen was also captured (Fig 3.3 f). It is evident from this image that there are no cellular structures in the exudate, leading to the conclusion that it is the released contents of the secretory cavity.

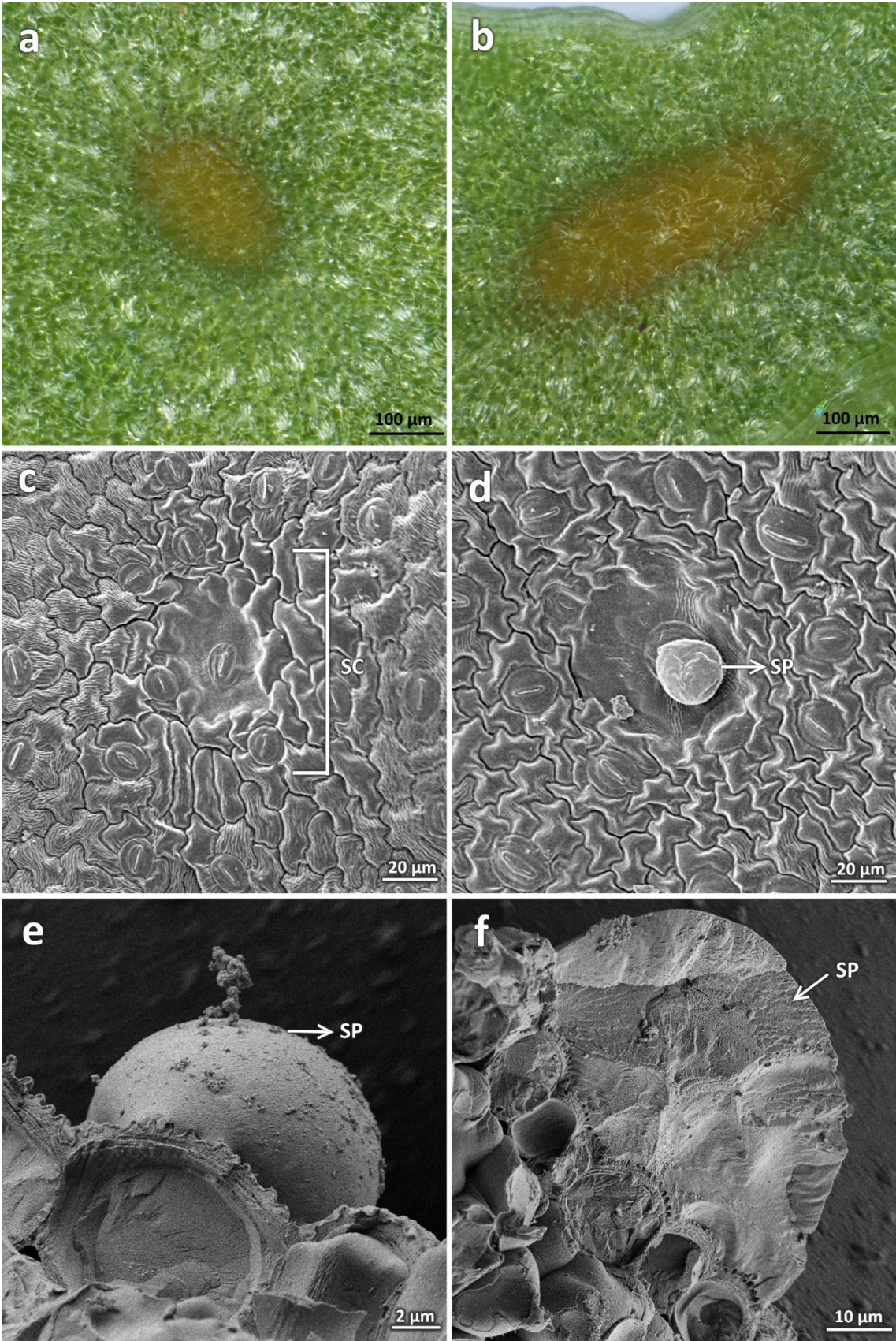


Figure 3. 3 Secretory cavities of *Tagetes minuta*: a) Stereomicrograph of rounded secretory cavity on the abaxial leaf surface. b) Ellipsoid secretory cavity found alongside the leaf margin. c) SEM of secretory cavity on abaxial leaf surface, in close relation to the stomata. d) SEM of cavity showing exudation taking place. e) Cryo-SEM micrograph showing the oil exudate expelled due to vacuum pressure. f) Cross-section of the exudate with no apparent cellular components within. SC: secretory cavity; SP: secretory product.

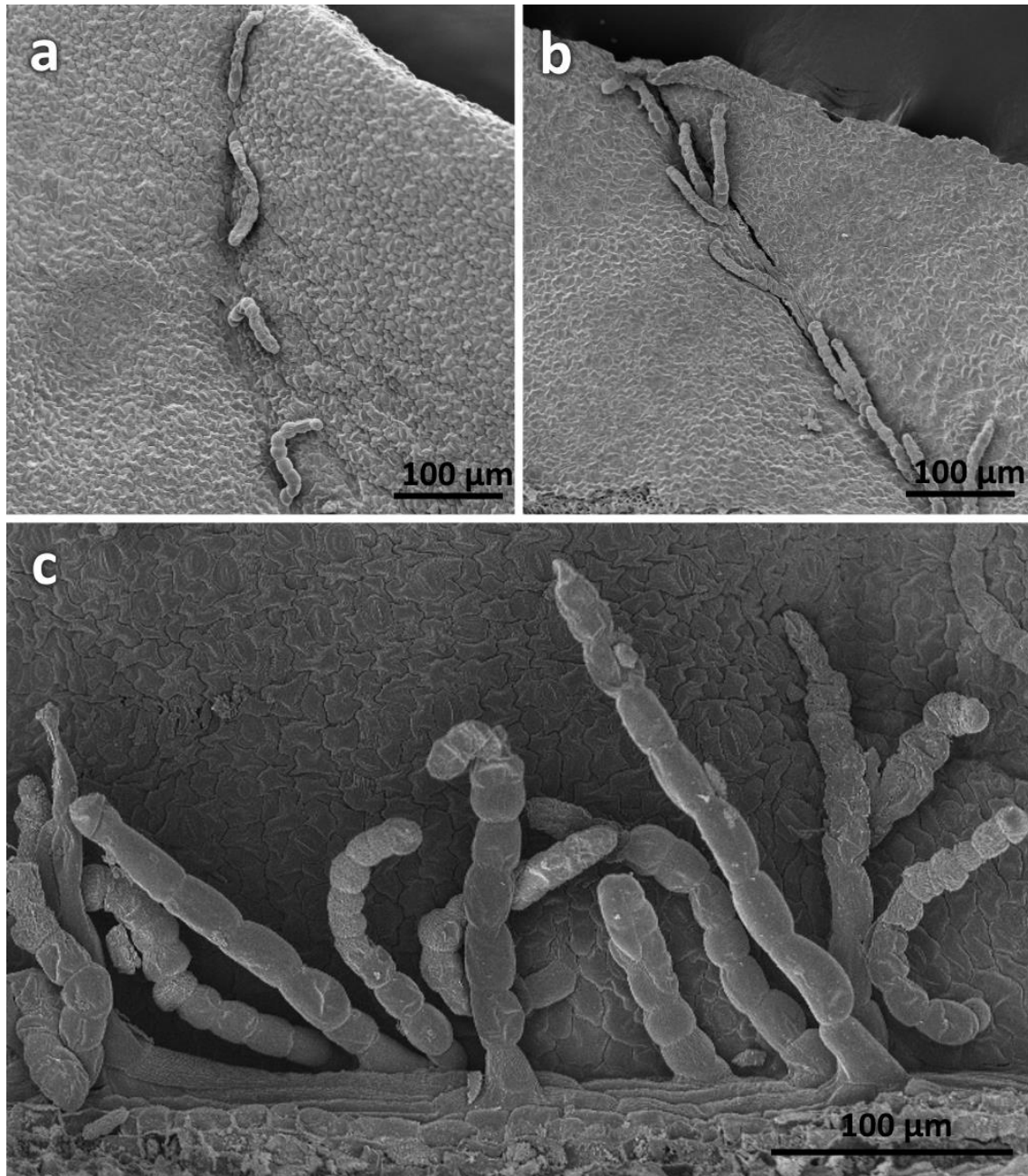


Figure 3. 4 Scanning electron micrographs of the non-glandular trichomes on the adaxial surface of young leaves of *Tagetes minuta*: a) The growth of non-glandular trichomes along the major leaf veins. b) Clustering of trichomes along the major leaf venation. c) Dense populations of non-glandular trichomes along the midvein of the leaf.

3.4 Non-glandular trichomes

Scanning electron microscopy shows the topology of the leaf. The trichomes of *T. minuta* do not densely cover the leaf surface, but are clustered around the main and lateral veins (Fig 3.4), with a more frequent occurrence on the adaxial surfaces of the emergent and young leaves. There is only one type of trichome that is found on the leaves of *T. minuta* and they appear to be non-glandular. Each trichome is uniseriate and multicellular with a rounded head, as evident by the segmentation in Figures 3.4 and 3.5. The length of the trichomes are not consistent and can range between 70 and 200 μm , where the longer trichomes are more frequently found on the mature leaves (Fig 3.5).

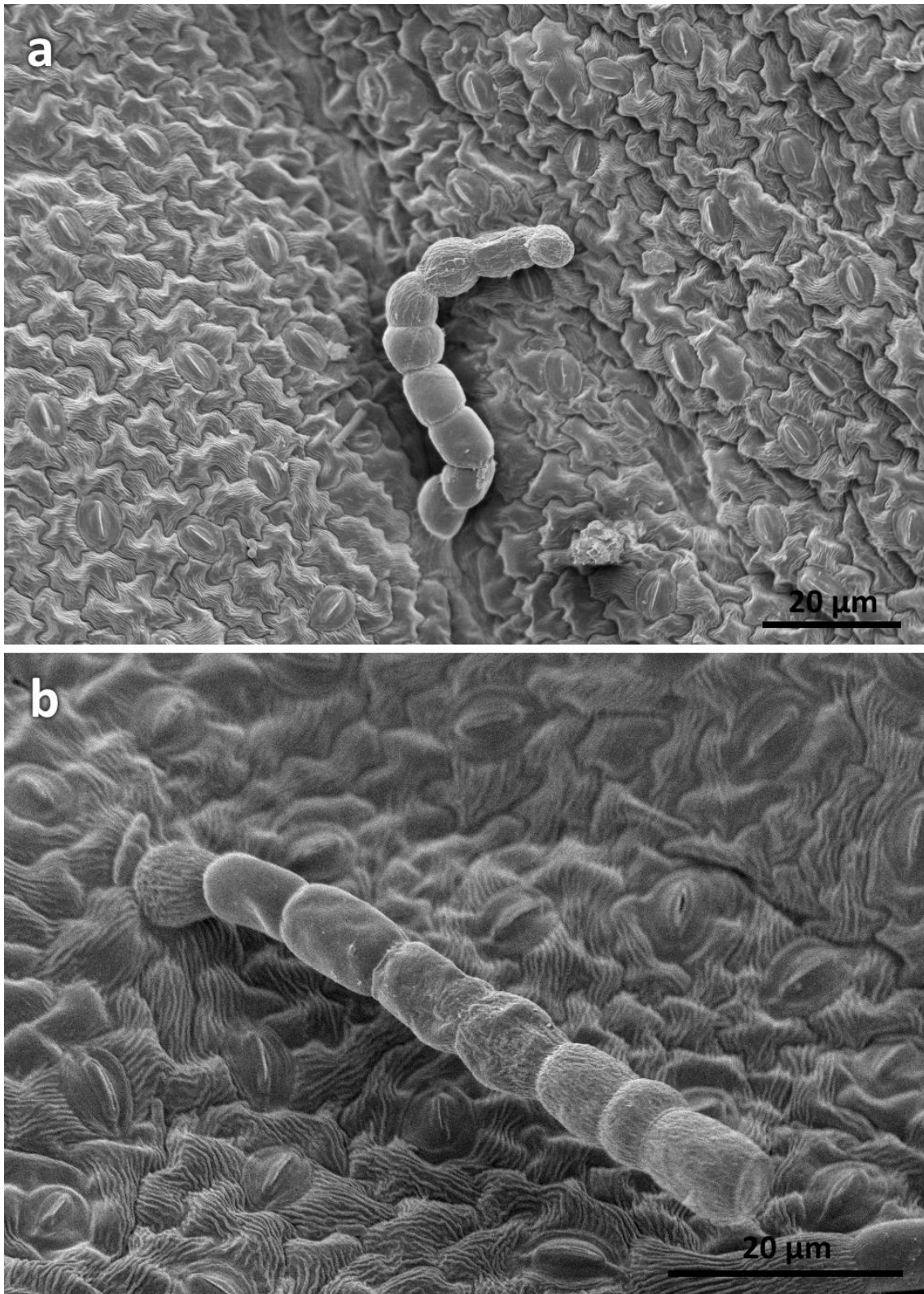


Figure 3. 5 Single non-glandular trichomes of *Tagetes minuta*: a) Single uniseriate non-glandular trichome on the adaxial surface of a young leaf. b) Non-glandular trichome on a mature leaf showing attachment to the leaf surface.

Trichomes are fine outgrowths of hair-like structures that are found on most angiosperm aerial organs, some gymnosperms and bryophytes (Johnson, 1975). They are highly diverse structures that are in contact with the external environment and thus function in response to different biotic and abiotic stimuli (Tooker et al., 2010; Li et al., 2018). Trichomes serve as the first line of defence against predators because they usually protrude from aerial surfaces and some types are capable of producing bioactive compounds that may attract and guide pollinators (Wagner, 1991; Hegebarth et al., 2016). Non-glandular trichomes are capable of enhancing plant defense systems by reducing UV radiation due to surface reflectance, and assisting through drought tolerance by reducing leaf temperatures and preventing stress from photoinhibition (Levin, 1973; Wagner, 1991; Werker, 2000). Szyndler et al. (2013) showed that trichomes are also capable of limiting movement of herbivores such as insects, restricting the damage inflicted on the plant tissues, while Kariyat et al. (2017) proved that non-glandular trichomes deter feeding by insects due to post-ingestive gut damage.

The functional usefulness of trichomes has led to increasing commercial value of the secretory metabolites in cosmetic, food, and pharmaceutical industries (Valkama et al., 2003; Balcke et al., 2017). Trichomes are highly variable and diverse foliar structures that provide mechanical and chemical barriers against herbivores (Fabricant and Farnsworth, 2001; Valkama et al., 2003). Trichome morphological traits have also been key characteristics in plant taxonomic studies.

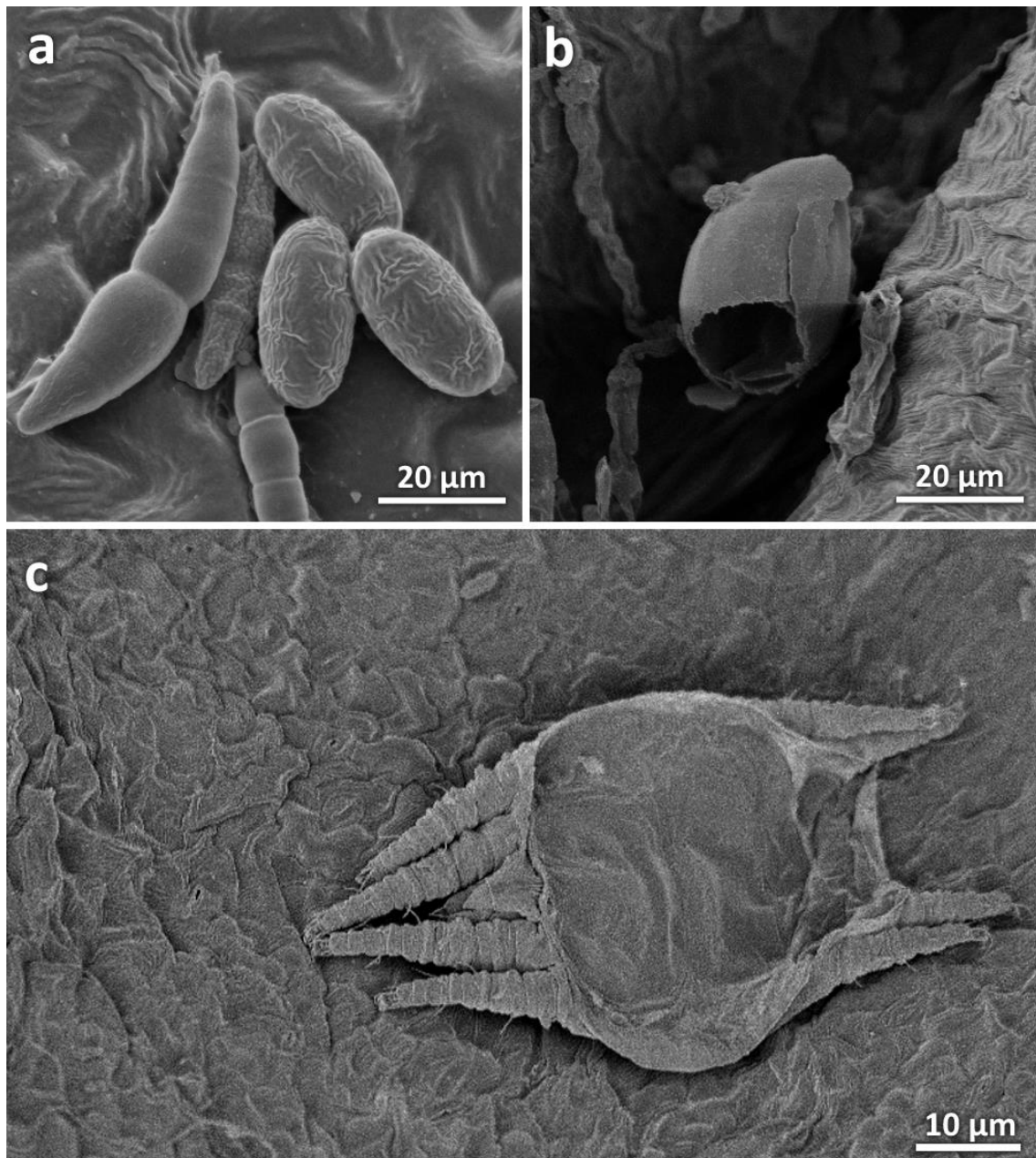


Figure 3. 6 Mites on the surface of *Tagetes minuta*: a) Scanning electron micrograph showing broad mite eggs and larvae on the abaxial surface of a young leaf. b) Micrograph showing empty egg case in the crevasse created by the midvein on the abaxial leaf surface. c) Micrograph of a scale mite from the family Tydeidae on the abaxial surface of a mature leaf.

3.5 Semi-thin sections of secretory cavities

The secretory cavities along the midvein are smaller (55 – 75 μm) than those found along the leaf margins and phyllaries (150 – 200 μm). They appear as elliptic glands that seem to take up the almost the entire width of the leaf blade. Figure 3.7 shows the development of the secretory cavity. The gland begins as a group of modified parenchymal cells that form concentric circles in the leaf blade, below the row of columnar epithelial cells on the adaxial leaf surface (Fig 3.7 a and b). As the cavity expands to accommodate the accumulated substances, the parenchymal cells elongate to form a multi-layered sheath with cutinised walls (Fig 3.7 d and e). As previously mentioned, the secretory cavity is limited by the chlorenchyma on the adaxial face, but grows adjacent to the epithelial cells on the abaxial face of the leaf. This leads to the conclusion that secretions are expelled from the abaxial leaf surface.

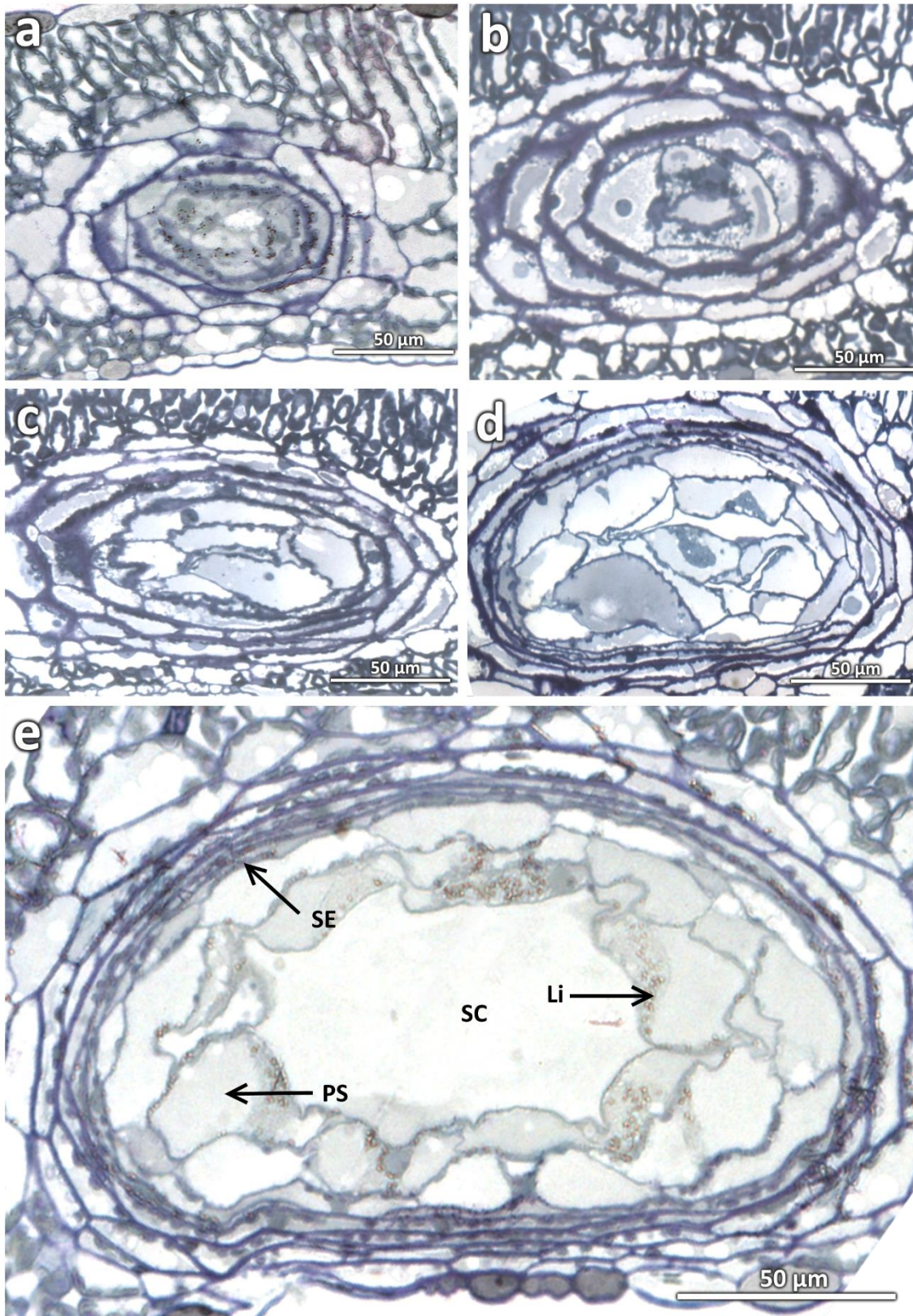


Figure 3. 7 Development of the secretory cavity in *Tagetes minuta*. a) Initiation of secretory cavity in emergent leaf. b) Cells differentiating in emergent leaf. c) Elongation of secretory epithelial cells in young leaf. d) Secretory epithelium extending under the chlorenchyma. e) Mature secretory cavity showing the movement of lipids into the schizolysigenous cavity. SE: secretory epithelium; SC: secretory cavity; PS: parenchyma sheath; Li: lipids.

The foliar cavity appears to form from the middle lamella where the cells at the centre pull apart (Fig 3.7 a and b). Once the lumen is developed (Fig 3.7 e), it appears that all interior cells release their secretory products (lipids) via holocrine secretion into the now schizolysigenous cavity. These cells undergo a process known as autolysis and has been described by Russin et al. (1992) for *Tagetes erecta*.

Many secretory cells are derived from other plant tissues, mainly parenchymatous and epidermal tissues (Buvat, 1989). In young leaves, the secretory cavities appear to be lysigenous, in which the intercellular substance is only partly dissolved during development, but are typically elongated in mature leaves, causing them to appear schizolysigenous (Buvat, 1989; Turner and Lange, 2015). The secretory epithelium is mainly responsible for the excretion of accumulated substances from the cavity, and can either cause the products to be diffused through the cuticle or released via distention of the epithelial lining itself (Buvat, 1989; Lopez et al., 2009).

Lopez et al. (2009) described the oil complex of *Tagetes minuta* from the standpoint of a senescent leaf. While the secretory cavity in a mature leaf (Fig 3.7 e) appears to be schizolysigenous, the secretory cavity in a senescent leaf appears lysigenous. The development of the secretory cavity from an emergent to a young leaf is shown in Figure 3.7 a – d. It can be seen that the secretory epithelium is comprised of cutinised parenchymal tissues that become narrow and elongated. Although the secretory cavity grows to fit the width of a leaf blade (Fig 3.7 e), they are limited on the adaxial face by a distinct row of chlorenchyma cells, which suggests that the leaf secretion occurs on the abaxial leaf surface.

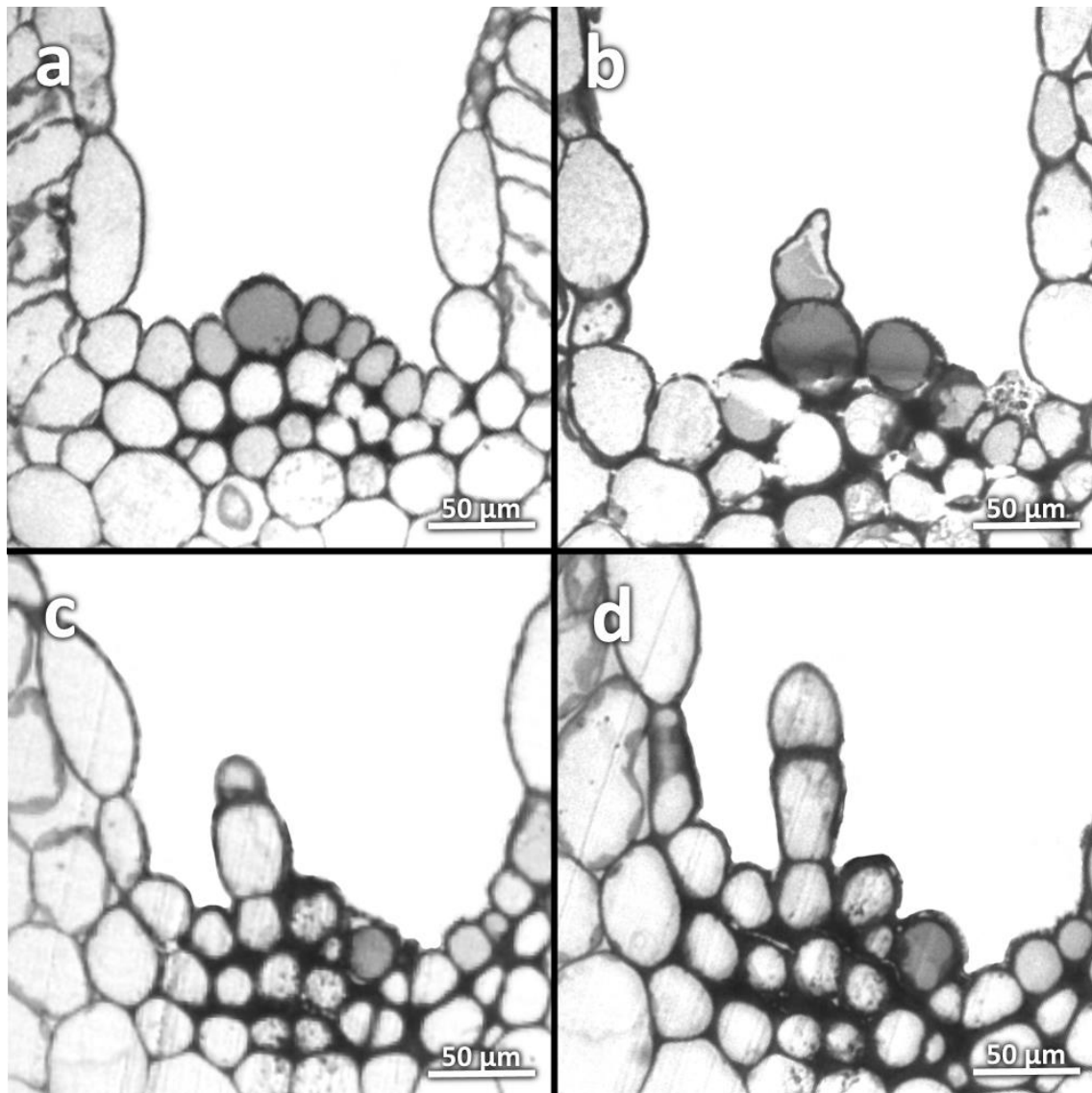


Figure 3. 8 Development of non-glandular trichome. a) Epithelial cells begin development by becoming cutinised. b) Cell undergoes periclinal division to create a tapering end of the now developing trichome. c) Cell division continues to create a uniseriate non-glandular trichome. d) Cutinised cells elongate to form a mature trichome.

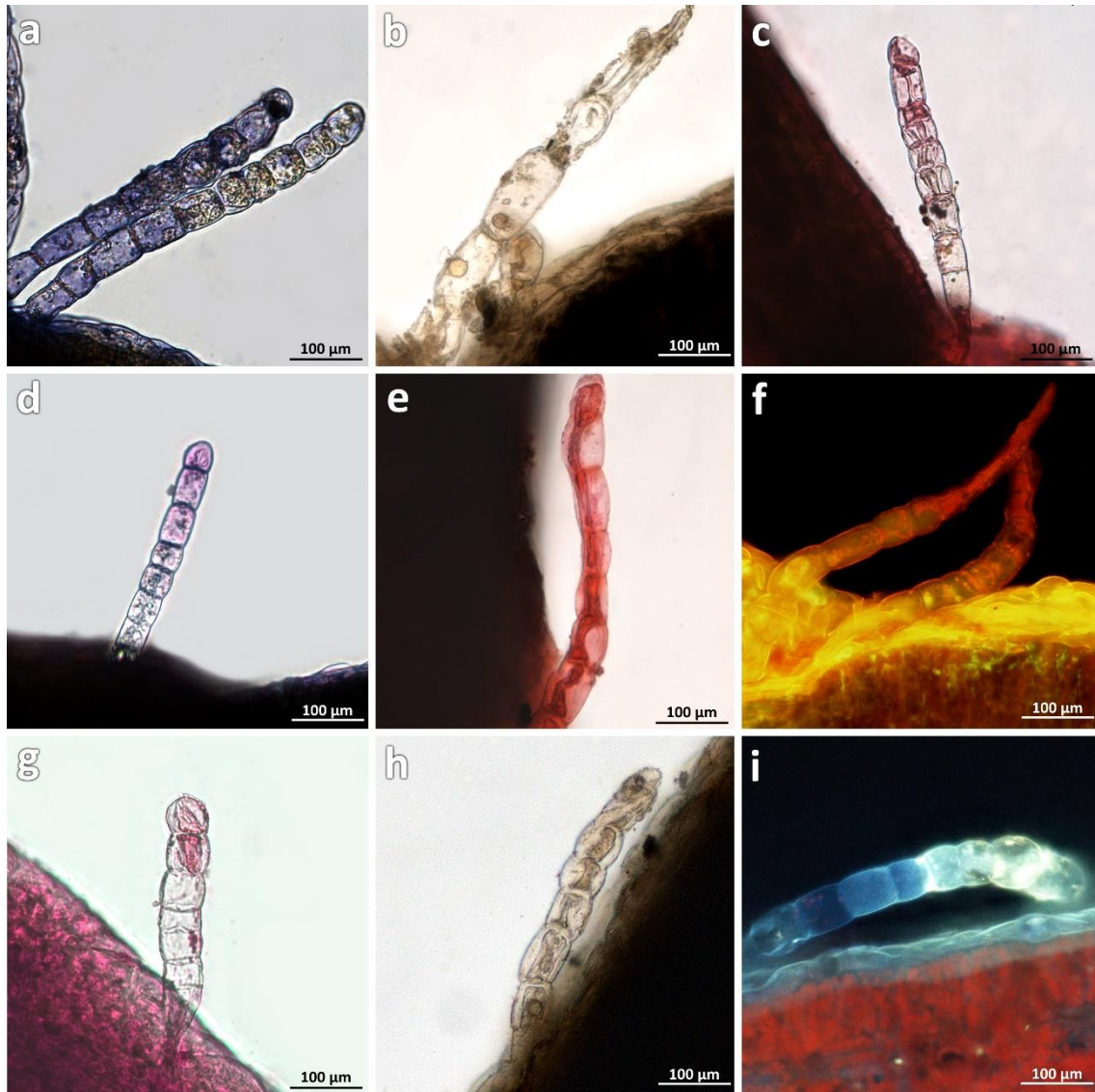


Figure 3. 9 Histochemical observations on the non-glandular trichomes of *Tagetes minuta*: a) Trichome positively stained with Coomassie Blue. b) Positive staining for alkaloids with Wagner's reagent. c) Ruthenium red staining of a trichome. d) Acidic lipids detected using Nile Blue stain. e) Positive test for lipids, stained with Sudan III&IV. f) Acridine orange stain used under UV light showing presence of lignins. g) Trichome stained with phloroglucinol, positive for lignins. h) Ferric chloride stain shows phenolics. i) Autofluorescence of a trichome under UV light shows presence of phenolic compounds.

3.6 Histochemical analyses of the non-glandular trichomes

The linear non-glandular trichomes were evaluated for the presence of histochemical compounds and localisation. It is evident that some of the bioactive compounds could be located within the cells of the trichomes, despite them being non-glandular. They were positively stained for lipids using Nile blue and Sudan III&IV and for lignins using phloroglucinol and acridine orange stains. Phenolic compounds were identified using ferric chloride and proteins were identified using the Coomassie blue stain. Alkaloids were present as deduced using Wagner's reagent, and ruthenium red stained positively for mucilages and pectins (Fig 3.9 a – i). The histochemical tests appears to localise the bioactive compounds in the apical cells of the trichomes, and occasionally, throughout the trichome cells. Figure 3.9 b shows a non-glandular trichome stained with Wagner's reagent, and the alkaloids appear as droplets throughout the trichome.

Non-glandular trichomes have shown to be metabolically active during the earliest stages of development (Levin, 1973; Mayekiso et al., 2008) but are thought to play only a minor role during the lifespan of the plant past the stage of development. Tozin et al. (2016) shows that while the traditional role of non-glandular trichomes has historically been protection of the plant material from predators, UV, and abiotic factors, they have the potential to produce, store, and liberate bioactive substances. While their work is primarily based on Lamiaceae and Verbenaceae species, a comparison can be drawn with *T. minuta*, which belongs to family Asteraceae. Chaffey (2006) first proposed that despite the lack of openings in the cuticle and cell walls of non-glandular trichomes, substances can traverse the body cells of the trichomes, which is visible in Figures 3.9 a, c, e, g, and h. Although the trichomes on *T. minuta* appear to be non-glandular, anatomically they are similar to the linear glandular trichomes found on other species in the Asteraceae family that aid in the storage and production of essential oils (Aschenbrenner et al., 2013; Bombo et al., 2017). This serves as the first study to histochemically analyse the contents and localisation in the non-glandular trichomes of *T. minuta*.

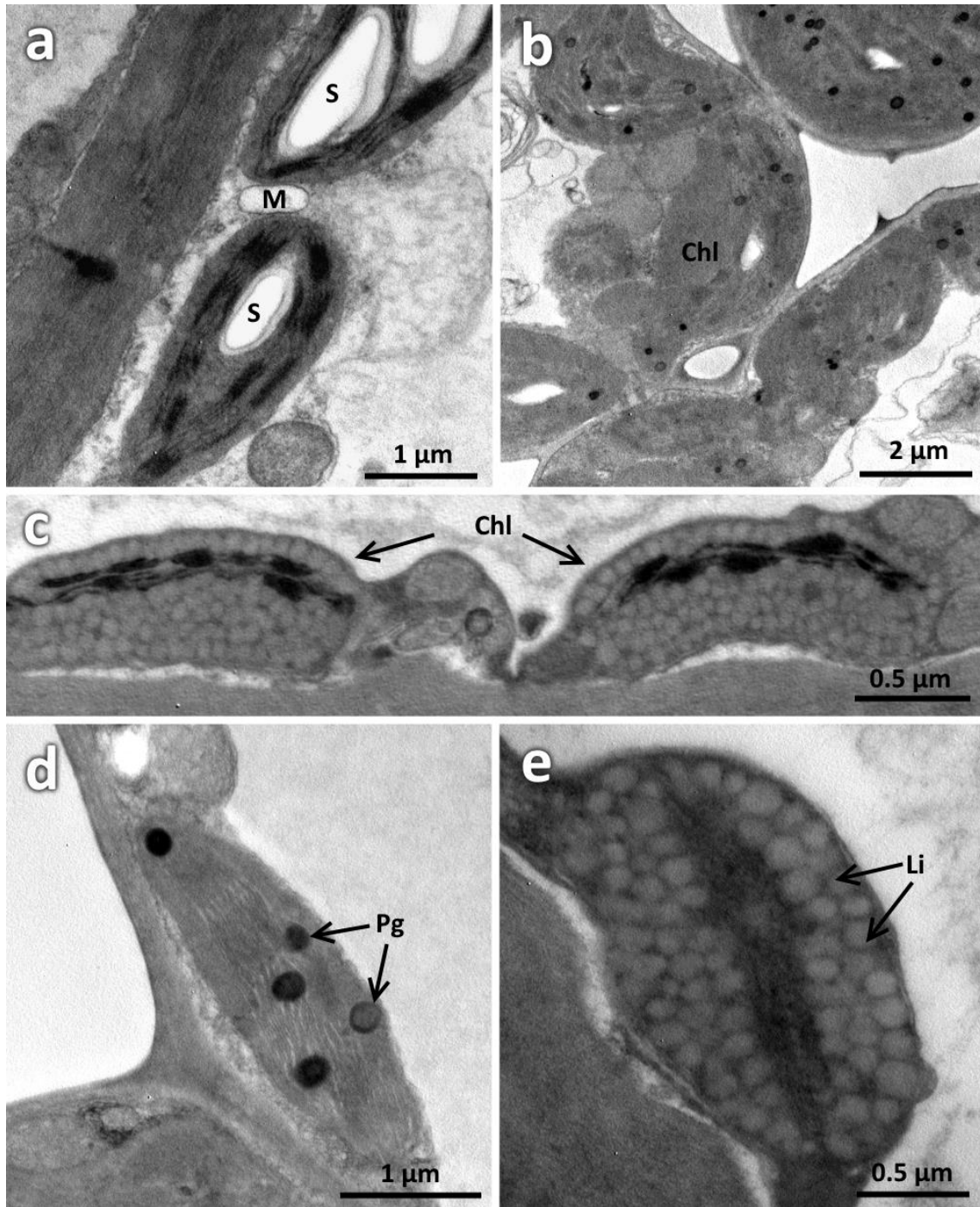


Figure 3. 10 Electron micrographs of plastids in leaves of *Tagetes minuta*: a) Chloroplast containing starch grains. b) Chloroplasts outside the secretory cavity. c) Elongated chloroplasts in the secretory epithelium containing lipids. d) Plastid containing plastoglobuli. e) Single chloroplast in the parenchymal sheath of the secretory cavity containing lipid globules. S: starch granules; M: mitochondria; Chl: chloroplast; Pg: plastoglobuli; Li: lipids.

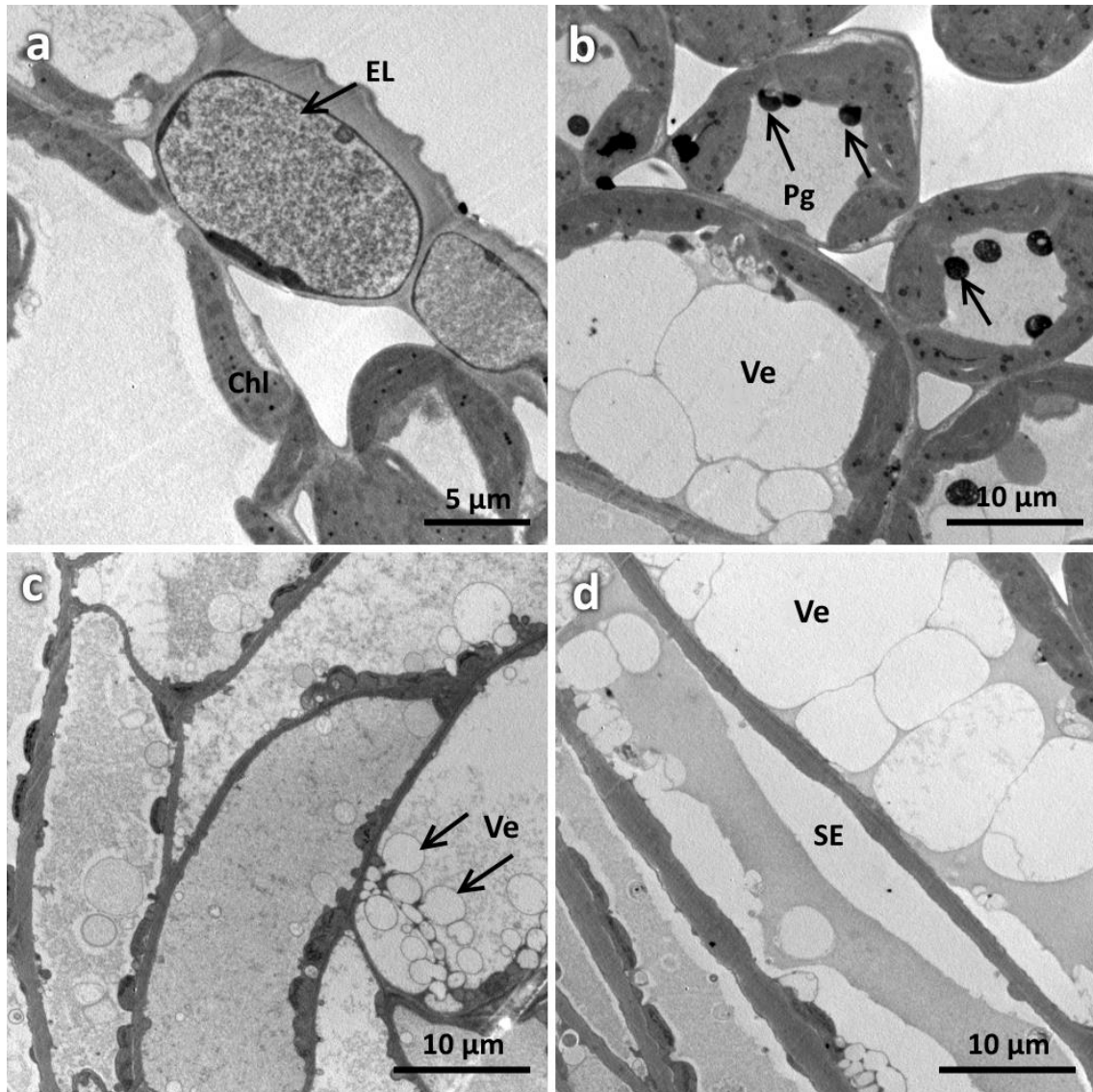


Figure 3. 11 Electron micrograph of cells within the oil complex: a) Epidermal layer showing electron-dense osmiophilic material within. b) Cells in the parenchymal sheath showing plastoglobuli. c) Elongated cells that form the secretory epithelium in a mature secretory cavity that contain vesicles. d) Secretory epithelial cells on the periphery of the secretory cavity containing vesicles. EL: epithelial layer; Chl: chloroplast; Pg: plastoglobuli; Ve: vesicle; SE: secretory epithelium.

3.7 Ultrastructure of the secretory cavities

The secretory cavities of *T. minuta* range in size from 75 to 200 μm across, meaning that they are not visible in their entirety using TEM. Figures 3.10 and 3.11 show parts of the parenchymal sheath and secretory epithelium that make up the secretory cavity, as well as the cells surrounding them. The changes in the plastids are evident from Figure 3.10 a – e, where primary starch granules are present in the chloroplasts of Figures 3.10 a and b. These plastids can be found in the neighbouring cells on the periphery of the secretory cavity and often contain plastoglobuli which appear as electron-dense material. Note the chloroplasts in these neighbouring cells with a normal thylakoid system. However, in the cells found in the secretory epithelium, the chloroplasts contain a dense population of what appear to be lipids surrounding the thylakoids and take up the space of the grana (Fig 3.10 c and e).

Sacchetti et al. (2001) assessed the ultrastructural characteristics of the secretory cavities of *Tagetes patula*, showing similar results to those above. The schizolysigenous spaces that are bordered by the parenchymal sheath (Figure 3.11 c and d) appears rich in plastids with electron-dense stroma and few thylakoids, which is a common feature in plants that exude essential oils (Lopez et al., 2009; Lizarraga et al., 2017). This may be strongly related to the production of terpene compounds such as thiophene that is prevalent in the leaves of *T. minuta* (Al-Musayeib et al., 2014; Ibrahim et al., 2018a). Also visible are the glandular cells which appear elongated and rich in vesicles.

3.8 Conclusion

The secretory cavities of *T. minuta* appear macroscopically on both the adaxial and abaxial leaf surfaces, and are pronounced in mature leaves. For the first time, the ultrastructural development of these secretory cavities shows the changes to the plastid system within the secretory epithelial lining. Trichomes on the leaves of *T. minuta* appear to be linear, uniseriate, and non-glandular. However, the histochemical analysis indicated the storage of various histocompounds, suggesting that non-glandular trichomes in the Asteraceae family have potential biological role that is more than protection against predators and abiotic factors.

CHAPTER 4: PHYTOCHEMICAL ANALYSES AND ANTIBACTERIAL POTENTIAL OF *TAGETES MINUTA* L.

4.1 Abstract

Phytochemical analysis was carried out on the crude organic solvent extracts derived from the leaves of *T. minuta*. Alkaloids, sterols, saponins, terpenoids, phenols, and lipids were detected from the extracts. Gas-chromatography mass-spectrometry (GC-MS) was carried out to reveal that the constituents with the highest percentage were 9-octadecen-1-ol (4.51 %), β -sitosterol (6.07 %), olean-12-en-3-one (7.47 %), and 3-methyl-1-butanol (14.77 %). Preliminary antibacterial activity was performed using the methanolic extract which showed inhibitory activity against selected gram positive and gram negative bacteria (*P. aeruginosa*, *E. coli*, *S. aureus*, MRSA, and *B. subtilis*). This study shows that *T. minuta* contains bioactive compounds that have pharmacological and medicinal uses.

Keywords: antibacterial; bioactive compounds; GC-MS; methanol extract; *Tagetes minuta*

4.2 Introduction

Plant material has been used in traditional medicine for millennia in both developing and developed countries due its ease of access and lesser risk of side effects (Qazi Majaz and Molvi Khurshid, 2016). The use of ethnomedicine is becoming increasingly popular in modern societies as natural alternatives to synthetic products and has become a socio-cultural phenomenon of third world countries (Dixit et al., 2013).

In South Africa, healthcare is largely polarised between Western medical therapies and traditional African healthcare systems. Although concurrent usage of traditional healers and allopathic providers of medicine is common, allopathic healthcare facilities are often limited and not easily accessible to most in South Africa (Bisi-Johnson et al., 2017). This has resulted in the medicinal plant industry in South Africa being supported by approximately 30 million local consumers with almost 70 thousand species of plants being used for medicinal purposes, many of which are threatened by overharvesting and international trade (Street and Prinsloo, 2013; Xego et al., 2016). The indiscriminate overharvesting coupled with extensive land degradation has affected the availability of medicinal plants that can be naturally foraged, resulting in an increasing demand for medicinal plant material (Phondani et al., 2016; Tanga et al., 2018).

In order to establish strategies to protect endemic medicinal plants, it is vital that they are screened for the bioactive phytochemicals responsible for their therapeutic properties. This will ensure regulation for use of wild populations of medicinal plants by putting into place mitigative measures such as systematic plant cultivation for the production and monitoring of this underutilised resource (Tanga et al., 2018). Moreover, many isolated phytometabolites from medicinal plants have led to the development of novel drugs and therapies to treat several human diseases such as cancer and diabetes (Hosseinzadeh et al., 2015; Shakya, 2016; Kudumela and Masoko, 2017).

Tagetes minuta belongs to the Asteraceae family, and its essential oils are renowned for its medicinal, ornamental, and therapeutic values (Dixit et al., 2013; Rajvanshi and Dwivedi, 2017). The essential oils of *T. minuta* has been researched for its nematocidal (Gutierrez et al., 2006), cosmetic (Farjana et al., 2009), food additive (Nandita et al., 2012), and antimalarial (Kyarimpa et al., 2014) properties.

Phytochemical analyses of *T. minuta* essential oil show that the plant is rich in alkaloids, phenolic compounds, flavonoids, and thiophenes which are responsible for its therapeutic properties (Chamorro et al., 2008; Meshkatalasadat et al., 2010; Devika and Koilpillai, 2012). The oil has been reported as having a high inhibitory effect on both gram positive and gram negative bacteria and fungi (Hethelyi et al., 1986). Therapeutically, *T. minuta* has several reported medicinal benefits such as remedies for respiratory inflammations, stomach pains, chest infections, coughs, and congestion (Shirazi et al., 2014). It also has a healing effect on wounds, cuts, and calluses (Rahimi et al., 2010; Maity et al., 2011).

This study was undertaken to examine the qualitative phytochemical composition using phytochemical tests, determine the quantitative chemical composition using GC-MS, and elucidate the preliminary antibacterial potential in the crude methanolic extract of *T. minuta* leaves.

4.3 Methods and Materials

4.3.1 Plant collection

Fresh leaves of *T. minuta* were collected from the UKZN Westville campus (29.817°S 30.940°E) and air-dried for 6 weeks at room temperature (24°C). A voucher specimen was deposited at the UKZN Westville Herbarium (accession number 18216, voucher number 01).

4.3.2 Extraction with organic solvents

Ten grams of *T. minuta* powdered leaf material were placed in a round bottom flask containing 100 ml of hexane. The flask was attached to Soxhlet apparatus and boiled for three 3-hour sessions to obtain the crude plant extract. This procedure was then repeated using the same leaf material for chloroform and methanol, respectively. The crude extracts were filtered through Whatman No. 1 filter paper and the stored in airtight jars at 4°C for further analysis.

4.3.3 Qualitative phytochemical analyses

a) Detection of carbohydrates

Molisch's test – two drops of α -naphthol were added to 2 ml of extract and gently shaken. One ml of concentrated sulphuric acid was slowly poured along the side of the test tube and allowed to stand. The formation of a red-purple ring at the junction of the two liquids is indicative of the presence of carbohydrates (Phani Deepthi Yadav et al., 2013).

Benedict's test – One ml of Benedict's reagent was added to 1 ml of filtrate and boiled for 2 min in a water bath at 100°C. An orange-red precipitate indicates the presence of reducing sugars (Phani Deepthi Yadav et al., 2013).

Fehling's test – One ml each of Fehling's solutions A and B were mixed into 1 ml of extract and boiled in a water bath. The formation of a red precipitate indicates the presence of carbohydrates (Phani Deepthi Yadav et al., 2013).

b) Detection of amino acids

Ninhydrin test – two drops of ninhydrin reagent were mixed into 2 ml of extract. A purple colour indicates the presence of amino acids and proteins (Minj et al., 2015).

c) Detection of alkaloids

Mayer's test – three drops of potassium mercuric iodide solution were added to 2 ml of filtrate. A yellow-orange precipitate confirms the presence of alkaloids (Surendra et al., 2016).

Wagner's test – two drops of Wagner's reagent were added to 1 ml of extract. A brown precipitate indicates the presence of alkaloids (Surendra et al., 2016).

Dragendorff's test – two drops of Dragendorff's reagent were added to 1 ml of extract. An orange-red precipitate indicates the presence of alkaloids (Surendra et al., 2016).

d) Detection of saponins

Foam test – two ml of extract were diluted using 5 ml of distilled water and vigorously shaken for 5 min. A persistent foam later above the mixture indicates the presence of saponins (Bargah, 2015).

e) Detection of sterols

Salkowski's test – three ml of chloroform and 2 drops of concentrated sulphuric acid was added to 2 ml of extract and gently shaken. A red ring in the chloroform layer and green precipitate in the extract indicates the presence of sterols (Bargah, 2015).

f) Detection of terpenoids

Sulphuric acid test – two ml of chloroform was added to 5 ml of extract and shaken gently. Three ml of sulphuric acid was poured gently along the side of the test tube. A red-brown ring indicates the presence of terpenes (Bargah, 2015).

g) Detection of phenolic compounds

Ferric chloride test – two drops of 5% ferric chloride was added to 2 ml of filtrate. A green-black precipitate indicates the presence of phenolic compounds (Surendra et al., 2016).

h) Detection of fixed fats and oils

Filter paper test – One drop of extract was placed on Whatman No. 1 filter paper and left to dry. A persistent oily residue present on the filter paper indicates a positive test for fixed fats and oils (Minj et al., 2015).

4.3.4 Gas chromatography–mass spectrometry (GC-MS)

Five grams of powdered leaf material was submerged in 50 ml of methanol in a round bottom flask and boiled for two 3 hr sessions. The crude extracts were filtered through Whatman No. 1 filter paper and stored in an airtight jar at 4°C until analysed. The extract was analysed by GC-MS using a QP-2010 Ultra Shimadzu system with a Rx-5SilMS fused silica column of length 30 m (0.25 µm internal diameter and 0.1 µm film thickness). Helium was used as the carrier gas at a constant pressure of 69 kPa. The flow rate was 0.96 ml/min with a total flow of 4.9 ml/min, along with a linear velocity of 36.7 cm/s at purge flow of 3.0 ml/min. The injection port temperature was set at 250°C. The temperature of the oven was initially set to 50°C for 1 min. The temperature was then increased to 310°C at a rate of 5°C/min and was maintained for 10 min. The MS was taken at 70 eV. The mass selective detector was operated in the scan mode between 50 and 800 m/z. Peak identification was carried out by comparison of the mass spectra with mass spectra data available on database of NIST and WILEY libraries (Kataria et al., 2016) The chemical compounds present in the crude methanolic extract of *T. minuta* were expressed as percentages based on peak area.

4.3.5 Antibacterial activity screening

The crude methanolic extract was first dried to a powder and re-suspended in deionized water to avoid antibacterial activity from the methanol (Valle et al., 2016) and adjusted to a final concentration of 1 mg/ml.

The preliminary antibacterial activity of the crude aqueous extract was evaluated against *Escherichia coli* (ATCC 25218), *Staphylococcus aureus* (ATCC 29213), methicillin-resistant *Staphylococcus aureus* (ATCC BAA-1683), *Bacillus subtilis* and *Pseudomonas aeruginosa* (ATCC 25215). Agar plates were prepared using Mueller Hilton agar which was poured into sterile petri dishes to set at room temperature. The bacterial strains were cultured in a nutrient broth for 18 hrs at 37°C before being standardised using the 0.5 McFarland turbidity standard. The bacterial cultures were then swabbed uniformly onto the plates using sterile cotton swabs. Five-millimetre wells were aseptically punched using an agar corer (gel puncture). The samples were pipetted into the wells (90 µl), and the plates were incubated at 37°C. The antibacterial activity was assessed after 24 hrs by measuring the diameter of the zone of inhibition (mm).

4.4 Results and Discussion

The preliminary phytochemical screening of *T. minuta* crude methanolic extract was performed qualitatively for three organic solvents, viz. hexane, chloroform, and methanol, and these results are presented in table 4.1. The crude hexane extract tested positively for the presence of alkaloids, saponins, sterols, terpenoids, and fixed fats and oils. The crude chloroform extract tested positively for the presence of carbohydrates, alkaloids, sterols, terpenoids and fixed fats and oils. The crude methanolic extract tested positively for the presence of carbohydrates, alkaloids, amino acids, terpenoids, phenols, and fixed fats and oils.

These bioactive compounds provide the plant with protection against pathogens, predators, diseases, and abiotic factors (Saxena et al., 2013). A similar phytochemical profile was identified for the essential oil of *T. erecta* (Rajvanshi and Dwivedi, 2017) who suggested that these classes of compound are responsible for antifungal, antibacterial, and anti-inflammatory properties of the plant. According to Shakya (2016), medicinal plants that contain sterols and saponins exhibit antimicrobial and anticancer properties. Alkaloids, flavonoids, terpenes, saponins, and phenolic compounds have been reported to possess various pharmacological and therapeutic effects, including antimicrobial, antioxidant, anti-diabetic, and anti-inflammatory activity (Abdul et al., 2018).

The chemical constituents of the crude methanolic extract of *T. minuta* were analysed using GC-MS, as is evident from the chromatogram in figure 4.1. The separation of all 108 bioactive compounds were identified by retention time and height percentage. Twenty-four out of the 108 compounds displayed a peak percentage greater than 1 and are presented in this study as table 4.2. Compounds with a peak area less than 1% were considered as low-level compounds (Appendix A) (Pakkirisamy et al., 2017).

The compounds with the highest composition percentage were 9-octadecen-1-ol (4.51 %), β -sitosterol (6.07 %), olean-12-en-3-one (7.47 %), and 3-methyl-1-butanol (14.77 %). These results differ greatly as compared to the chemical profiling of the essential oils of *T. minuta*, where monoterpenes, sesquiterpenes, limonene, and tagetones are often the most abundant compounds (Shahzadi et al., 2010; Shirazi et al., 2014; Rezaei et al., 2018). The compound 9-octadecen-1-ol is a long-chain aliphatic alcohol that is known to

decrease low-density lipoprotein (LDL) cholesterol and increase high-density lipoprotein (HDL) cholesterol and is most commonly synthetically produced as a lipid-lowering drug for high cholesterol patients (Santos et al., 2015). Additionally, Shen et al. (2018b) has shown that 9-octadecen-1-ol is also a large constituent of *Bidens pilosa*. This becomes important when paired with the findings of Cid et al. (2016) who studied the effects of co-cropping *B. pilosa* with *T. minuta*, claiming that their similar chemical profile aids their ability to bioaccumulate metals and act as an herbicide.

Beta-sitosterol is a nontoxic isoprenoid that has displayed anticancer effects against breast cancer, prostate cancer, colon cancer, lung cancer, stomach cancer, ovarian cancer, and leukaemia by interference of multiple cell signalling pathways (Bin Sayeed and Ameen, 2015). Ge et al. (2018) and Oladosu et al. (2018) claim that the effects of β -sitosterol and olean-12-en-3-one on cancer cells in vitro are weak as compared to other oleanane-type triterpenoids, but still exhibit antibacterial, antiviral, and gastroprotective properties.

Kyarimpa et al. (2014) and Athuman et al. (2016) studied the repellence of the malaria-carrying mosquito, *Anopheles gambiae*, using essential oils from *T. minuta*. Both studies concluded that some constituents in the essential oil causes 100 % mortality of mosquito larvae as well as adult mosquitoes, but the compound is not isolated. In 2015, Zohdy et al. established the use of 3-methyl-1-butanol as an odor-bait for *Anopheles* mosquitoes. This chemical compound produced by both plants and animals acts a lure for mosquitoes. This implies that *T. minuta* has the potential to act as lure for malaria-carrying mosquitoes, as well as acting as an insecticide.

The presence of these phytochemicals make *T. minuta* a considerable candidate for the production and optimisation of valuable compounds with pharmacological and therapeutic benefits.

Table 4. 1 : Qualitative phytochemical analysis of the crude leaf extracts of *Tagetes minuta* (n=3).

Phytochemical compound	Test	Hexane extract	Chloroform extract	Methanol extract
Carbohydrates	Molisch's	–	+	+
	Benedict's	–	+	++
	Fehling's	–	+	–
Alkaloids	Mayer's	+	+	++
	Wagner's	++	+	+
	Dragendorff's	+	++	+
Amino acids	Ninhydrin	–	–	+
Saponins	Foam	+	–	–
Sterols	Salkowski's	+	+	–
Terpenoids	Sulphuric acid	+	+	+
Phenols	Ferric chloride	–	–	+
Fixed fats & oils	Filter paper	+	+	+

– Absent, + Present, ++ Intense positive reaction

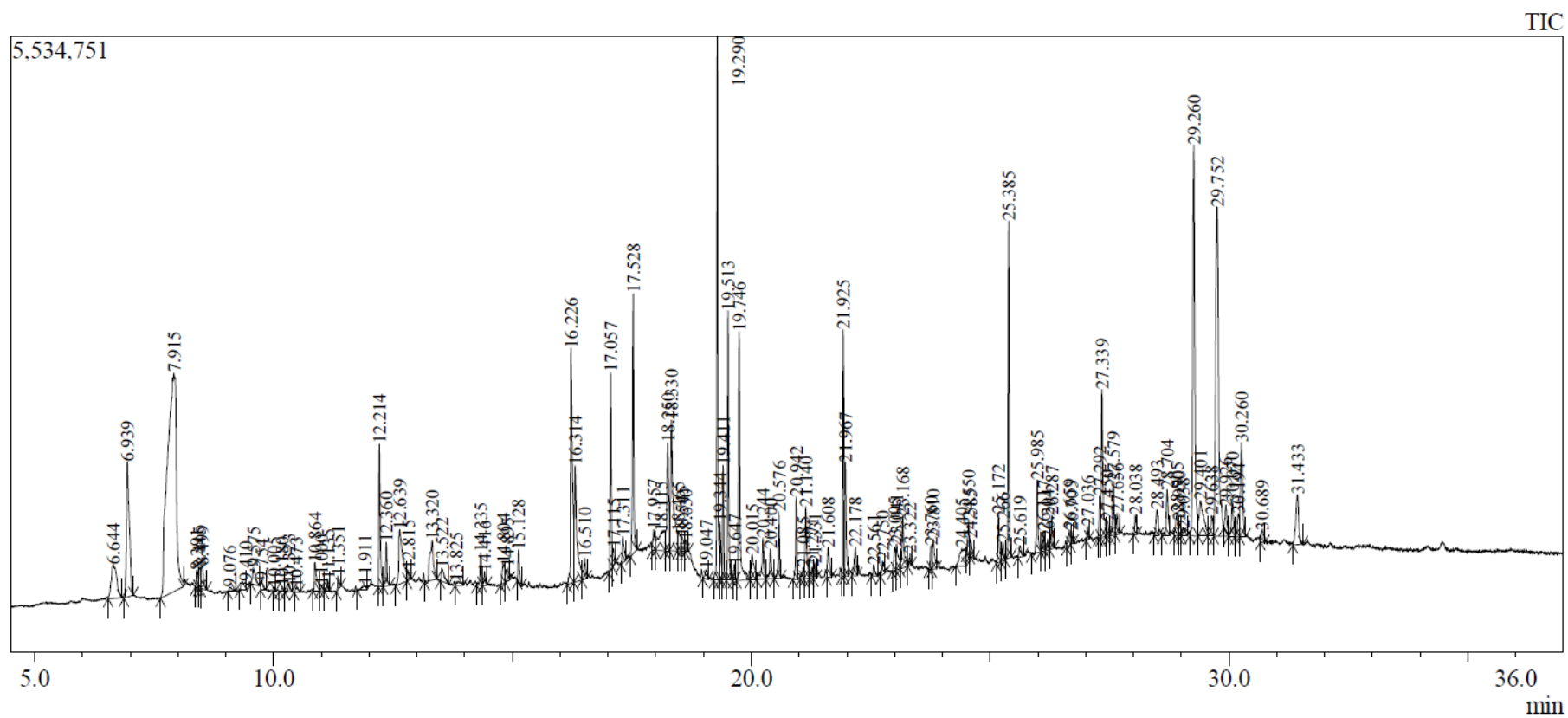


Figure 4.1 GC-MS chromatogram of crude methanolic extract of *Tagetes minuta* leaves

Table 4. 2 : Phytochemical compounds with % peak area >1 in the methanolic extract of *T. minuta* by GC-MS.

Peak	Compound name	Retention time(min)	Area %	Molecular formula	Molecular weight (g/mol)	CAS number
1	D-Limonene	6.664	1.43	C ₁₀ H ₁₆	136.23	138-86-3
2	Valeric acid	6.939	2.99	C ₅ H ₁₀ O ₂	102.13	109-52-4
3	3-methyl-1-butanol	7.915	14.77	C ₆ H ₁₂ O ₂	116.16	110-45-2
20	Pyrrolidine	12.214	1.37	C ₄ H ₉ N	71.12	123-75-1
22	Benzaldehyde	12.639	1.65	C ₇ H ₆ O	106.12	100-52-7
24	Diethyl pyrocarbonate	13.320	1.04	C ₆ H ₁₀ O ₅	162.14	1609-47-8
32	5-pyrimidinol,2-methyl-	16.226	3.15	C ₆ H ₆ N ₂ OS	142.18	4874-33-3
33	Supinine	16.314	2.22	C ₁₅ H ₂₅ NO ₄	283.37	551-58-6
35	Phytyl acetate	17.057	1.77	C ₂₂ H ₄₂ O ₂	338.57	10236-16-5
38	Heptadecanol-1	17.528	2.48	C ₁₇ H ₃₆ O	256.47	1454-85-9
41	Rivastigmine	18.250	1.41	C ₁₄ H ₂₂ N ₂ O ₂	250.34	123441-03-2
42	Pentadecanoic acid	18.330	2.71	C ₁₅ H ₃₀ O ₂	242.40	1002-84-2
47	9-octadecen-1-ol, (Z)-	19.920	4.51	C ₁₈ H ₃₆ O	268.48	143-28-2
49	Limonen-6-ol, pivalate	19.411	1.02	C ₁₅ H ₂₄ O ₂	236.36	10121-28-5
50	Nonadecanol-1	19.513	2.35	C ₁₉ H ₄₀ O	284.53	1454-84-8
52	Phytol	19.746	2.64	C ₂₀ H ₄₀ O	296.54	150-86-7
63	2-chloro-4.6-dimetoxypyrimidine	21.925	2.12	C ₆ H ₇ ClN ₂ O ₂	174.58	13223-25-1
64	Oleamide	21.967	1.23	C ₁₈ H ₃₅ NO	281.48	301-02-0
79	Squalene	25.385	2.59	C ₃₀ H ₅₀	410.73	111-02-4
89	1-heptacosanol	27.339	1.83	C ₂₇ H ₅₆ O	396.74	2004-39-9
99	β-sitosterol	29.260	6.07	C ₂₉ H ₅₀ O	414.72	83-46-5
100	Heptadecanoic acid	29.401	1.20	C ₁₇ H ₃₄ O ₂	270.46	506-12-7
102	Olean-12-en-3-one	29.752	7.47	C ₃₀ H ₄₈ O	424.71	638-97-1
106	α-amyrin	30.260	1.50	C ₃₀ H ₅₀ O	426.73	638-95-9

Table 4. 3: Preliminary screening of antibacterial activity of silver nanoparticles derived from leaves of *T. minuta* (n=3, mean values represented).

Bacterial strains	Zone of Inhibition (mm)	Antibiotic
Methicillin-resistant <i>Staphylococcus aureus</i>	16	0
<i>Escherichia coli</i>	10	18
<i>Staphylococcus aureus</i>	10	0
<i>Bacillus subtilis</i>	12	6
<i>Pseudomonas aeruginosa</i>	13	9

(mm) = inhibition zone including diameter of gel puncture

The antibacterial efficacy of the crude methanolic extract from *T. minuta* leaves are summarised in table 4.3 and were assessed by measuring the diameter of the inhibition zone of each well. The crude extract exhibited varying degrees of inhibition against 5 bacterial strains (MRSA, *E. coli*, *S. aureus*, *B. subtilis*, and *P. aeruginosa*). The antibiotic used for the gram-positive bacteria was streptomycin and gentamycin for gram-negative bacteria. In general, the crude methanolic extract proved to be more effective against gram-positive than gram-negative bacteria.

The antibacterial effects are similar to the activity shown from the essential oils of *T. patula* (Rondon et al., 2006) and *T. erecta* (Tripathi et al., 2012). These studies report flavonoids, alkaloids, and phenolic compounds are responsible for the antibacterial effects of extracts from *Tagetes* species (Tripathy et al., 2017).

4.5 Conclusion

Tagetes minuta has proved to be an important medicinal plant for human use as well as an insecticide and herbicide. Its applications extend pharmaceutically to include antidiabetic, anti-inflammatory, anticancer, and antimicrobial activities as evidenced from the phytochemicals found in abundance in the methanolic extract from the leaves

of *T. minuta*. The results of this study show potential for research regarding the regulation, use, and development of bioactive compounds sourced from medicinal plants. Additionally, the plethora of pharmacologically useful compounds sourced from *T. minuta* makes a convincing case for the status to be changed from invasive species to underutilised medicinal plant crop in South Africa.

CHAPTER 5: GREEN SYNTHESIS OF SILVER NANOPARTICLES FROM *TAGETES MINUTA* L. AND ITS ANTIBACTERIAL POTENTIAL

5.1 Abstract

The plant mediated synthesis of metallic nanoparticles is a fast-growing area of interest in the field of nanotechnology due to its eco-friendly approach. This study demonstrated the green synthesis of silver nanoparticles (AgNPs) using *Tagetes minuta* leaf extract. The AgNPs were characterised using UV-visible spectroscopy, transmission electron microscopy (TEM), energy dispersive X-ray (EDX) analysis and Fourier transform infrared (FTIR) spectroscopy. UV-visible spectrum of synthesised silver nanoparticles showed maximum peak at 442 nm. TEM revealed that the particles were spherical in shape and size ranging from 10 to 50 nm. The EDX spectrum confirmed the presence of silver metal. Preliminary antibacterial activity was determined using the agar well diffusion method, which showed growth inhibition against selected gram-positive and gram-negative bacteria.

Keywords: Antibacterial activity; energy dispersive x-ray; FTIR spectroscopy; silver nanoparticles; UV-visible spectrometry

5.2 Introduction

Nanotechnology is the blanket term for the synthesis, manipulation, and application of materials and structures that range between 1 and 100 nm, and is currently one of the most active research fields in material science (Sarsar et al., 2013; Padalia et al., 2015; Khatoon et al., 2017). Size, distribution, and morphology of nanoparticles determines their biological effectiveness (Krishnamurthy et al., 2012). Noble metal nanoparticles such as gold, silver, and platinum show promising applications in the fields of biotechnology, bioengineering, solar energy conversion, medicine, and water treatment (Dahl et al., 2007; Sharma et al., 2009).

Traditionally, nanoparticles are produced using chemical and physical methods, but these methods often face several caveats in the way of costs and environmental damage (Ramya and Subapriya, 2012). Green chemistry and green synthesis methods have since been adopted in the efforts of reducing both costs and generated hazardous waste, as well as decreasing the risk of safety concern over the products (Kaler et al., 2010). The biological method of synthesising nanoparticles occurs by redox reaction that builds towards larger and more complex systems beginning at the molecular level (Ramya and Subapriya, 2012). Based on green chemistry perspectives, the selection of an environmentally benign solvent and nontoxic chemicals in the synthesis of nanoparticles are imperative (Sharma et al., 2009). Natural material from microorganisms, enzymes, and plants are used for green synthesis of silver nanoparticles (Kotakadi et al., 2014; Vidhu and Philip, 2014).

Silver has been used as an antimicrobial agent for many decades, but the rising interest in the properties of metallic silver in the form of silver nanoparticles (AgNPs) is focused towards the increasing threat of antibiotic resistance (Roy and Das, 2015; Ojo et al., 2018). Ahmed et al. (2016) claimed that silver is the least toxic metal to animal cells that is used as an antimicrobial, and is effective against over 650 microorganisms from different classes such as gram-negative and gram-positive bacteria, fungi, and viruses. In order for silver to have any antimicrobial properties, it must first be in its ionized form, as the positive charge on the Ag^+ ions is vital in forming nanoparticles (Ahmed et al., 2016; AlSalhi et al., 2016). In conjunction, the medicinal properties of plants are attributed to its phytochemicals, which are in a position to reduce, cap, and stabilise Ag^+ ions (Chinnasamy et al., 2017; Tiwary and Jha, 2017). Organic chemicals present in plant

aqueous extracts (e.g. carbohydrates, proteins, phenols, flavonoids, terpenoids, alkaloids) are capable of donating an electron that results in the reduction of Ag^+ ions to Ag^0 (Roy and Das, 2015; Tiwary and Jha, 2017).

Nanotechnology also allows for the exploitation of antimicrobial properties of silver, as they are used in the form of nanoparticles. Silver nanoparticles display a large surface area to volume ratio – which allows for broad contact with the nuclear content of the bacteria, thus enabling the inactivation of DNA replication leading to growth inhibition (Ojo et al., 2017). It has been reported that AgNPs attach to the cell walls of bacteria and disturb the cell wall permeability and cellular respiration (Singh et al., 2008; Roy and Das, 2015).

Tagetes minuta is an aromatic herbaceous plant belonging to the Asteraceae family that has been reported for its high-grade essential oil that shows numerous uses in beverage, cosmetic, and pharmaceutical industries (Shirazi et al., 2014). It is found along river banks, forest margins, dry wooded valleys and hillsides in KwaZulu-Natal since its naturalisation in South Africa. The leaves of *T. minuta* are used in the preparation of traditional remedies for the management of stomach ailments, headaches, diarrhoea, malaria, and epilepsy (Karimian et al., 2014; Kyarimpa et al., 2014; Igwaran et al., 2017). The pharmacological effects of the leaf extracts are purported to be the result of various secondary metabolites including essential oils particularly abundant in monoterpenes, sesquiterpenes, flavonoids, aromatics, and thiophenes (Bansal et al., 1999; Brene et al., 2009; Sadia et al., 2013). The aims of this study were to employ the use of aqueous leaf extracts of *T. minuta* in the biosynthesis of AgNPs, characterise the particles, as well as to observe its antimicrobial activity against both gram-positive and gram-negative bacteria.

5.3 Methods and Materials

5.3.1 Collection of plant material

Fresh leaves of *T. minuta* were collected from the UKZN Westville campus (29.817°S 30.940°E) and air-dried for 6 weeks. A voucher specimen was confirmed and deposited at the UKZN Westville Herbarium (accession number 18216, voucher number 01).

5.3.2 Methanol extraction

The air-dried leaves were ground into a fine powder using a blender. Thirty grams of ground material was placed in a round bottom flask containing 50 ml of methanol. The flask was attached to Soxhlet apparatus and boiled for two 3-hour sessions to obtain the crude plant extract. The extract was filtered using filter paper (Whatman No. 1) and stored in an airtight jar at 4°C.

5.3.3 Fresh water extraction

Ten grams of fresh leaves were thoroughly washed with distilled water. The leaves were cut into small pieces and boiled for 10 min in 100 ml distilled water and filtered through Whatman No. 1 filter paper and stored in a concealed jar. The filtrate was used for the synthesis of silver nanoparticles.

5.3.4 Green synthesis of AgNPs

Aqueous solution (1 mM) of silver nitrate (AgNO_3) was prepared and used for the synthesis of AgNPs. The ratio of 1 ml methanol extract to 19 ml silver nitrate solution was used for the reduction of Ag^+ ions. The solution was then incubated in a hot water bath at 60°C until a colour change was observed. This process took 30 minutes. AgNP solution was centrifuged at 16000 rpm (20°C) for 5 min on the Eppendorf Centrifuge 5415R. Thereafter, the pellet was suspended in deionized water.

5.3.5 Characterisation of AgNPs

a) UV–Visible spectroscopy

UV–Vis spectra of synthesized nanoparticles were monitored on a spectrophotometer (Shimadzu UV-1800) in 350–700 nm range at a resolution of 2 nm.

b) Energy dispersive X-ray analysis

A drop of the AgNP solution was placed on a glass cover slip, mounted onto a brass stub and left to dry. The stub was then sputter coated with gold in a Polaron SC500 sputter coater and viewed with a Zeiss Ultra Plus field emission scanning electron microscope (FE-SEM) at 5 kV. Silver nanoparticle information by EDX microanalysis of elements present was captured using Aztec software coupled to an Oxford X-MAX detector (Oxford instruments, UK).

c) Fourier transform infrared (FTIR) spectral analysis

Each sample was centrifuged at 10000 rpm (Beckman Coulter Avanti J-E Centrifuge) for 30 min. The resulting pellet was suspended in deionized water and was used for further characterisation. Spectroscopic measurements of the sample (200 μ l) were determined using a PerkinElmer FTIR Spectrum One spectrophotometer in the diffuse reflectance mode operating at a spatial resolution of 4 cm^{-1} .

d) Transmission electron microscopy

A copper grid was submerged in the silver nanoparticles sample and thereafter air-dried. The size, shape, and overall morphology of the AgNPs was determined using the Zeiss UltraPlus FEGSEM at 200 kV.

5.3.6 Antibacterial screening

The preliminary antibacterial activity of the synthesised AgNPs was evaluated against *Escherichia coli* (ATCC 25218), *Staphylococcus aureus* (ATCC 29213), methicillin-resistant *Staphylococcus aureus* (ATCC BAA-1683), *Bacillus subtilis* and *Pseudomonas aeruginosa* (ATCC 25215). Mueller Hilton agar medium was prepared and poured into

sterile petri dishes to set at room temperature. The bacterial cultures were swabbed uniformly onto the plates using sterile cotton swabs. Wells of 5 mm in diameter were made using an agar corer (gel puncture). The samples were pipetted into the wells (90 μ l), and the plates were incubated at 37°C. The effect of the samples on the bacteria was assessed 24 hours later by measuring diameter of the zone of inhibition (mm).

5.4 Results and Discussion

The fresh suspension of *T. minuta* was a light green in colour (Fig 5.1 a). However, after the addition of silver nitrate and exposing to heat in a 60°C water bath for 30 mins, the suspension turned a dark brown colour (Fig 5.1 b). The reduction of silver ions into silver nanoparticles during exposure to the plant extract is indicated by this colour change. It appears that the intensity of the colour reaction was directly proportional to the formation of the AgNPs. The UV-vis spectra recorded from the methanolic extract of *T. minuta* is presented in Fig 5.2, where the maximum absorption peak is shown to be at 442 nm. Surface plasmon resonance (SPR) is the collective oscillation of electrons in the conduction band on a nanoparticle surface (Suman et al., 2014). Siddiqui et al. (2018) claimed that the absorption band from 400 to 500 nm represents the dipole component of the SPR of silver nanoparticles. This implies that the peak wavelength, width, and effect of these resonances yield a unique spectral fingerprint for a plasmonic nanoparticle with a distinct size and shape. Using high-resolution TEM, Mock et al. (2002) showed that silver nanoparticles that peak in the range of 410 – 500 nm are spherical; whereas in the range of 500 – 700 nm, particles are usually triangular or pentagonal. This observation strongly suggests that the AgNPs synthesised in this study were spherical in shape.

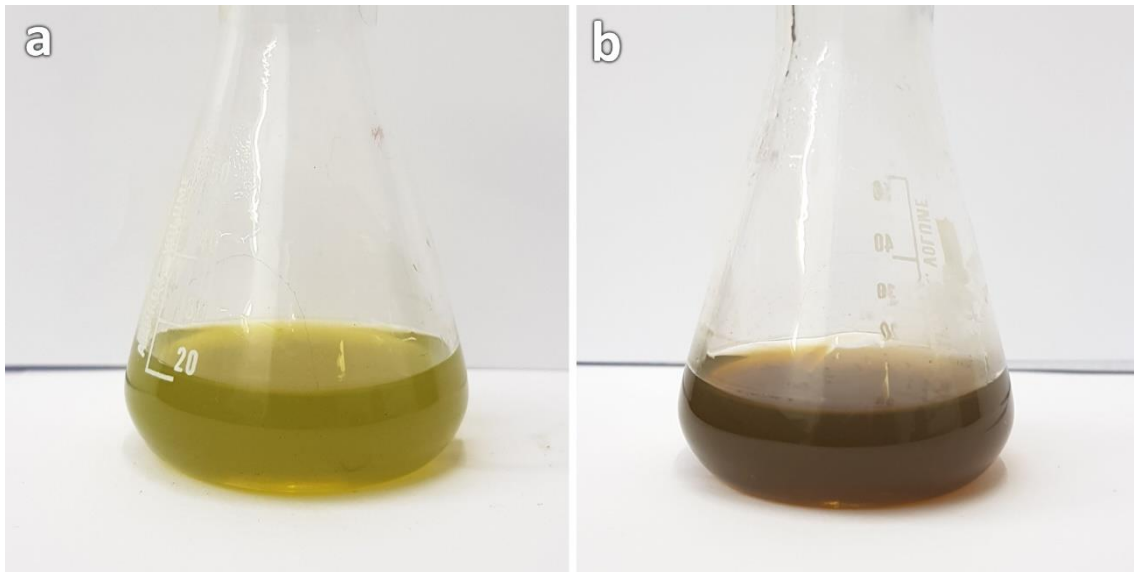


Figure 5. 1 Images of silver nanoparticle synthesis using *T.minuta* extract from leaves: a) Silver nitrate solution with leaf extract. b) Synthesised silver nanoparticle solution after heating for 30 minutes.

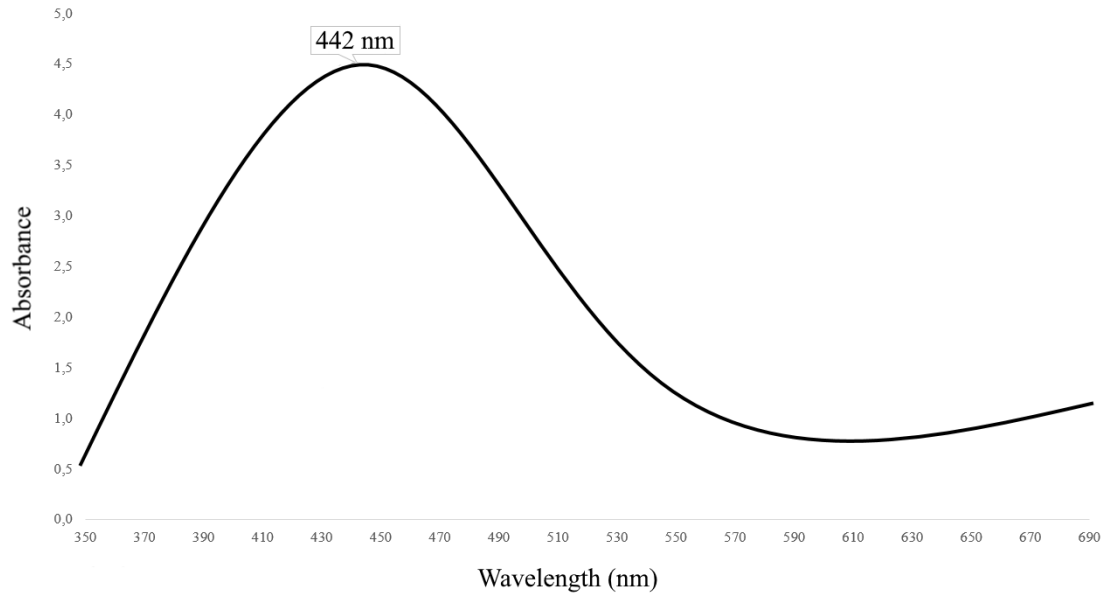


Figure 5. 2 UV-Vis absorption spectra of reduction of silver ions to silver nanoparticles after 30 min reaction.

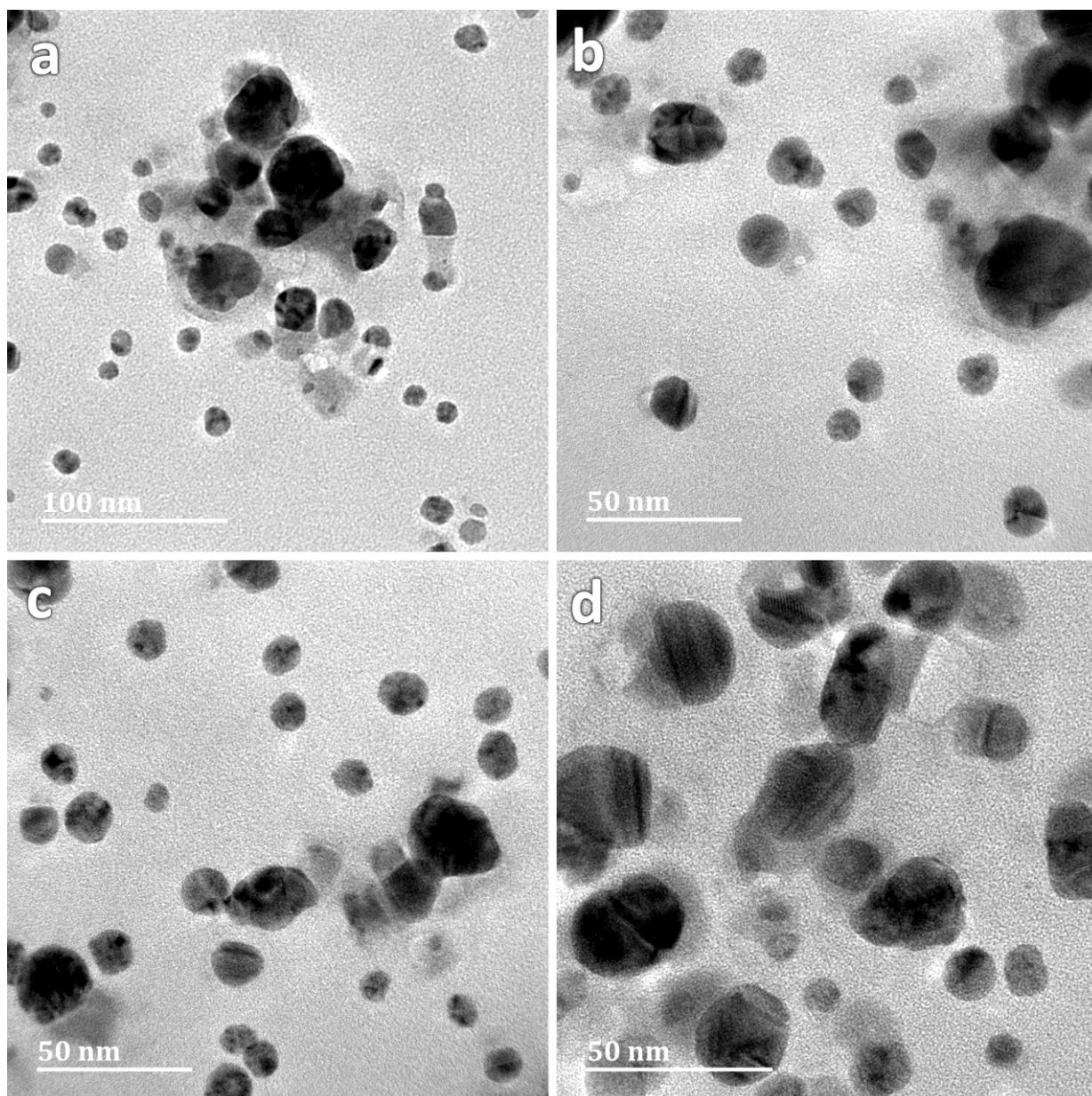


Figure 5. 3 HR-TEM images of silver nanoparticles in low and high magnification.

The shape and size of the AgNPs from *T. minuta* leaf extracts are depicted in Fig 5.3. The optical and electronic properties of AgNPs are significantly influenced by their shape (Kim et al., 2007). The particles appear to be uniformly spherical. The sizes ranged from 7 – 42 nm and the average diameter was found to be 11.75 nm (Fig 5.4). Similarly-shaped silver nanoparticles were synthesised using *T. patula* leaf extract (Elemike et al., 2018) and *T. erecta* flower extract (Padalia et al., 2015). The AgNPs were predominantly

monodispersed and stable. Organic material derived from the plant extraction process causes the inherent functional group capping, which in turn offers stability and prevents agglomeration (Shaik et al., 2014).

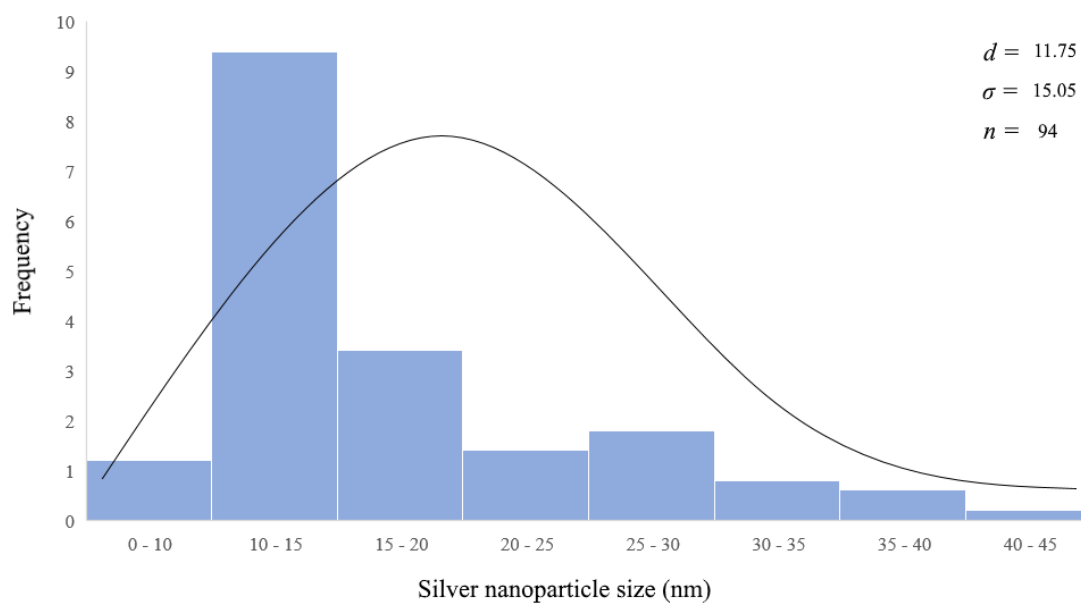


Figure 5. 4 Frequency histogram for silver nanoparticle size range.

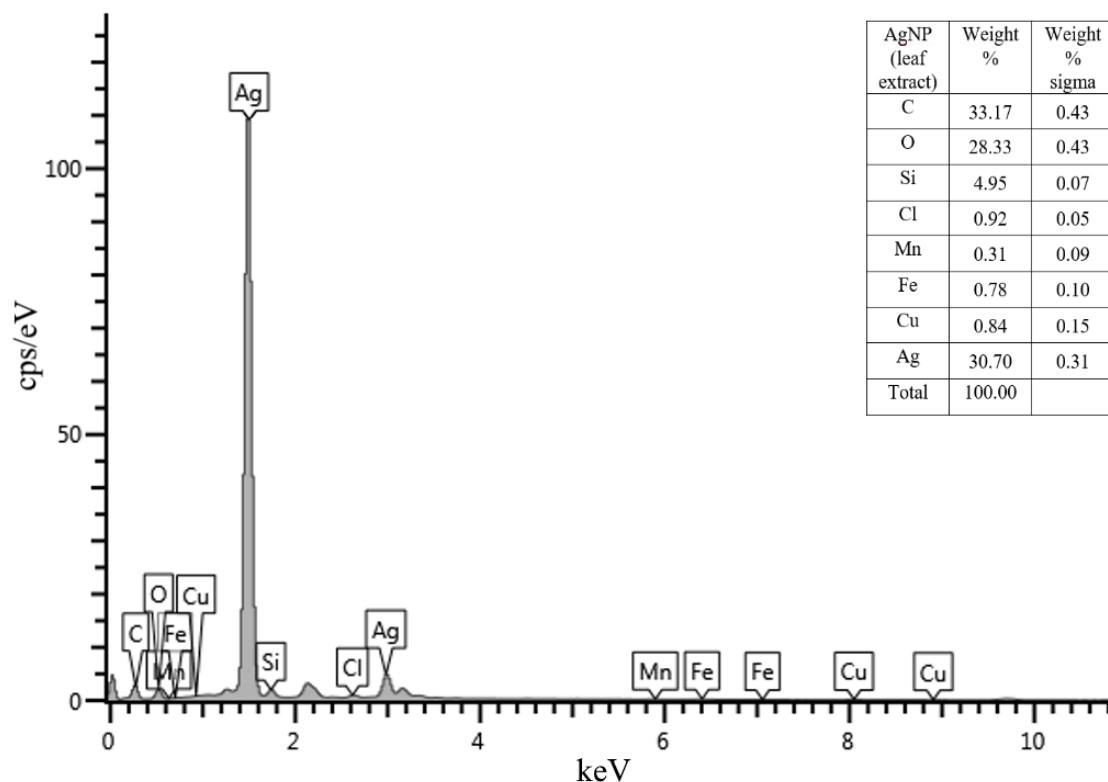


Figure 5. 5 EDX spectrum of synthesised silver nanoparticles using leaf extract of *Tagetes minuta*.

A strong signal of silver is evident from the EDX spectrum at 1.5 keV and a weaker signal at 3 keV (Fig 5.5) confirming the presence of elemental silver. A similar spectral profile for silver has been reported by Hedaginal and Taranath (2017) for the leaf extract of *Thunbergia alata*. Weak signals of carbon, oxygen, iron, manganese, silicon, chlorine, and copper are also evident. The presence of silicon, carbon, and copper is likely to be from the support glass cover slip and grid used in the methodology for EDX. Signals of other trace elements may be the result of x-ray emission from organic compounds involved in the capping of the nanoparticles and are bound to the surface of the nano-silver (Singh et al., 2015).

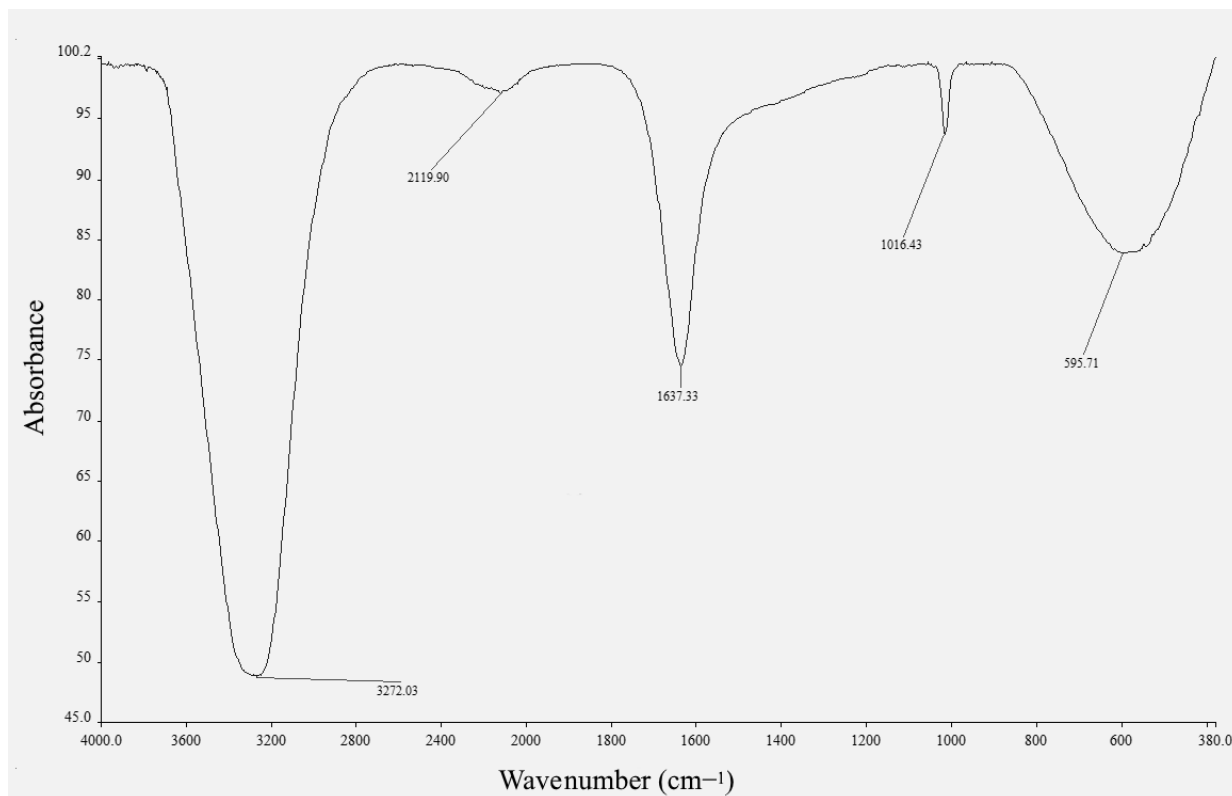


Figure 5. 6 FTIR spectrum of the synthesised silver nanoparticles using leaf extract of *Tagetes minuta*.

The known active ingredients in *T. minuta* are terpenoids viz. limonene, caryophyllene, and eucarvone (Tiwari et al., 2016; Igwaran et al., 2017); amines viz. pyrrolidine (Meshkalasadat et al., 2010); ketones viz. tagetone, dihydrotagetone, tagetenone (Gil et al., 2002; Mohammad et al., 2010); and hydrocarbons viz. ocimene (Igwaran et al., 2017). The FTIR spectrum analysis of biosynthesised silver nanoparticles are displayed in Fig 5.6 which manifest absorption peaks located at the regions between 600 cm^{-1} and 3300 cm^{-1} in order to identify the functional groups of the extract involved in the reduction of the synthesised AgNPs. Prominent peaks on the FTIR spectrum are marked at 3272 cm^{-1} , 2119 cm^{-1} , 1637 cm^{-1} , 1016 cm^{-1} , and 595 cm^{-1} . The absorption peak at 3272 cm^{-1} is assigned to -OH stretching in alcohols and phenolic compounds, which indicates the possible involvement of the known terpenoids (Awwad et al., 2013; Elemike et al., 2018). The peak at 2119 cm^{-1} suggest $\text{-C}\equiv\text{C}$ and -CH groups that are found in terpenoid ring structures and is close to that reported for aliphatic aldehydes (Shaik et al., 2014;

Hedaginal and Taranath, 2017). The absorption peak at 1637 cm^{-1} arose due to C=C stretches that are typical of aliphatic and aromatic amine structures and alkenes (Jha et al., 2018). Peaks below the value 1300 cm^{-1} are usually indicative of C–C and C–O groups, but are not as reliably interpreted due to a larger number of different vibrations (Kumar et al., 2017).

Table 5. 1 : Preliminary screening of antibacterial activity of silver nanoparticles derived from leaves of *T. minuta* (n=3, mean values represented).

Bacterial strains	Zone of Inhibition (mm)	Antibiotic
Methicillin-resistant <i>Staphylococcus aureus</i>	9	0
<i>Escherichia coli</i>	11	10
<i>Staphylococcus aureus</i>	8	0
<i>Bacillus subtilis</i>	9	6
<i>Pseudomonas aeruginosa</i>	7	9

(mm) = inhibition zone including diameter of gel puncture

The antibacterial efficacy of silver nanoparticles synthesised from *T. minuta* leaves are summarised in table 5.1 and were assessed by measuring the diameter of the zone of inhibition of each well. The AgNPs exhibited varying degrees of inhibition against 5 bacterial strains (MRSA, *E. coli*, *S. aureus*, *B. subtilis*, and *P. aeruginosa*). The antibiotic used for the gram-positive bacteria was streptomycin and gentamycin for gram-negative bacteria. In general, the silver nanoparticles were more effective against gram-positive than gram-negative bacteria.

The AgNPs were least effective against *E. coli* and *P. aeruginosa*, which showed inhibition zones very similar to that of the antibiotic (gentamycin). Sondi and Salopek-Sondi (2014) demonstrated silver nanoparticles penetrating the bacterial cell walls of *E. coli*, but growth inhibition was dependent on the concentration of the AgNPs used, and in most instances would only delay the growth of the bacterial colonies. Pal et al. (2007)

studied the effects of nanoparticle shape against gram-negative bacteria, and found that spherical and rod-shaped nanoparticles are less effective than triangular-shaped nanoparticles. This may explain the ineffectiveness of the AgNPs synthesised in this study against *P. aeruginosa*.

The bacterial growth of the gram-positive bacteria (MRSA, *S. aureus*, and *B. subtilis*) was more severely inhibited by the AgNPs synthesised in this study. Guzman et al. (2012) highlighted the importance of the size of AgNPs against gram-positive bacteria, concluding that silver particles between 9 and 14 nm in diameter showed the highest activity. In Fig 5.4, it is evident that the silver nanoparticles synthesised in this study that were under 15 nm in diameter were the most frequent, which likely contributed to the higher antibacterial activity. It has been reported that AgNPs induce the inactivation of DNA replication and thus protein synthesis in gram-positive bacteria by interacting with present thiol groups (Ojo et al., 2017).

5.5 Conclusion

This study provided a simple and rapid method for the biosynthesis of AgNPs using *T. minuta* aqueous leaves extract. The secondary metabolites present in *T. minuta* perform the dual function of formation and stabilisation of AgNPs through the action of various terpenoid and amine compounds identified. The AgNPs were further confirmed by using UV-Vis spectroscopy, EDX, and FTIR techniques. The shape of the nanoparticles was determined to be spherical using HR-TEM. The biosynthesised AgNPs also exhibited antimicrobial activity against selected gram-positive and gram-negative bacteria strains, which is in part due to the size and shape of the AgNPs. Hence, this study supports the efficiency of plant mediated green synthesis of AgNPs, which has the potential to be utilised in various clinical applications.

CHAPTER 6: GENERAL CONCLUSIONS AND RECOMMENDATIONS FOR FURTHER RESEARCH

6.1 Main findings

Tagetes minuta L. is an annual herb that is used as ethnomedicine worldwide. It is reported to have numerous medicinal benefits such as treatment for respiratory inflammations, stomach pains, chest infections, coughs, and as well as a healing effect on wounds, cuts, and calluses. Despite its rich literature in ethnomedicinal uses, the phytochemicals that are responsible for its therapeutic properties have not been reported on. Additionally, the foliar structures that produce, store, and exude these phytochemicals are not well understood. The aims of this study were to critically analyse the leaves of *T. minuta* with regard to its micromorphology, histochemistry, phytochemistry, green synthesis of silver nanoparticles, and potential for antibacterial activity.

The leaves of *T. minuta* contain two types of foliar structures, viz. non-glandular trichomes and secretory cavities. In Chapter 3, the leaves were studied using stereomicroscopy, scanning electron microscopy (SEM), and transmission electron microscopy (TEM). Stereomicroscopy showed a sparse coverage of trichomes that group along the midvein and major venation network, suggesting that they do not play a large role in physical protection to the plant. The secretory cavities can be seen macroscopically and appear as large pellucid yellow glands between 70 and 200 μm in diameter. Scanning electron microscopy revealed the secretory cavity openings along the anomocytic stoma. The trichomes were deduced to be uniseriate and non-glandular, reaching up to 200 μm in length. TEM was used to view the cells within the secretory cavity, which showed an increase in lipid and vesicle production within the organelles as compared to surrounding cells. Histochemical analyses showed that the non-glandular trichomes were able to store various classes of phytochemicals, in contrast to the literature suggesting non-glandular trichomes are incapable of phytochemicals. This work is novel in terms of the micromorphology of *T. minuta*.

Crude organic solvent extracts derived from the leaves of *T. minuta* were investigated in Chapter 4. Phytochemical tests were used to determine the main chemical classes present in the hexane, chloroform, and methanol crude extracts, revealing the presence of carbohydrates,

alkaloids, amino acids, sterols, saponins, terpenoids, phenols, and lipids. The crude methanolic extract was further subjected to analysis using GC-MS, which showed that the compounds with the highest composition percentage were 9-octadecen-1-ol (4.51 %), β -sitosterol (6.07 %), olean-12-en-3-one (7.47 %), and 3-methyl-1-butanol (14.77 %). These compounds are discussed in Chapter 4 as having various pharmacological benefits. Antibacterial screening using the methanolic extract showed greater growth inhibition on gram positive than gram negative bacteria.

Green synthesis of silver nanoparticles was achieved in Chapter 5 using the methanolic extract. Using TEM, the nanoparticles were proved to be spherical in shape and ranged between 10 and 50 nm in size. The presence of elemental silver was determined using EDX analysis and polymeric chemical groups assessed using FTIR spectroscopy. The silver nanoparticles proved to have a greater effect on the growth inhibition of gram positive bacteria.

6.2 Future recommendations

With regard to microscopy, TEM analysis could be taken further to include the intracellular components of the non-glandular trichomes to determine whether they produce as well as store secondary metabolites. Future research could compare and contrast the percentage composition of phytochemicals from the organic solvent extracts to that of the essential oils of *T. minuta*, as well as compare percentage composition from extracts taken at different growth development and flowering stages of the plant. Silver nanoparticles derived from the methanolic extract can be further investigated in terms of antimicrobial activity in order to determine the minimum inhibitory concentrations. Additionally, *T. minuta* can be used in cell culture for possible propagation, changing its status in South Africa from invasive weed to underutilised medicinal crop.

CHAPTER 7: REFERENCES

- Abdul, W.S., Hajrah, N.H., Sabir, J.S.M., Al-Garni, S.M., Sabir, M.J., Kabli, S.A., Saini, K.S., Bora, R.S., 2018. Therapeutic role of *Ricinus communis* L. and its bioactive compounds in disease prevention and treatment. *Asian Pacific Journal of Tropical Medicine* 11, 177–185.
- Achika, J.I., Arthur, D.E., Gerald, I., Adedayo, A., 2014. A review on the phytoconstituents and related medicinal properties of plants in the Asteraceae family. *IOSR Journal of Applied Chemistry* 7, 1–8.
- Adebooye, O.C., Hunsche, M., Noga, G., Lankes, C., 2012. Morphology and density of trichomes and stomata of *Trichosanthes cucumerina* (Cucurbitaceae) as affected by leaf age and salinity. *Turkish Journal of Botany* 36, 328–335.
- Adedeji, O., Jewoola, O.A., 2008. Importance of leaf epidermal characters in the Asteraceae family. *Notulae Botanicae Horti Agrobotanici Cluj-Napoca* 36, 7–16.
- Agrawal, A.A., 2006. Macroevolution of plant defense strategies. *Trends in Ecology and Evolution* 22, 103–109.
- Agrawal, A.A., Fishbein, M., 2006. Plant defense systems. *Ecology* 87 Supplement, 132–149.
- Ahmed, S., Ahmad, M., Swami, B.L., Ikram, S., 2016. A review on plants extract mediated synthesis of silver nanoparticles for antimicrobial applications: a green expertise. *Journal of Advanced Research* 7, 17–28.
- Algotsson, E., 2009. Biological Diversity. In Strydom, H.A. and King, N.D., eds. *Environmental Management in South Africa*. Cape Town: Juta, 97–125.
- Al-Musayeib, N.M., Mohamed, G.A., Ibrahim, S.R.M., Ross, S.A., 2014. New thiophene and flavonoid from *Tagetes minuta* leaves growing in Saudi Arabia. *Molecules* 19, 2819–2828.
- AlSalhi, M.S., Devanesan, S., Alfuraydi, A.A., Vishnubalaji, R., Munusamy, M.A., Murugan, K., Nicoletti, M., Benelli, G., 2016. Green synthesis of silver nanoparticles using *Pimpinella anisum* seeds: antimicrobial activity and cytotoxicity on human neonatal skin stromal cells and colon cancer cells. *International Journal of Nanomedicine* 11, 4439–4449.

Andreotti, R., Garcia, M.V., Cunha, R.C., Barros, J.C., 2013. Protective action of *Tagetes minuta* (Asteraceae) essential oil in the control of *Rhipicephalus microplus* (Canestrini, 1887) (Acari: Ixodidae) in a cattle pen trial. *Veterinary Parasitology* 197, 341–345.

Arora, K., Batish, D.R., Singh, H.P., Kohli, R.K., 2015. Allelopathic potential of the essential oil of wild marigold (*Tagetes minuta* L.) against some invasive weeds. *Journal of Environmental and Agricultural Sciences* 3, 56–60.

Arora, S. and Kumar, G., 2018. Micro-morphological descriptions on *Cenchrus* species from Rajasthan (India). *Annals of Plant Sciences* 7, 2141–2145.

Aschenbrenner, A., Horakh, S., Spring, O., 2013. Linear glandular trichomes of *Helianthus* (Asteraceae): morphology, localization, metabolite activity and occurrence. *Annals of Botany* 5, 28–37.

Athuman, I., Innocent, E., Machumi, F., Augustino, S., Kisinza, W., 2016. Repellency properties of oils from plants traditionally used as mosquito repellents in Longido district, Tanzania. *International Journal of Mosquito Research* 3, 4–8.

Awwad, A.M., Salem, N.M., Abdeen, A.O., 2013. Green synthesis of silver nanoparticles using carob leaf extract and its antibacterial activity. *International Journal of Industrial Chemistry* 4, 29–35.

Balandrin, M.F., Klocke, J.A., Wurtele, E.S., Bollinger, W.H., 1985. Natural plant chemicals: source of industrial and medicinal materials. *Science* 228, 1154–1160.

Balcke, G.U., Bennewitz, S., Bergau, N., Athmer, B., Henning, A., Majovsky, P., Jimenez-Gomez, J.M., Hoehenwarter, W., Tissier, A., 2017. Multi-omics of tomato glandular trichomes reveals distinct features of central carbon metabolism supporting high productivity of specialized metabolites. *The Plant Cell*, 29, 960–983.

Balunas, M.J. and Kinghorn, A.D., 2005. Drug discovery from medicinal plants. *Life Sciences* 78, 431–441.

Bandana, K., Raina, R., Kumari, M., Rani, J., 2018. *Tagetes minuta*: an overview. *International Journal of Chemical Studies* 6, 3711–3717.

- Bansal, R.P., Bahl, S.N., Garg, A.A., Sharma, N.S., Ram, M., Kumar, S., 1999. Variation in quality of essential oil distilled from vegetative and reproductive stages of *Tagetes minuta* crop grown in north Indian plains. *Journal of Essential Oil Research* 11, 747–752.
- Bargah, R.K., 2015. Preliminary test of phytochemical screening of crude ethanolic and aqueous extract of *Moringa pterygosperma* Gaertn. *Journal of Pharmacognosy and Phytochemistry* 4, 7–9.
- Barkley, T.M., Brouillet, L., Strother, J.L., 2006. The Asteraceae Family. *Flora of North America* 19, 3–12.
- Bartoli, A., Galati, B.G., Tortosa, R.D., 2011. Anatomical studies of the secretory structures: glandular trichomes and ducts in *Grindelia pulchella* Dunal (Astereae, Asteraceae). *Flora* 206, 1063–1068.
- Bezerra, L.D.A., Mangabeira, P.A.O., de Oliveira, R.A., Costa, L.C.D.B., da Cunha, M., 2018. Leaf blade structure of *Verbesina macrophylla* (Cass.) F.S. Blake (Asteraceae): ontogeny, duct secretion mechanism and essential oil composition. *Plant Biology (Stuttgart, Germany)* 20, 433–443.
- Bin Sayeed, M.S. and Amen, S.S., 2015. Beta-sitosterol: a promising but orphan nutraceutical to fight against cancer. *Nutrition and Cancer* 1, 1–7.
- Bisi-Johnson, M.A., Obi, C.L., Samuel, B.B., Eloff, J.N., Okoh, A.I., 2017. Antibacterial activity of crude extracts of some South African medicinal plants against multidrug resistant etiological agents of diarrhoea. *BMC Complementary and Alternative Medicine* 17, 321–329.
- Bombo, A.B., Filartiga, A.L., Garcia, V.L., Apezato-da-Gloria, B., 2017. Secretory structures in *Aldama* species (Heliantheae – Asteraceae): Morphology, histochemistry and composition of essential oils. *Flora* 228, 39–49.
- Bremer, K., 1987. Tribal interrelationships of the Asteraceae. *Cladistics* 3, 210–253.
- Bremer, K., Jansen, R.K., Karis, P.O., Kallersjo, M., Keeley, S.C., Kim, K., Michaels, H.J., Palmer, J.D., Wallace, R.S., 1992. A review of the phylogeny and classification of the Asteraceae. *Nordic Journal of Botany* 12, 141–148.

- Brene, K., Tournayre, P., Fernandez, X., Meierhenrich, U.J., Brevard, H., Joulain, D., 2009. Identification of odour impact compounds of *Tagetes minuta* essential oil: comparison of two GC-olfactometry methods. *Journal of Agricultural and Food Chemistry* 57, 8572–8580.
- Brewer, C.A., Smith, W.K., Vogelmann, T.C., 1991. Functional interaction between leaf trichomes, leaf wettability and the optical properties of water droplets. *Plant, Cell, & Environment* 14, 955–962.
- Buda, G.J., Isaacson, T., Matas, A.J., Paolilo, D.J. and Rose, J.K.C., 2009. Three-dimensional imaging of plant cuticle architecture using confocal scanning laser microscopy. *The Plant Journal* 60, 378–385.
- Buvat, R., 1989. Ontogeny, cell differentiation, and structure of vascular plants. Springer-Verlag Berlin Heidelberg, 56.
- Cappellari, L.D.R., Santoro, M.V., Nievas, F., Giordano, W., Banchio, E., 2013. Increase of secondary metabolite content in marigold by inoculation with plant growth-promoting rhizobacteria. *Applied Soil Ecology* 70, 16–22.
- Cardellina, J.H., 2002. Challenges and opportunities confronting the botanical dietary supplement industry. *Journal of Natural Products* 65, 1073–1084.
- Chaffey, N., 2006. Esau's Plant Anatomy, Meristems, Cells, and Tissues of the Plant Body: Their Structure, Function, and Development. 3rd edn. *Annals of Botany* 99, 785–786.
- Chamorro, E.R., Ballerini, G., Sequeira, A.F., Velasco, G.A., Zalazar, M.F., 2008. Chemical composition of essential oil from *Tagetes minuta* L. leaves and flowers. *Journal of the Argentine Chemical Society* 96, 80–86.
- Chinnasamy, C., Tamilselvan, P., Karthik, V. and Karthik, B., 2017. Optimization and characterization studies on green synthesis of silver nanoparticles using response surface methodology. *Advances in Natural and Applied Sciences* 11, 214–221.
- Cid, C.V., Rodriguez, J.H., Salazar, M.J., Blanco, A., Pignata, M.L., 2016. Effects of co-cropping *Bidens pilosa* (L.) and *Tagetes minuta* (L.) on bioaccumulation of Pb in *Lactuca sativa* (L.) growing in polluted agricultural soils. *International Journal of Phytoremediation* 18, 908–917.

Colombo, P.M. and Rascio, N., 1977. Ruthenium red staining for electron microscopy of plant material. *Journal of Ultrastructure Research* 60, 135–139.

Cunningham, A.B., 1990. Whose knowledge and whose resources? Ethnobotanists as brokers between two worlds. Occasional paper 82. Institute of National Resources, Pietermaritzburg, South Africa, 7.

Dahl, J.A., Maddux, B.L., Hutchison, J.E., 2007. Toward greener synthesis. *Chemical Reviews* 107, 2228–2269.

Dauskardt, R.P.A., 1990. The changing geography of traditional medicine: urban herbalism on the Witwatersrand, South Africa. *GeoJournal* 22, 275–283.

Demarco, D., 2017. Histochemistry of single molecules: methods and protocols. *Methods in Molecular Biology* 1560, 313–330.

Devika, R. and Koilpillai, J., 2012. Phytochemical screening studies of bioactive compounds of *Tagetes erecta*. *International Journal of Pharma and Bio Sciences* 3, 596–602.

Dixit, P., Tripathi, S., Verma, N.K., 2013. A brief study on marigold (*Tagetes* species): A review. *International Research Journal of Pharmacy* 4, 43–48.

Elemike, E.E., Onwudiwe, D.C., Abiola, O.K., Ibe, K.A., 2018. Surface characterisation and reaction kinetics of silver nanoparticles mediated by the leaf and flower extracts of French marigold (*Tagetes patula*). *IET Nanobiotechnology* 12, 957–962.

Fabricant, D.S. and Farnsworth, N.R., 2001. The value of plants used in traditional medicine for drug discovery. *Environmental Health Perspectives* 109, 69–75.

Fahn, A., 1979. Secretory tissues in plants. Academic Press, London, 302.

Fahn, A., 2000. Structure and function of secretory cells. *Advances in Botanical Research* 31, 219–238.

Farjana, N., Rowshanul, H.M., Zahangir, A.S., Rezaul, M.K., Apurba, K.R., Shahriar, Z., 2009. Toxicological evaluation of chloroform fraction of flower of *Tagetes erecta* Linn. on rats. *International Journal of Drug Development and Research* 1, 161–165.

Filartiga, A.L., Bombo, A.B., Garcia, V.L., Appezzato-da-Gloria, B., 2017. Belowground organs of four Brazilian *Aldama* (Asteraceae) species: morphoanatomical traits and essential oil profile. *South African Journal of Botany* 113, 150–159. *Plant Biology* 20, 433–443.

Gakuubi, M.M., Wanzala, W., Wagacha, J.M., Dossaji, S., 2016. Bioactive properties of *Tagetes minuta* L. (Asteraceae) essential oils: A review. *American Journal of Essential Oils and Natural Products* 4, 27–36.

Galdon-Armero, J., Fullana-Pericas, M., Mulet, P.A., Conesa, M.A., Martin, C., Galmes, J., 2018. The ratio of trichomes to stomata is associated with water use efficiency in *Solanum lycopersicum* (tomato). *The Plant Journal* 96, 607–619.

Ge, Y., Zhang, H., Lei, J., Wang, K., 2018. Chemical constituents of *Viburnum odoratissimum* and their cytotoxic activities. *Chemistry of Natural Compounds* 54, 600–602.

Gil, A., Ghersa, C.M., Susana, P., 2002. Root thiophenes in *Tagetes minuta* L. accessions from Argentina: genetic and environmental contribution to changes in concentration and composition. *Biochemical Systematics and Ecology* 30, 1–13.

Gonzales, W.L., Negritto, M.A., Suarez, L.H., Gianoli, E., 2008. Induction of glandular and non-glandular trichomes by damage in leaves of *Madia sativa* under contrasting water regimes. *Acta Oecologica* 33, 128–132.

Gupta, H.S. and De, D.N., 1985. Uptake and accumulation of acridine orange by plant cells. *Proceedings of the National Academy of Sciences* 6, 653–660.

Gutierrez, R.M.P., Luna, H.H.S., Garrido, H., 2006. Antioxidant activity of *Tagetes erecta* essential oil. *Journal of the Chilean Chemical Society* 51, 883–886.

Guzman, M., Dille, J., Godet, S., 2012. Synthesis and antibacterial activity of silver nanoparticles against gram-positive and gram-negative bacteria. *Nanomedicine: Nanotechnology, Biology, and Medicine* 8, 37–45.

Hedaginal, B.R. and Taranath, T.C., 2017. Characterization and antimicrobial activity of biogenic silver nanoparticles using leaf extract of *Thunbergia alata* Bojer ex Sims. *International Journal of Pharmaceutical Sciences and Research* 8, 2070–2081.

Hegebarth, D., Buschhaus, C., Wu, M., Bird, D., Jetter, R., 2016. The composition of surface wax on trichomes of *Arabidopsis thaliana* differs from wax on other epidermal cells. *The Plant Journal* 88, 762–774.

Hethelyi, E., Danos, B., Tetenyi, P., 1986. GC-MS analysis of the essential oils of four *Tagetes* species and the anti-microbial activity of *Tagetes minuta*. *Flavour and Fragrance Journal* 1, 169–173.

Hosseinzadeh, S., Jafarikukhdan, A., Hosseini, A., Armand, R., 2015. The application of medicinal plants in traditional and modern medicine: a review of *Thysmusvulgaris*. *International Journal of Clinical Medicine* 6, 635–642.

Ibrahim, S.R.M. and Mohamed, G.A., 2017. Thiotagetin A, a new cytotoxic thiophene from *Tagetes minuta*. *Natural Product Research* 31, 543–547.

Ibrahim, S.R.M., Abdallah, H.M., El-Halawany, A.M., Esmat, A., Mohamed, G.A., 2018a. Thiotagetin B and tagetannins A and B, new acetylenic thiophene and digalloyl glucose derivatives from *Tagetes minuta* and evaluation of their *in vitro* antioxidative and anti-inflammatory activity. *Fitoterapia* 125, 78–88.

Igwaran, A., Iweriebor, B.C., Okoh, S.O., Nwodu, U.U., Obi, L.C., Okoh, A.I., 2017. Chemical constituents, antibacterial and antioxidant properties of the essential oil flower of *Tagetes minuta* grown in Cala community Eastern Cape, South Africa. *BMC Complementary and Alternative Medicine* 17, 351–361.

Jensen, W.A., 1962. *Botanical Histochemistry – principles and practice*. University of California, Berkeley. San Francisco and W. H. Freeman, 408.

Jha, B., Rao, M., Prasad, K., ha, A.K., 2018. Evaluation of antimicrobial activity of silver nanoparticles from *Piper betle* leaves against human and plant pathogens. *AIP Conference Proceedings* 1953, 030257.

Johnson, H.B., 1975. Plant pubescence: An ecological perspective. *Botanical Review* 41, 233–258.

Kaler, A., Patel, N., Banerjee, U.C., 2010. Green synthesis of silver nanoparticles. *Current Research and Information on Pharmaceutical Science* 11, 68–71.

Karimian, P., Kavooosi, G., Amirghofran, Z., 2014. Anti-oxidative and anti-inflammatory effects of *Tagetes minuta* essential oil in activated macrophages. *Asian Pacific Journal of Tropical Biomedicine* 4, 219–277.

Kariyat, R.R., Hardison, S.B., Ryan, A.B., Stephenson, A.G., De Moraes, C.M., Mescher, M.C., 2018. Leaf trichomes affect caterpillar feeding in an instar-specific manner. *Communicative and Integrative Biology* 11, 1–6.

Kariyat, R.R., Smith, J.D., Stephenson, A.G., De Moraes, C.M., Mescher, M.C., 2017. Non-glandular trichomes of *Solanum carolinense* deter feeding by *Manduca sexta* caterpillars and cause damage to the gut peritrophic matrix. *Proceedings of the Royal Society B* 284, 20162323.

Kataria, D., Chahal, K.K., Kumar, A., 2016. Chemical transformation of carotol isolated from carrot seed oil. *Asian Journal of Chemistry* 28, 1790–1792.

Khatoon, N., Mazumder, J.A., Sardar, M., 2017. Biotechnological applications of green synthesized silver nanoparticles. *Journal of Nanosciences: Current Research* 2, 107.

Kim, H.J., Han, J., Kim, S., Lee, H.R., Shin, J., Cho, J., Kim, Y.H., Lee, H.J., Kim, B., Choi, D., 2011. Trichome density of main stem is tightly linked to PepMoV resistance in chili pepper (*Capsicum annuum* L.). *International Journal of Plant Breeding Research* 122, 1051–1058.

Kim, J.S., Kuk, E., Yu, K.N., Kim, J.H., Park, S.J., Lee, H.J., Kim, S.H., Park, Y.K., Park, Y.H., Hwang, C.Y., Kim, Y.K., Lee, Y.S., Jeong, D.H., Cho, M.H., 2007. Antimicrobial effects of silver nanoparticles. *Nanomedicine* 3, 95–101.

Kimutai, A., Ngeiywa, M., Mulaa, M., Njagi, P.G.N., Ingonga, J., Nyamwamu, L.B., Ombati, C., Ngumbi, P., 2017. Repellent effects of the essential oils of *Cymbogon citratus* and *Tagetes minuta* on the sandfly, *Phlebotomus duboscqi*. *BMC Research Notes* 10, 99–103.

Kotakadi, V.S., Gaddam, S.A., Rao, Y.S., Prasad, T.N.V.K.V., Reddy, A.V., Gopal, D.V.R.S., 2014. Biofabrication of silver nanoparticles using *Andrographis paniculate*. *European Journal of Medicinal Chemistry* 73, 135–140.

Krishnamurthy, N.B., Nagaraj, B., Malakar, B., Liny, P., Dinesh, R., 2012. Green synthesis of gold nanoparticles using *Tagetes erecta* L. (marigold) flower extract and evaluation of their antimicrobial activities. *International Journal of Pharma and Bio Sciences* 3, 212–221.

- Kudumela, R.G. and Masoko, P., 2017. *In vitro* assessment of selected medicinal plants used by the Bapedi community in South Africa for treatment of bacterial infections. *Journal of Evidence-Based Integrative Medicine* 23, 1–10.
- Kumar, B., Smita, K., Cumbal, L., Debut, A., 2017. Green synthesis of silver nanoparticles using Andean blackberry fruit extract. *Saudi Journal of Biological Sciences* 24, 45–50.
- Kyarimpa, C.M., Böhmendorfer, S., Wasswa, J., Kiremire, B.T., Ndiege, I.O., Kabasa, J.D., 2014. Essential oil and composition of *Tagetes minuta* from Uganda. Larvicidal activity on *Anopheles gambiae*. *Industrial Crops and Products* 62, 400–404.
- Lawrence, B.M., 1996. Progress in essential oils, Myrtle oil. *Perfumer and Flavorist* 21, 57–58.
- Levin D.A., 1973. The role of trichomes in plant defense. *The Quarterly Review of Biology* 48, 3–15.
- Li, S., Tosens, T., Harley, P.C., Jiang, Y., Kanagendran, A., Grosberg, M., Jaamets, K., Niinemets, U., 2018. Glandular trichomes as a barrier against atmospheric oxidative stress: Relationships with ozone uptake, leaf damage, and emission of LOX products across a diverse set of species. *Plant, Cell and Environment* 41, 1263–1277.
- Lizarraga, E., Mercado, M.I., Galvez, C., Ruiz, A.I., Ponessa, G.I., Catalan, C.A.N., 2017. Morpho anatomical characterization and essential oils of *Tagetes terniflora* and *Tagetes minuta* (Asteraceae) growing in Tucuman (Argentina). *Boletín de la Sociedad Argentina de Botánica* 52, 55–68.
- Lopez, M.L., Bonzani, N.E., Zygadlo, J.A., 2009. Allelopathic potential of *Tagetes minuta* terpenes by a chemical, anatomical and phytotoxic approach. *Biochemical Systematics and Ecology* 36, 882–890.
- Machado, S.R., Canaveve, Y., Rodrigues, T.M., 2017. Structure and functioning of oil cavities in the shoot apex of *Metrodorea nigra* A. St.-Hil. (Rutaceae). *Protoplasma* 254, 1661–1674.
- Madikizela, B., Kambizi, L., McGaw, L.J., 2017. An ethnobotanical survey of plants used traditionally to treat tuberculosis in the eastern region of O.R. Tambo district, South Africa. *South African Journal of Botany* 109, 231–236.

- Maheshwari, J.K., 1972. *Tagetes minuta* Linn. In Shimla hills. Journal of Bombay Natural History Society 69, 451.
- Maity, N., Newma, N.K., Abedy, M.K., Sarkar, B.K., Mukherjee, P.K., 2011. Exploring *T. erecta* Linn flower for the elastase, hyaluronidase and MMP-1 inhibitory activity. Journal of Ethnopharmacology 137, 1300–1305.
- Mander, M., Ntuli, L., Diederichs, N., Mavundla, K., 2007. Economics of the traditional medicine trade in South Africa: healthcare delivery. South African Health Review 1, 189 – 196.
- Matsuki, S., Sano, Y., Koike, T., 2004. Chemical and physical defence in early and late leaves in three heterophyllous birch species native to Northern Japan. Annals of Botany 93, 141–147.
- Mayekiso, B., Magwa, L.L., Cooposamy, R., 2008. The morphology and ultrastructure of glandular and non-glandular trichomes of *Pteronia incana* (Asteraceae). African Journal of Plant Sciences 2, 50–60.
- Meshkatsadat, M.H., Safaei-Ghomi, J., Moharrampour, S., Nasser, M., 2010. Chemical characterization of volatile components of *Tagetes minuta* L. cultivated in south west of Iran by nano scale injection. Digest Journal of Nanomaterials and Biostructures 5, 101–106.
- Milan, P., Hayashi, A. H., Appezzato-da-Gloria, B., 2006. Comparative leaf morphology and leaf anatomy of three Asteraceae species. Brazilian Archives of Biology and Technology 49, 135–144.
- Minj, E., Britto, S.J., Marandi, R.R., Kindo, I., George, M., 2015. Phytochemical analysis and antimicrobial activity of *Putranjiva roxburghii* Wall. World Journal of Pharmacy and Pharmaceutical Sciences 5, 1157–1166.
- Mo, Y., Yang, R., Liu, L., Gu, X., Yang, X., Wang, Y., Zhang, X., Li, H., 2016. Growth, photosynthesis and adaptive responses of wild and domesticated watermelon genotypes to drought stress and subsequent re-watering. Journal of Plant Growth Regulation 79, 229–241.
- Mock, J.J., Barbic, M., Smith, D.R., Schultz, D.A., Schultz, S., 2002. Shape effects in plasmon resonance of individual colloidal silver nanoparticles. Journal of Chemical Physics 116, 6755–6759.

Mohammad, H., Javad, S., Saeid, M., Morasaalsadat, N., 2010. Chemical characterization of volatile components of *Tagetes minuta* L. cultivated in south west of Iran by nano scale injection. Digest Journal of Nanomaterials and Biostructures 5, 101–106.

Monteiro, W.R., Fahn, A., Caldeira, W., de Moraes Castro, M., 1999. Ultrastructural observations on the foliar secretory cavities of *Porophyllum lanceolatum* DC. (Asteraceae). Flora 194, 113–126.

Nafiu, M.O., Hamid, A.A., Muritala, H.F., Adeyemi, S.B., 2017. Preparation, Standardization, and Quality Control of Medicinal Plants in Africa, in: Medicinal Spices and Vegetables from Africa. Academic Press, 171–204.

Nair, R. and Chanda, S.V., 2007. Antibacterial activities of some medicinal plants of the western region of India. Turkish Journal of Biology 31, 231–236.

Nandita, D., Shivendu, R., Proud, S., Rahul, J., Swati, M., Arabi, M., 2012. Antibacterial activity of leaf extract of Mexican marigold (*Tagetes erecta*) against different gram positive and gram negative bacterial strains. Journal of Pharmaceutical Research 5, 4201–4203.

Ngarivhume, T., van't Klooster, C.I.E.A., de Jong, J.T.V.M., Van der Westhuizen, J.H., 2015. Medicinal plants used by traditional healers for the treatment of malaria in the Chipinge district in Zimbabwe. Journal of Ethnopharmacology 159, 224–237.

Ojo, O.A., Oyinloye, B.E., Ojo, A.B., Afolabi, O.B., Peters, O.A., Olaiya, O., Fadaka, A., Jonathan, J., Osunlana, O., 2017. Green synthesis of silver nanoparticles (AgNPs) using *Talinum triangulare* (Jacq.) Willd. leaf extract and monitoring their antimicrobial activity. Journal of Bionanoscience 11, 292–296.

Ojo, O.A., Oyinloye, B.E., Ojo, A.B., Basiru, A., Olayide, I., Idowu, O., Olasehinde, O., Fadugba, A., Adewunmi, F., 2018. Green-route mediated synthesis of silver nanoparticles (AgNPs) from *Syzygium cumini* (L.) Skeels polyphenolic-rich leaves extract and investigation of their antimicrobial activity. IET Nanobiotechnology 12, 305–310.

Oladosu, I.A., Aiyelaagbe, O.O., Afieroho, O.E., 2018. A novel normethylfriedelane-type isoprenoid from *Syzygium guineense* stem bark. Chemistry of Natural Compounds 54, 112–116.

- Padalia, H., Moteriya, P., Chanda, S., 2015. Green synthesis of silver nanoparticles from marigold flower and its synergistic antimicrobial potential. *Arabian Journal of Chemistry* 8, 732–741.
- Pakkirisamy, M., Kalakandan, S.K., Ravichandran, K., 2017. Phytochemical screening, GC-MS, FT-IR analysis of methanolic extract of *Curcuma caesia* Roxb (black turmeric). *Pharmacognosy Journal* 9, 952–956.
- Pal, S., Tak, Y.K., Song, J.M., 2007. Does the antibacterial activity of silver nanoparticles depend on the shape of the nanoparticle? A study of the gram-negative bacterium *Escherichia coli*. *Applied and Environmental Microbiology* 73, 1712–1720.
- Phani Deepthi Yadav, C.H.S.D., Bharadwaj, N.S.P., Yedukondalu, M., Methushala, C.H., Kumar, A.R., 2013. Phytochemical evaluation of *Nyctanthes arbortristis*, *Nerium oleander* and *Catharathnus roseus*. *Indian Journal of Research in Pharmacy and Biotechnology* 1, 333–338.
- Phondani, P.C., Bhatt, I.D., Negi, V.S., Kothiyari, B.P., Bhatt, A., Maikhuri, R.K., 2016. Promoting medicinal plants cultivation as a tool for biodiversity conservation and livelihood enhancement in Indian Himalaya. *Journal of Asia-Pacific Biodiversity* 9, 39–46.
- Rahimi, R., Shams-Ardekani, R.M.R., Abdollahi, M., 2010. A review of the efficacy of traditional Iranian medicine for inflammatory bowel disease. *World Journal of Gastroenterology* 16, 4504–4514.
- Rajvanshi, S.K. and Dwivedi, D.H., 2017. Screening of secondary phytometabolite of hydro-distilled essential oil from fresh flower and leaves of African marigold (*Tagetes erecta* L.). *International Journal of Minor Fruits, Medicinal and Aromatic Plants* 3, 1–7.
- Ramya, M. and Subapriya, M.S., 2012. Green synthesis of silver nanoparticles. *International Journal of Pharma Medicine and Biological Sciences* 1, 54–61.
- Rezaei, F., Jamei, R., Heidari, R., 2018. Evaluation of volatile profile, fatty acids composition and *in vitro* bioactivity of *Tagetes minuta* growing wild in northern Iran. *Advanced Pharmaceutical Bulletin* 8, 115–121.

- Rondon, M., Velasco, J., Hernandez, J., Pecheneda, M., Rojas, J., Morales, A., Carmona, J., Diaz, T., 2006. Chemical composition and antibacterial activity of the essential oil of *Tagetes patula* L. (Asteraceae) collected from the Venezuela Andes. *Revista Latinoamericana de Química* 34, 32–36.
- Roy, S. and Das, T.K., 2015. Plant mediated green synthesis of silver nanoparticles – a review. *International Journal of Plant Biology and Research* 3, 1044–1053.
- Russin, W.A., Uchytel, T.F., Durbin, R.D., 1992. Isolation of structurally intact secretory cavities from leaves of African marigold, *Tagetes erecta* L. (Asteraceae). *Plant Science* 85, 115–119.
- Sacchetti, G., Romagnoli, C., Bruni, A., Poli, F., 2001. Secretory tissue ultrastructure in *Tagetes patula* L. (Asteraceae) and thiophene localization through x-ray microanalysis. *Phyton (Horn, Austria)* 41, 35–48.
- Sadia, S., Khalid, S., Qureshi, R., Bajwa, A.A., 2013. *Tagetes minuta* L., a useful underutilized plant of family Asteraceae: a review. *Pakistan Journal of Weed Sciences Research* 19, 179–189.
- SANBI, 2015. *Tagetes minuta* L. National Assessment: Red List of South African Plants version 2015.1. <http://redlist.sanbi.org/> (Accessed on 2017/06/25)
- Santos, S.A.O., Vilela, C., Freire, C.S.R., Abreu, M.H., Rocha, S.M., Silvestre, A.J.D., 2015. *Chlorophyta* and *Rhodophyta* macroalgae: A source of health promoting phytochemicals. *Food Chemistry* 183, 122–128.
- Sarsar, V., Selwal, K.K., Selwal, K., 2013. Green synthesis of silver nanoparticles using leaf extract of *Mangifera indica* and evaluation of their antimicrobial activity. *Journal of Microbiology and Biotechnology Research* 3, 27–32.
- Saxena, M., Saxena, J., Nema, R., Singh, D., Gupta, A., 2013. Phytochemistry of medicinal plants. *Journal of Pharmacognosy and Phytochemistry* 1, 168–182.
- Schilmiller, A.L., Last, R.L., Pichersky, E., 2008. Harnessing plant trichome biochemistry for the production of useful compounds. *The Plant Journal* 54, 702–711.
- Scrivanti, L.R., Zunino, M.P., Zygadlo, J.A., 2003. *Tagetes minuta* and *Schinus areira* essential oils as allelopathic agents. *Biochemical Systematics and Ecology* 31, 563–572.

Senatore, F., Napolitano, F., Mohamed, M., Harris, P.J., Mnkeni, P.N., Henderson, J., 2004. Antibacterial activity of *Tagetes minuta* L. (Asteraceae) essential oil with different chemical composition. *Flavour and Fragrance Journal* 19, 574–578.

Shahzadi, I. and Shah, M.M., 2015. Acylated flavonol glycosides from *Tagetes minuta* with antibacterial activity. *Frontiers in Pharmacology* 6, 195–199.

Shahzadi, I., Hassan, A., Khan, U.W., Shah, M.M., 2010. Evaluating biological activities of the seed extracts from *Tagetes minuta* L. found in Northern Pakistan. *Journal of Medicinal Plant Research* 4, 2108–2112.

Shaik, S., Mkize, L., Khumalo, M., Singh, N., 2014. *Tetradenia riparia*-mediated synthesis of nano-gold particles. *Digest Journal of Nanomaterials and Biostructures* 9, 567–573.

Shakya, A.K., 2016. Medicinal plants: future source of new drugs. *International Journal of Herbal Medicine* 4, 59–64.

Sharma, V.K., Yngard, R.A., Lin, Y., 2009. Silver nanoparticles: green synthesis and their antimicrobial activities. *Advances in Colloid and Interface Science* 145, 83–96.

Shen, Q., Zhang, L., Liao, Z., Wang, S., Yan, T., Shi, P., Liu, M., Fu., X., Pan, Q., Wany, Y., Lv, Z., Lu, X., Zhang, F., Jiang, W., Ma., Y., Chen, M., Hao, X., Li, L., Tang, Y., Lv, G., Zhou, Y., Sun, X., Brodelius, P.E., Rose, J.K.C., Tang, K., 2018a. The genome of *Artemisia annua* provides insight into the evolution of Asteraceae family and artemisin biosynthesis. *Molecular Plant*, 1–13.

Shen, Y., Zhouliang, S., Shi, P., Wang, G., Wu, Y., Li, S., Zheng, Y., Huang, L., Lin, L., Lin, X., Yao, H., 2018b. Anticancer effect of petroleum ether extract from *Bidens pilosa* L and its constituents' analysis by GC-MS. *Journal of Ethnopharmacology* 217, 126–133.

Shirazi, M.T., Gholami, H., Kavooosi, G., Rowshan, V., Tafsiry, A., 2014. Chemical composition, antioxidant, antimicrobial and cytotoxic activities of *Tagetes minuta* and *Ocimum basilicum* essential oils. *Food Science and Nutrition* 2, 146–155.

Siddiqui, M.N., Redwhi, H.H., Achilias, D.S., Kosmidou, E., Vakalpoulou, E., Ioannidou, M.D., 2018. Green synthesis of silver nanoparticles and study of their antimicrobial properties. *Journal of Polymers and the Environment* 26, 423–433.

Singh, M., Singh, S., Prasad, S., Gambhir, I.S., 2008. Nanotechnology in medicine and antibacterial effects of silver nanoparticles. *Archives of Applied Science Research* 2, 76–81.

Singh, V., Shrivastava, A., Wahi, N., 2015. Biosynthesis of silver nanoparticles by plants crude extracts and their characterization using UV, XRD, TEM and EDX. *African Journal of Biotechnology* 14, 2554–2567.

Singh, V., Singh, B., Kaul, V.K., 2003. Domestication of wild marigold (*Tagetes minuta* L.) as a potential economic crop in Western Himalaya and North Indian plains. *Economic Botany*, 57, 535–544.

Singh, V., Singh, B., Sood, R.P., 1995. Herb, oil yield, oil content and constituent variation at different stages of *Tagetes minuta*. *Indian Perfumery* 39, 102–106.

Sletvold, N. and Agren, J., 2012. Variation in tolerance to drought amongst Scandinavian populations of *Arabidopsis lyrata*. *Evolutionary Ecology* 26, 559–577.

Sondi, I. and Salopek-Sondi, B., 2004. Silver nanoparticles as antimicrobial agent: a case study on *E. coli* as a model for gram-negative bacteria. *Journal of Colloid and Interface Science* 275, 177–182.

Spurr, A.R., 1969. A low-viscosity epoxy resin embedding medium for electron microscopy. *Journal of Ultrastructure Research* 26, 31–43.

Spyropoulou, E., Haring, M., Schuurink, R., 2014. RNA sequencing on *Solanum lycopersicum* trichomes identifies transcription factors that activate terpene synthase promoters. *BMC Genomics* 15, 402.

Street, R.A. and Prinsloo, G., 2013. Commercially important medicinal plants of South Africa: a review. *Journal of Chemistry* 2013, 1–16.

Suman, T.Y., Rajasree, S.R.R., Ramkumar, R., Rajthilak, C., Perumal, P., 2014. The green synthesis of gold nanoparticles using an aqueous root extract of *Morinda citrifolia* L. *Spectrochimica Acta Part A: Molecular and Biomolecular Spectroscopy* 118, 11–16.

Surendra, T.V., Roopan, S.M., Arasu, M.V., Al-Dhabi, N.A., Sridharan, M., 2016. Phenolic compounds in drumstick peel for the evaluation of antibacterial, hemolytic and photocatalytic activities. *Journal of Photochemistry and Photobiology* 161, 463–471.

Szyndler, M.W., Haynes, K.F., Potter, M.F., Corn, R., Loudon, C., 2013. Entrapment of bed bugs by leaf trichomes inspires microfabrication of biomimetic surfaces. *Journal of The Royal Society Interface* 10, 20130174.

Tanga, M., Lewu, F.B., Oyedeji, O.A., Oyedeji, O.O., 2018. Cultivation of medicinal plants in South Africa: A solution to quality assurance and consistent availability of medicinal plant materials for commercialization. *Academia Journal of Medicinal Plants* 6, 168–177.

Tankeu, S.Y., Vermaak, I., Viljoen, A.M., Sandasi, M., Kamatou, G.G.P., 2013. Essential oil variation of *Tagetes minuta* in South Africa – a chemometric approach. *Biochemical Systematics and Ecology* 51, 320–327.

Tattini, M., Matteini, P., Saracini, E., Traversi, M.L., Giordano, C., Agati, G., 2006. Morphology and biochemistry of non-glandular trichomes in *Cistus salvifolius* L. leaves growing in extreme habitats of the Mediterranean basin. *Journal of Plant Biology* 9, 411–419.

Tereschuk, M.L., Riera, M.V.Q., Castro, G.R., Abdala, L.R., 1997. Antimicrobial activity of flavonoids from leaves of *Tagetes minuta*. *Journal of Ethnopharmacology* 56, 227–232.

Tiwari, A., Goswami, P., Bisht, B.S., Chauhan, A., Verma, R.S., Padalia, R.C., 2016. Essential oil composition of African marigold (*Tagetes minuta* L.) harvested at different growth stages in foothills agroclimatic conditions of North India. *American Journal of Essential Oils and Natural Products* 4, 4–7.

Tiwary, M. and Jha, A.K., 2017. Biosynthesis of silver nanoparticles using plant extracts: new approach in agriculture and pharmaceuticals: a review. *International Journal for Innovative Research in Multidisciplinary Field* 3, 1–7.

Tolke, E.E.A.D., Lacchia, A.P.S., Demarco, D., Carmello-Guerreiro, S.M., 2017. Pericarp ontogeny of *Tapirira guianensis* Aubl. (Anacardiaceae) reveals a secretory endocarp in young stage. *Acta Botanica Brasilica* 31, 319–329.

Tooker J.F., Peiffer, M., Luthe, D.S., Felton, G.W., 2010. Trichomes as sensors: detecting activity on the leaf surface. *Plant Signaling and Behaviour* 5, 73–75.

Tozin, L.R.S., Silva, S.C.M., Rodrigues, T.M., 2016. Non-glandular trichomes in Lamiaceae and Verbenaceae species: morphological and histochemical features indicate more than physical protection. *New Zealand Journal of Botany* 54, 446–457.

- Tripathi, B., Bhatia, R., Walia, S., Kumar, B., 2012. Chemical composition and evaluation of *Tagetes erecta* (var. Pusa narangi genda) essential oil for its antioxidant and antimicrobial activity. *Biopesticides International* 8, 138–146.
- Tripathy, B., Satyanarayana, S., Khan, K.A., Raja, K., Tripathy, S., 2017. Preliminary phytochemical screening and comparison study of in vitro antioxidant activity of selected medicinal plants. *International Journal of Pharmacy and Life Sciences* 8, 5598–5604.
- Turner, G.W. and Lange, B.M., 2015. Ultrastructure of grapefruit secretory cavities and immunocytochemical localization of (+)- limonene synthase. *International Journal of Plant Sciences* 176, 643–661.
- Turner, G.W., Berry, A.M., Gifford, E.M., 1998. Schizogenous secretory cavities of *Citrus limon* (L.) Burm. F. and a reevaluation of the lysigenous gland concept. *International Journal of Plant Sciences* 159, 75–88.
- Valkama, E., Salminen, J.P., Koricheva, J., Pihlaja, K., 2003. Comparative analysis of leaf trichome structure and composition of epicuticular flavonoids in Finnish birch species. *Annals of Botany* 91, 643–655.
- Valle, D.L., Cabrera, E.C., Puzon, J.J.M., Rivera, W.L., 2016. Antimicrobial activities of methanol, ethanol and supercritical CO₂ extracts of Philippine *Piper betle* L. on clinical isolates of gram positive and gram negative bacteria with transferable multiple drug resistance. *PLoS ONE* 11, e0146349.
- Valverde, P.L., Fornoni, J., Nunez-Farfan, J., 2001. Defensive role in leaf trichomes in resistance to herbivorous insects in *Datura stramonium*. *Journal of Evolutionary Biology* 14, 424–432.
- Van Wyk, B.E., Van Oudtshoorn, B., Gericke, N., 2009. Medicinal plants of South Africa (2nd eds), Briza Publication, Pretoria, South Africa, 366.
- Vasudevan, P., Kashyap, S., Sharma, S., 1997. *Tagetes*: a multipurpose plant. *Bioresource Technology* 62, 29–35.
- Venkatachalam, K.V., Kjonaas, R., Croteau, R., 1984. Development and essential oil content of secretory glands of sage (*Salvia officinalis*). *Plant Physiology* 76, 148–150.

- Vidhu, V.K., Philip, D., 2014. Spectroscopic, microscopic and catalytic properties of silver nanoparticles synthesized using *Saraca indica* flower. *Spectrochimica Acta Part A: Molecular and Biomolecular Spectroscopy* 117, 102–108.
- Vidic, D., Āavar Zeljkoviā, S., Dizdar, M., Maksimoviā, M., 2016. Essential oil composition and antioxidant activity of four Asteraceae species from Bosnia. *Journal of Essential Oil Research* 28, 445–457.
- Wagner, G.J., 1991. Secreting glandular trichomes: more than just hairs. *Plant Physiology* 96, 675–679.
- Wagner, G.J., Wang, E., Shepherd, R.W., 2004. New approaches for studying and exploiting an old protuberance, the plant trichome. *Annals of Botany* 93, 3–11.
- War, A.R., Paulraj, M.G., Ahmad, T., Buhroo, A.A., Hussain, B., Ignacimuthu, S., Sharma, H.C., 2012. Mechanisms of plant defense against insect herbivores. *Plant Signaling and Behavior* 7, 1306–1320.
- Werker, E., 2000. Trichome diversity and development, in: Hallahan, D.L., Gray, J.C. (Eds.). *Advances in Botanical Research* 31, 1–30.
- Werker, E., Putievsky, e., Ravid, U., Dudai, N., Katzir, I., 1994. Glandular hairs, secretory cavities, and the essential oil in the leaves of tarragon (*Artemisia dracunculus* L.). *Journal of Herbs, Spices & Medicinal Plants* 2, 19–32.
- Weryszko-Chmielewska, E., Chwil, M., 2014. Structures of *Heracleum sosnovskii* Manden. stem and leaves relaeasing photodermatitis-causing substances. *Acta Agrobotanica* 67, 25–32.
- Xego, S., Kambizi, L., Nchu, F., 2016. Threatened medicinal plants of South Africa: case study of the family Hyacinthaceae. *African Journal of Traditional, Complementary and Alternative Medicines* 13, 169–180.
- Zarate, R. and Yeoman, M.M., 1994. Studies of the cellular localization of the phenolic pungent principle of ginger, *Zingiber officinale* Roscoe. *New Phytologist* 126, 295–300.
- Zohdy, S., Derfus, K., Andrianjafy, M.T., Wright, P.C., Gillespie, T.R., 2015. Field evaluation of synthetic lure (3-methyl-1-butanol) when compared to non odor-baited control in capturing *Anopheles* mosquitoes in varying land-use sites in Madagascar. *Parasites and Vectors* 8, 145–151.

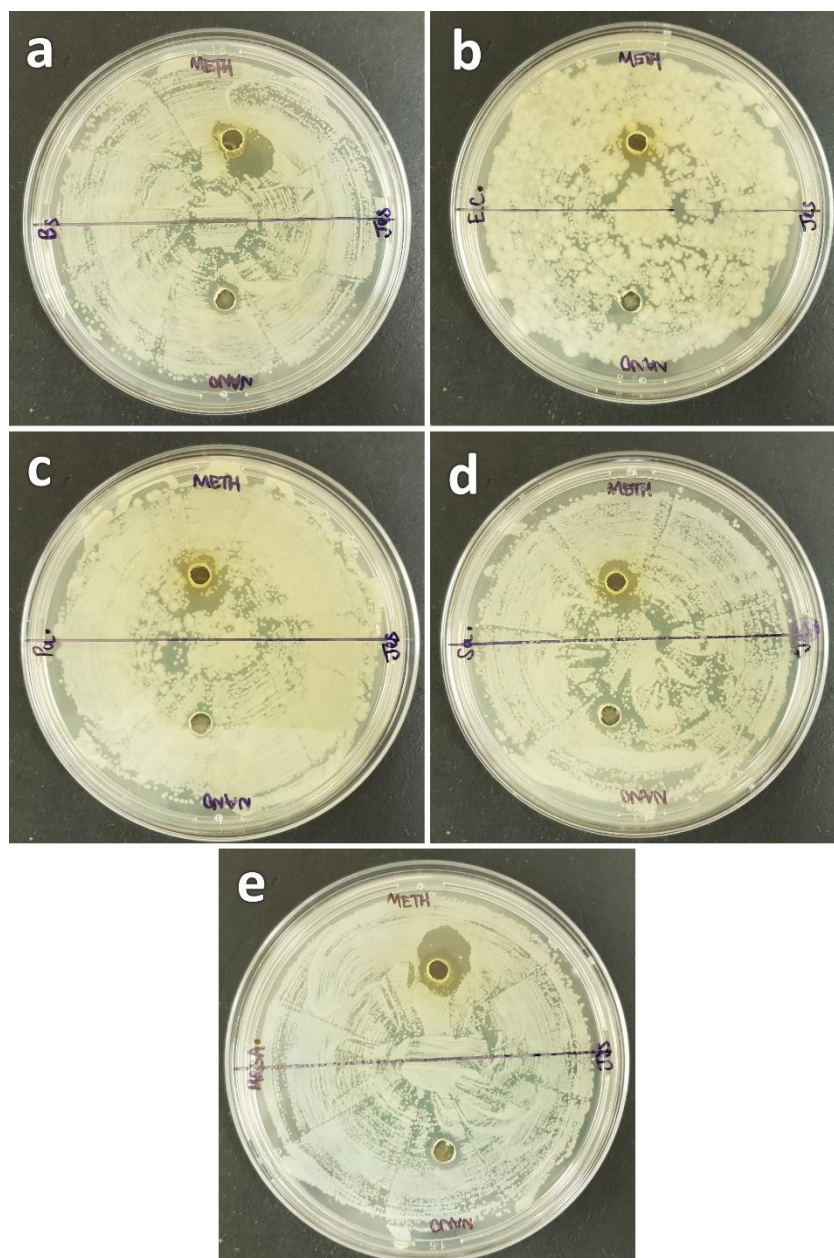
Zuber, J.A. and Takala-Harrison, S., 2018. Multidrug-resistant malaria and the impact of mass drug administration. *Infection and Drug Resistance* 11, 299–306.

APPENDIX A - Table A 1:

Peak#	R.Time	I.Time	F.Time	Area	Area%	Height	Height%
1	6.644	6.540	6.830	2475343	1.43	305415	0.52
2	6.939	6.870	7.065	5172418	2.99	1214597	2.07
3	7.915	7.635	8.110	25551453	14.77	1965752	3.36
4	8.391	8.360	8.425	373730	0.22	158212	0.27
5	8.445	8.425	8.475	460746	0.27	182581	0.31
6	8.499	8.475	8.600	733765	0.42	206025	0.35
7	9.076	9.035	9.210	166274	0.10	39712	0.07
8	9.410	9.290	9.435	418634	0.24	67678	0.12
9	9.575	9.530	9.700	597234	0.35	153526	0.26
10	9.754	9.725	9.840	222873	0.13	85746	0.15
11	10.005	9.985	10.040	78377	0.05	40521	0.07
12	10.180	10.120	10.225	54567	0.03	39881	0.07
13	10.323	10.235	10.385	190054	0.11	69122	0.12
14	10.473	10.430	10.550	189707	0.11	42762	0.07
15	10.864	10.825	10.965	864017	0.50	253745	0.43
16	11.000	10.965	11.055	180956	0.10	54479	0.09
17	11.135	11.055	11.170	194769	0.11	104562	0.18
18	11.351	11.315	11.405	287690	0.17	124240	0.21
19	11.911	11.740	11.960	195463	0.11	44214	0.08
20	12.214	12.190	12.295	2372374	1.37	1282959	2.19
21	12.360	12.295	12.440	779796	0.45	393721	0.67
22	12.639	12.555	12.795	2851558	1.65	491053	0.84
23	12.815	12.795	12.885	233794	0.14	98098	0.17
24	13.320	13.160	13.415	1792820	1.04	360421	0.62
25	13.522	13.485	13.665	498037	0.29	117008	0.20
26	13.825	13.800	13.970	245570	0.14	30429	0.05
27	14.335	14.245	14.370	549423	0.32	289600	0.49
28	14.416	14.370	14.465	253555	0.15	119412	0.20
29	14.804	14.750	14.850	655961	0.38	179654	0.31
30	14.895	14.850	14.945	484252	0.28	121913	0.21
31	15.128	15.100	15.190	561492	0.32	293400	0.50
32	16.226	16.145	16.285	5455648	3.15	2113614	3.61
33	16.314	16.285	16.455	3842620	2.22	1044798	1.78
34	16.510	16.455	16.560	589457	0.34	191216	0.33
35	17.057	17.020	17.100	3065541	1.77	1777349	3.04
36	17.115	17.100	17.150	273270	0.16	155771	0.27
37	17.311	17.275	17.365	601541	0.35	236896	0.40
38	17.528	17.475	17.605	4288951	2.48	2338540	3.99
39	17.957	17.920	17.995	501712	0.29	187455	0.32
40	18.115	17.995	18.200	1705988	0.99	170376	0.29
41	18.250	18.200	18.285	2445611	1.41	970341	1.66
42	18.330	18.285	18.455	4681544	2.71	1177665	2.01
43	18.465	18.455	18.530	685365	0.40	175309	0.30
44	18.545	18.530	18.610	473479	0.27	133099	0.23
45	18.630	18.610	18.680	278621	0.16	105578	0.18
46	19.047	18.985	19.105	275184	0.16	82367	0.14
47	19.290	19.215	19.325	7795999	4.51	4890010	8.35
48	19.344	19.325	19.380	1062698	0.61	523327	0.89
49	19.411	19.380	19.475	1762495	1.02	1031791	1.76
50	19.513	19.475	19.570	4057257	2.35	2421745	4.14
51	19.647	19.615	19.675	247735	0.14	142030	0.24
52	19.746	19.690	19.975	4571191	2.64	2231339	3.81
53	20.015	19.975	20.090	877977	0.51	227600	0.39
54	20.244	20.110	20.305	1137957	0.66	369897	0.63
55	20.400	20.305	20.480	755299	0.44	269534	0.46

APPENDIX A - Table A 2:

Peak#	R.Time	I.Time	F.Time	Area	Area%	Height	Height%
56	20.576	20.480	20.625	1063615	0.61	600340	1.03
57	20.942	20.870	20.980	1326686	0.77	744388	1.27
58	21.085	21.025	21.100	237568	0.14	107791	0.18
59	21.140	21.100	21.215	1617781	0.94	648561	1.11
60	21.271	21.215	21.300	302096	0.17	99132	0.17
61	21.331	21.300	21.370	287996	0.17	133405	0.23
62	21.608	21.575	21.685	759598	0.44	268752	0.46
63	21.925	21.890	21.950	3666052	2.12	2216104	3.78
64	21.967	21.950	22.035	2123946	1.23	1021565	1.74
65	22.178	22.100	22.220	689392	0.40	258051	0.44
66	22.561	22.515	22.645	240467	0.14	99909	0.17
67	22.750	22.705	22.800	392331	0.23	127309	0.22
68	23.005	22.950	23.025	526010	0.30	213253	0.36
69	23.041	23.025	23.115	751470	0.43	236051	0.40
70	23.168	23.115	23.275	1371395	0.79	462323	0.79
71	23.322	23.275	23.350	215801	0.12	110260	0.19
72	23.760	23.715	23.775	436480	0.25	207484	0.35
73	23.810	23.775	23.880	946092	0.55	268133	0.46
74	24.405	24.280	24.505	1311187	0.76	156761	0.27
75	24.550	24.500	24.575	682415	0.39	318119	0.54
76	24.585	24.575	24.670	406895	0.24	152903	0.26
77	25.172	25.125	25.225	902466	0.52	431517	0.74
78	25.266	25.225	25.315	380720	0.22	161762	0.28
79	25.385	25.315	25.450	4487899	2.59	3028899	5.17
80	25.619	25.585	25.690	334326	0.19	103527	0.18
81	25.985	25.860	26.060	1366573	0.79	654169	1.12
82	26.117	26.060	26.150	359406	0.21	183331	0.31
83	26.204	26.150	26.240	216541	0.13	99484	0.17
84	26.287	26.240	26.340	588350	0.34	300580	0.51
85	26.659	26.595	26.685	436412	0.25	140883	0.24
86	26.703	26.685	26.750	214715	0.12	115740	0.20
87	27.036	27.010	27.070	206387	0.12	121676	0.21
88	27.292	27.255	27.310	698051	0.40	374589	0.64
89	27.339	27.310	27.420	3165144	1.83	1330794	2.27
90	27.450	27.420	27.495	426807	0.25	143313	0.24
91	27.579	27.495	27.620	1195394	0.69	483541	0.83
92	27.656	27.620	27.710	489203	0.28	188866	0.32
93	28.038	28.005	28.075	392391	0.23	179691	0.31
94	28.493	28.435	28.530	649891	0.38	230451	0.39
95	28.704	28.595	28.765	1236661	0.71	414492	0.71
96	28.905	28.860	28.940	622545	0.36	211501	0.36
97	28.950	28.940	29.000	297200	0.17	133813	0.23
98	29.038	29.000	29.130	386469	0.22	68799	0.12
99	29.260	29.175	29.350	10496560	6.07	3513650	6.00
100	29.401	29.350	29.550	2084159	1.20	320259	0.55
101	29.638	29.550	29.680	807344	0.47	185278	0.32
102	29.752	29.680	29.990	12928684	7.47	2958970	5.05
103	29.926	29.885	29.990	634287	0.37	209259	0.36
104	30.070	29.990	30.125	968688	0.56	307442	0.53
105	30.194	30.125	30.220	642711	0.37	205207	0.35
106	30.260	30.220	30.350	2595856	1.50	844430	1.44
107	30.689	30.655	30.745	406402	0.23	108545	0.19
108	31.433	31.335	31.545	1897867	1.10	451311	0.77
				172991224	100.00	58554448	100.00

APPENDIX B – Antibacterial activity

Appendix B: Antibacterial activity of crude methanolic leaf extract and silver nanoparticles synthesised from the leaves of *Tagetes minuta* against gram positive and gram negative bacteria: a) *Bacillus subtilis*. b) *Escherichia coli*. c) *Pseudomonas aeruginosa*. d) *Staphylococcus aureus*. e) Methicillin-resistant *Staphylococcus aureus*.